Universidade do Minho
Escola de Engenharia

Pedro Daniel da Silva Ramôa

Design of a knee orthosis locking system

Pedro Daniel da Silva Ramôa Design of a knee orthosis locking system
UMinho | 2012

Outubro de 2012

Universidade do Minho
Escola de Engenharia

Pedro Daniel da Silva Ramôa

Design of a knee orthosis locking system

Tese de Mestrado
Engenharia Mecatrónica

Trabalho efectuado sob a orientação do
Professor Doutor João Paulo Flores Fernandes

e co-orientação do
Professor Doutor Jaime Francisco Cruz Fonseca

Outubro de 2012

Acknowledgements

In first place, I would like to thank my parents, my participation in this project was possible due to their hard work. I would also like to dedicate this thesis to Cidália, my brother Rui and to my sister-in-law Paula, their support during this project was very important to me, they were always there for me. To company Thermopista, a big thank you, specially to Alexandre and Susana. I would also like to thank the people from CT2M, specially to Pedro Moreira.

To my supervisors, Paulo Flores and Jaime Fonseca, I would like to thank them for their guidance during this project.

Pedro Ramôa

Abstract

The main goal of this work was to design a mechatronic locking system for a Stance Control Knee Ankle Foot Orthosis (SCKAFO). This mechanism should be able to perform two different functions. The first one is to lock the orthosis during the stance phase of human gait, in which contact between the foot and the ground exists. The second function deals with the unlock of the orthosis during the swing phase, in which there is no contact between the foot and the ground, allowing the flexion of the knee.

Biomechanics of human gait play an important role in the mechanical design of the locking system, since the motion characteristics associated with pathological and non-pathological exhibit different behaviors. Thus experimental gait studies was considered for pathological and non-pathological, in order to analyze the kinematic properties(joint angles and trajectories) and kinetic (ground reaction forces, joint forces and moments) of the human gait.

In the context of the present work sensors were used to detect the key points that characterize the human gait, allowing for the correct mechanism performance. These sensors are placed in anatomical relevant locations and calculate, not only the joint angles, but also the angular acceleration. The data read by these sensors is interpreted by a microcontroller that controls the actuation system in order to lock or unlock the mechanism. An innovative solution is presented here, which differs from the currently available solutions or in the scientific literature. The new approach is able to work without foot sensors and cables used with the purpose to lock/unlock the orthosis. With this approach it is expected that the locking/unlocking operation will be effective, safe and quick for the user.

Resumo

O objetivo principal deste projeto foi desenvolver um sistema mecatrónico para ortóteses do tipo *Stance Control Knee Ankle Foot Orthosis* (SCKAFO). Este mecanismo permite realizar duas funções distintas. A primeira consiste no bloqueio da ortótese durante a fase de apoio da marcha humana, onde se verifica contacto entre o pé e o solo. A segunda função incide no desbloqueio da ortótese durante a fase de balanço da marcha humana, onde não se verifica contacto entre o pé e o solo, permitindo a flexão do joelho.

Os conceitos biomecânicos da marcha humana assumem uma elevada importância no projeto mecânico deste mecanismo, uma vez que as características associadas à marcha natural e patológica demonstram comportamentos distintos. Por isso serão consideradas análises experimentais, com o objetivo de caracterizar cinematicamente (ângulos e trajetórias das articulações e segmentos anatómicos) e cineticamente (forças de contacto entre o pé e o solo, momentos e forças nas articulações) a marcha humana.

No contexto do presente trabalho foram utilizados sensores de forma a detetar pontos-chave da marcha humana, permitindo um correto funcionamento do mecanismo. Os sensores serão colocados nos segmentos anatómicos de maior interesse para este estudo e irão possibilitar o cálculo dos ângulos das articulações e as suas acelerações angulares. A informação gerada pelos sensores será interpretada por um microcontrolador, que irá controlar um sistema de atuação, permitindo bloquear ou desbloquear a ortótese. Com este trabalho, pretende-se desenvolver uma abordagem inovadora, que difere de todas as soluções comerciais e apresentadas na literatura científica. Esta solução permite um funcionamento sem a necessidade de recorrer a sensores plantares (colocados no pé) e sem presença de cabos ao longo do membro inferior. Com esta abordagem pretende-se desenvolver um mecanismo que realize a operação de bloqueio e desbloqueio de modo eficaz, seguro e rápido para o seu utilizador.

"First of all, let me assert my firm belief that the only thing we have to fear is fear itself - nameless, unreasoning, unjustified terror which paralyzes needed efforts to convert retreat into advance."

Franklin D. Roosevelt

Contents

List of Figures

List of Tables

LIST OF TABLES

Abbreviations

FA	Feet Adjacent
HR	Heel Rise
I^2C	Inter-Integrated Circuit
IC	Initial Contact
IMU	Inertial Measurement Unit
KAFO	Knee Ankle Foot Orthosis
OI	Opposite iInitial contact
OT	Opposite Toe off
PCB	Printed Circuit Board
PWM	Pulse Width Modulation
SCKAFO	Stance Control Knee Ankle Foot Orthosis
SPI	Serial Peripheral Interface
TO	Toe Off
TV	Tibia Vertical

Chapter 1

Introduction

1.1 Motivation

The muscular weakness of the lower limbs induces difficulties in the knee flexion/extension movement which results in a gait disorder. According to Moreira and Flores (2011) the gait disorder can be the result of several diseases, such as: peripheral neurological diseases, central neurological diseases and muscular diseases. A person with muscular weakness does not have the necessary muscular strength to maintain the knee at full extension during the entire stance phase, that is the contact between the foot and the ground exists. Thus a theoretical aid is required to help people to be able to keep the knee fully extended during gait.

According to Russell et al. (1997), in 1994 there were 989 thousand people using knee braces in the United States of America, which represents 0,35% of the total population, estimated in 260 million. In Portugal, it is know that 6.10% of the population has some type of disability, and 24,59% of all disabilities are motor related. In 2001 there were 610 thousand people with disabilities in Portugal (INE, 2002).

Currently, it is known that the number of different solutions to compensate the muscular weakness of the lower limbs is still small. In Portugal the most common solutions available in the market to solve this problem are the wheelchair and the KAFO (Knee-Ankle-Foot-Orthosis). The wheelchair has two negative effects. The first one is a slowdown in the physiotherapy process because the person stays seated down most of the day without using the muscles of the lower limbs. The second one is the need to adapt the house with ramps or elevators, making it wheelchair accessible. The KAFO solution does not need these requirements and limitations. In turn, the KAFO device is a static orthosis that does not allow the flexion of the knee while walking compensating the muscular weakness. This type of orthosis is becoming an obsolete model, the impossibility of flexing the knee during the swing phase is a great disadvantage. According to Bernhardt et al. (2006), the percentage of KAFOs rejection is between 58% and 78% due to several reasons.

Some companies such as Ottobock and Becker introduced to the market a new type of orthosis. The SCKAFO has one advantage compared to the KAFO that is, it unlocks the orthosis during the swing phase allowing to flex the knee and has the same behaviour of KAFO during the stance phase. This type of device is called a dynamic orthosis. However, the SCKAFO orthosis are still in an early stage of development. Thus, the main motivation for this work comes from the interest to contribute for the development of this type of orthosis making more accessible and stable.

1.2 Objectives and Thesis Structure

This work aims to develop a mechatronic locking system for a Stance-Control-Knee-Ankle-Foot-Orthosis (SCKAFO) which will be different from the ones currently available, mainly in what concerns with the need to include fast sensors and cables. With this approach also intends to perdict the locking of the mechanism, making available a larger period for the locking system to act correctly.

The specific goals of this work can be listed as follows:

- To perform an exhaustive study of the available SCKAFOs;
- To characterize the human gait with and without pathologies;
- To design a new mechanical system for orthosis locking system;
- To develop an electronic system that allows for the control and actuation the orthosis locking system;
- To build a data acquisition in order to access the influence of the developed locking system in the human gait;
- To develop of a functional prototype for verification and validation purpose.

The present dissertation is divided in six main chapters described below.

Chapter one presents the characterization of state of the art in order to evidence the different solutions by the companies with commercial solutions. In addition, a brief discussion on this thesis contribution can be found in this chapter.

Chapter two deals with the description of the lower limbs elements, followed by studies on the non-pathological human gait and pathological gait as well. Special emphasis is given to both bibliographical and experimental studies.

Chapter three describes the problem to be solved, the limitations and assumptions that the locking system must fulfill. Furthermore, in this chapter the proposed mechanical solutions and their characteristics are analyzed taking in account the critical points of the mechanism and the maximum strength. In this chapter will also be explained the reasons for the chosen materials.

Chapter four shows the electronic parts suitable for this project, such as sensors or microcontrollers are discussed. The fundamental reasons to select the components are presented in this process. The data acquisition software developed is also demonstrated in this chapter.

In Chapter five the new concept of locking mechanism is presented as well as the corresponding performance. In this chapter the materials, the costs and the process of the construction of the physical prototype are discussed. The relation between the electronic system and the locking mechanism can also be found in this chapter. Finally, all the tests performed as well as the concept validation is object of study in this chapter.

The Chapter six contains the issues addressed in the conclusions and the future work are presented.

In Appendices A to D it is possible to see the technical drawings and summary of the results of stress simulations. In Appendix E is presents the schematics from the developed boards.

1.3 State-of-the-Art

As result of the technology evolution over the last decades, the quality of the orthosis has been increasing. The use of new versatile and lighter materials improved the functionality and comfort of the orthosis without compromising the safety of the user. The use of new materials also allowed to improve the orthosis aesthetically.

At the end of the 80's decade and beginning of 90's decade of last century, the first SCKAFOs were presented. However with the introduction of electronics, the orthosis gained new capabilities that would not be possible before, because they were purely mechanical devices.

The first mechanical SCKAFO was presented in 1989 by *Becker Orthopedic* company. The *UTX* model was the first of a generation of mechanical SCKAFOs (Edeer and Martin, 2010). This *UTX* with some improvements is currently available. Since 1989, other pure mechanical SCKAFOs were introduced namely, *Becker FullStride* and *SafetyStride*, or *Ottobock Free Walk*. Figure 1.1 shows the mechanical SCKAFOs developed by *Becker Orthopedic*. In this type of orthosis the locking system is activated by a movement of the lower limb, usually is the dorsiflexion (Figure 1.2a). This type of orthosis demonstrate a major disadvantage, a person with foot dropping is unable to activate the locking system. In spite of the aesthetically differences, the working principle is the same, the movement of dorsiflexion is responsible for the locking/unlocking of the mechanism (Bedard, 2010).

(a) *Becker UTX* (b) *Becker SafetyStride* (c) *Becker FullStride*

Figure 1.1: *Becker*'s mechanical orthosis (Bedard, 2010)

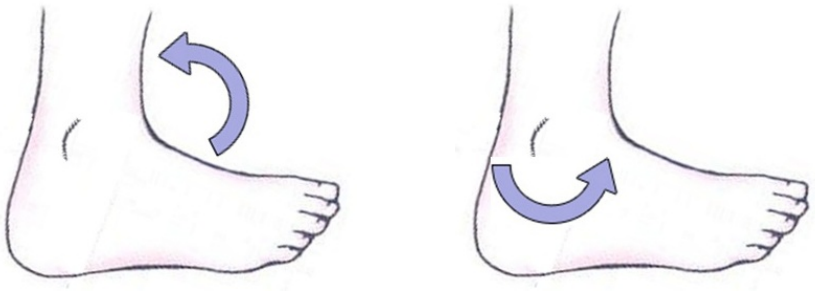

(a) Dorsiflexion (b) Ankle rotation

Figure 1.2: Foot movements

The *UTX* and the *FullStride* models are presented in Figure 1.1, and they have a similar locking system to the *Ottobock Free Walk* as it is shown in Figure 1.4b, This locking system is composed by a ratchet/pawl mechanism as Figures 1.3a and 1.3b illustrate.

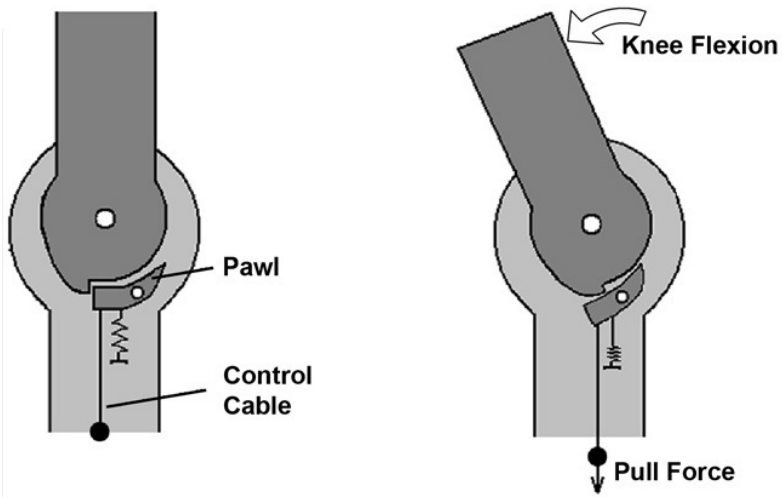

(a) Locked mechanism (b) Unlocked mechanism

Figure 1.3: *UTX*'s mechanism (Yakimovich et al., 2009)

This mechanical orthosis have a cable along the shank, visible in Figures 1.1 and 1.3, which is moved according to the movement of the ankle. According to Yakimovich et al. (2009), it is necessary 10° of dorsiflexion to unlock this orthosis. When the user is performing the dorsiflexion, the cable follows the movement of the ankle which pulls away the pawl from the ratchet and consequently, unlocking the orthosis allowing the flexion of the knee. In turn, to lock the orthosis, the knee must be totally extended and dorsiflexion should not exist.

There are other fundamental issues associated with the *UTX* orthosis, mainly (Bedard, 2010):

- The typical *UTX* orthosis weight less than two kilograms and has several design variations suiting the diferent types of diseases;
- This model is indicated to: Quadriceps weakness as a result of Poliomyelitis; Multiple Sclerosis; Cerebrovascular Accident; Femoral Nerve; Incomplete SCI; Inclusion Body Myositis; Genu recurvatum;
- The user must have muscular force in the lower limbs equal or greater than Grade 3, that is, the joint can move against the gravity;
- The user must weight less than 120kg and the knee at full-extension must be at least 10°.

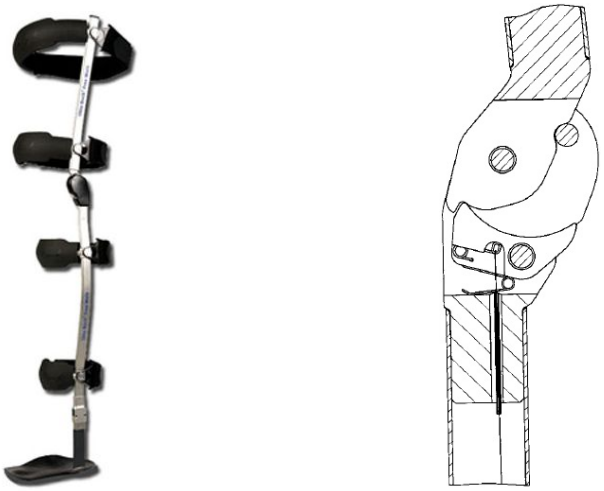

(a) *Ottobock Free Walk* (Network, 2012)

(b) *Free Walk*'s mechanism (OttoBock, 2008c)

Figure 1.4: *Ottobock Free Walk* and corresponding mechanism

The fundamental information about the *Free Walk* orthosis can be listed below:

- The *Free Walk* orthosis weight is 780 grams; (OttoBock, 2008c)
- This model is indicated to: Central nervous system disorders (Stroke, brain tumors, craniocerebral injury, multiple sclerosis, and others); Spinal cord diseases (Injury in the spinal cord, Myatrophic lateral sclerosis, Post-polio syndrome, Post-polio syndrome, and others); (OttoBock, 2008b)

- The *Free Walk* model have two variations, one to users with a bodyweight up to 80kg, and other to users with a bodyweight up to 120kg; (OttoBock, 2008b)
- The knee in full-extension must be at least 10°; (OttoBock, 2008c)
- The user must have muscular force in the lower limbs equal or greater than Grade 3. (OttoBock, 2008c)

The *SafetyStride* model from *Becker* has a different mechanism from the remaining of the presented mechanical SCKAFOs. Instead of a mechanism composed by a ratchet and a pawl, this model has a clutch and a lever (see Figure 1.5). With the clutch, the orthosis is able to lock in any position without the need of having the knee fully extended. This is a major advantage when compared with other mechanical SCKAFOs. The lever locks the orthosis during the swing phase (when the knee is flexed and there is no contact between the foot and the ground), allowing only the movement of extension of the knee. At the end of the stance phase, the lever unlocks the orthosis. This working principle is similar to the *Fillauer* orthosis, illustrated in Figure 1.6.

Figure 1.5: *Becker SafetyStride*'s mechanism (Orthotics, 2012b)

The *Becker* orthosis gives the following information about the *SafetyStride* (Bedard, 2010):

- The *SafetyStride* is indicated for people with: Quadriceps weakness as a result of Poliomyelitis; Multiple Sclerosis; Cerebrovascular Accident; Femoral Nerve and Incomplete SCI; Inclusion Body Myositis; Genu recurvatum;
- The weight limit is 100kg;
- The person should not have any spascity in hip, knee or ankle.

The company *Fillauer* presented a mechanical SCKAFO, called *Stance Phase Lock* (*SPL*) which uses the same mechanism of *Becker UTX* but with the working principle of the *Becker SafetyStride*. According to Yakimovich et al. (2009) the locking mechanism is actuated by gravity. When the thigh is anterior to the body the weight pawl falls into the ratchet locking the orthosis, as shown in Figure 1.6b. With the thigh posterior to the body, the weight pawl will fall away from the ratchet (see Figure 1.6c), unlocking the orthosis, allowing the flexion of the knee.

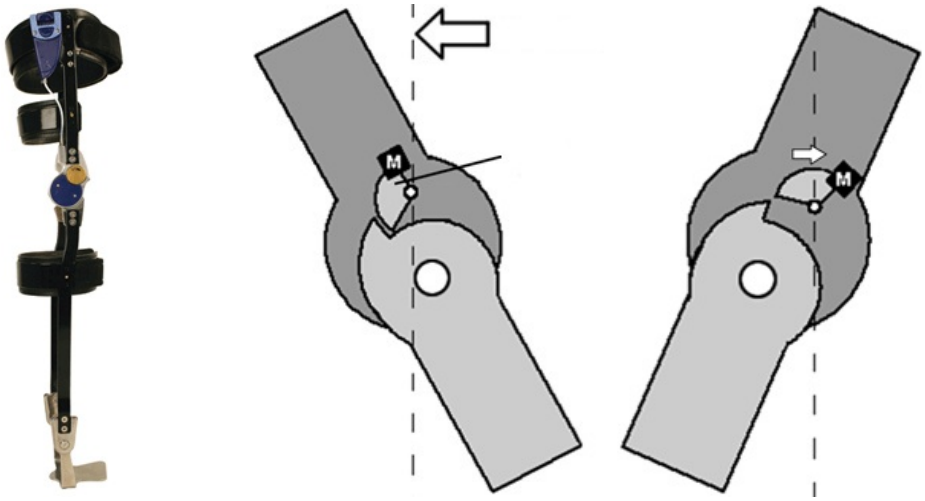

(a) *Fillauer* SCKAFO (Cascade, 2012a) (b) Locked mechanism (Yakimovich et al., 2009) (c) Unlocked mechanism (Yakimovich et al., 2009)

Figure 1.6: *Fillauer SPL* and respective mechanism

Fillauer launched to the market a new orthosis, named *Stance Phase Lock 2* (see Figure 1.7a), developed by *Basko Healthcare*, a *Fillauer* affiliate in The Netherlands. The locking mechanism, illustrated in Figure 1.7b, is very similar to the prior model, with some improvements, namely: it has two locking positions (0° and 15°); it has a *cylindrical bumper with extended wear*; and Teflon bushings for sideloading. These characteristics improve the locking mechanism safety, increase the durability and reduces the friction.

Stance Phase Lock 2 indications and contraindications are listed below:

- The *Stance Phase Lock 2* is indicated for people with: Post-polio; Spinal involvement; Cerebral vascular accident; Peripheral paresis/paralysis; Nerve inflammations; Neurological failures; Myopathies; Multiple sclerosis. (Fillauer, 2012)
- Contraindications: Central paresis/paralysis, Hip flexion contracture. (Fillauer, 2012)

(a) *Fillauer* SCKAFO (Cascade, 2012b)

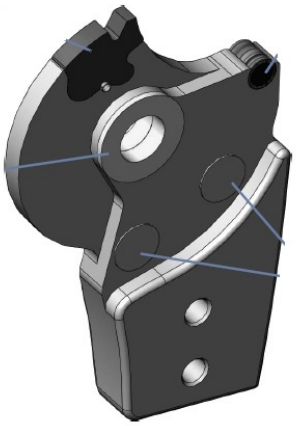

(b) *SPL2* mechanism (Fillauer, 2012)

Figure 1.7: *Fillauer SPL2* and respective mechanism

The mechanism from *Horton*'s SCKAFO, illustrated in Figure 1.8 has a different working principle from the *Becker*'s or *Ottobock*'s SCKAFO. In this model the locking mechanism is activated by the contact between the foot and the ground. With the contact the stirrup is forced to move upwards, causing the pushrod to move the cam into the friction ring, locking the orthosis. When the contact between the heel and the ground no longer exists, the stirrup moves downwards by the force of gravity moving the cam away from the friction ring, unlocking the orthosis and allowing to the person to flex the knee (Yakimovich et al., 2009).

(a) *Horton* SCKAFO (Orthotics, 2012a)

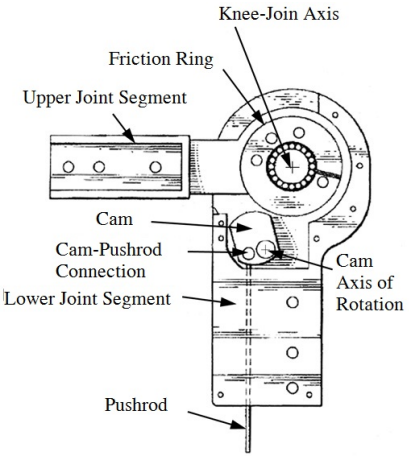

(b) Mechanism (Yakimovich et al., 2009)

Figure 1.8: *Horton Stance Control KAFO* and respective mechanism

Becker has two other mechanical orthosis, namely the *GX-Knee* and the other is *Load Response*. *GX-Knee* comes with a pneumatic spring to help the knee extension and can be used alone (see Figure 1.9a) or with *Becker FullStride* and *SafetyStride* as *GX-Assist* (Figure 1.9b). The *GX-Knee* orthosis does not have locking mechanism, the only purpose of this orthosis is to assist the knee extension movement. This mechanism is similar to the ones used to the elevation of cars trunks. The *Load Response* has a similar mechanism to the *SafetyStride*, it is *equipped with a preloaded spiral torsional spring that mimics the ability of ther quadriceps muscle to absorb ground reaction forces from heel strike* (see Figure 1.10).

(a) *Becker GX-Knee* (b) *Becker SafetyStride* with *GX-Assist*

Figure 1.9: *Becker GX-Knee* and *SafetyStride* with *GX-Assist* (Bedard, 2010)

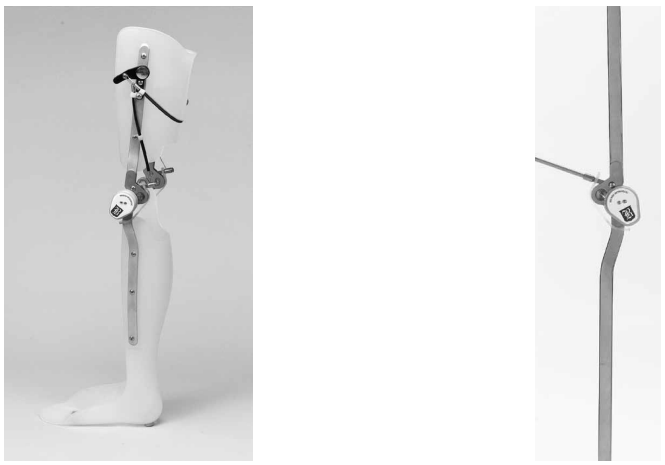

(a) *Becker Load Response* (b) *Load Response*'s mechanism

Figure 1.10: *Becker Load Response* and corresponding mechanism (Bedard, 2010)

According to Edeer and Martin (2010), SCKAFOs controlled by a microcontroller, such as *Becker E-Knee* or *Ottobock Sensor Walk* were introduced. The *E-Knee* model (see Figure 1.11a) uses a electromagnetic mechanism (see Figure 1.11b) to lock the orthosis with foot sensors to control the orthosis, as it is shown in Figure 1.12. When the pressure sensors on the foot detects contact with the ground, the electromagnetic coil is activated and forces the contact between the two ratchet plates allowing the motion only in one way (knee extension). When the pressure sensors no longer detect the contact between the ground and the foot, the coil is deactivated and the spring forces the separation between the two sprocket wheels.

(a) *Becker E-Knee* (Bedard, 2010)

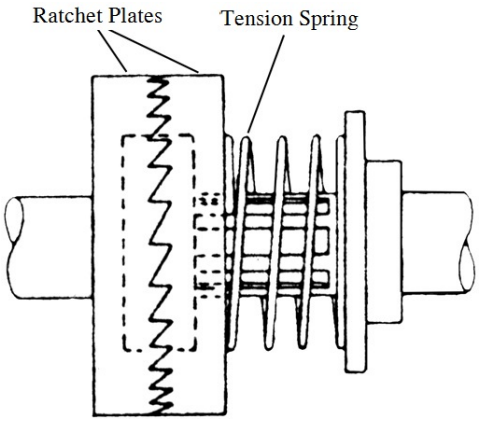

(b) *E-Knee* mechanism (Yakimovich et al., 2009)

Figure 1.11: *Becker E-Knee* and corresponding mechanism

The *E-Knee* model is equipped with four foot sensors as shown in Figure 1.12, one placed on the big toe (sensor 1), one located on the first metatarsal (sensor 2), one situated on the fifth metatarsal (sensor 3), and one placed on the heel (sensor 4).This set sensors is used because the foot touches the ground differently depending on the disease. For instance, a person with foot drop has a different contact area between the foot and the ground when compared to a person with lateral trunk bending.

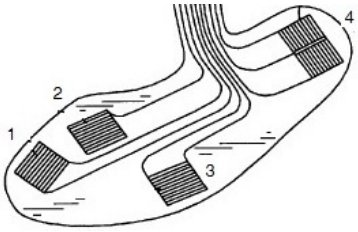

Figure 1.12: *E-Knee*'s sensors (Naft et al., 2003)

Becker E-Knee additional features, namely:

- The *Becker E-Knee* is indicated to people with: Quadriceps weakness as a result of Poliomyelitis; Multiple Sclerosis; Cerebral vascular Accident; Femoral Nerve; Incomplete SCI; Inclusion Body Myositis (Bedard, 2010);
- Contraindications: Users with bodyweight superior to 100kg; Spasticity in hip, knee or ankle; Fixed varus or valgus deformity at the knee superior to 15°; Substantial leg length discrepancy (Bedard, 2010).

Ottobock Sensor Walk has five sensors, four located on the foot and one placed at the knee level. *Sensor Walk* uses a wrap spring clutch as locking mechanism as it is shown in Figure 1.12. When the contact between the foot and the ground does not exist (end of the stance phase) by the sensors placed on the foot, the microcontroller unlocks the mechanism making it a free swing orthosis. At the middle of the swing phase, the knee sensor detects the motion of the shank and the microcontroller will lock the orthosis, allowing only the extension movement and blocking the flexion movement.

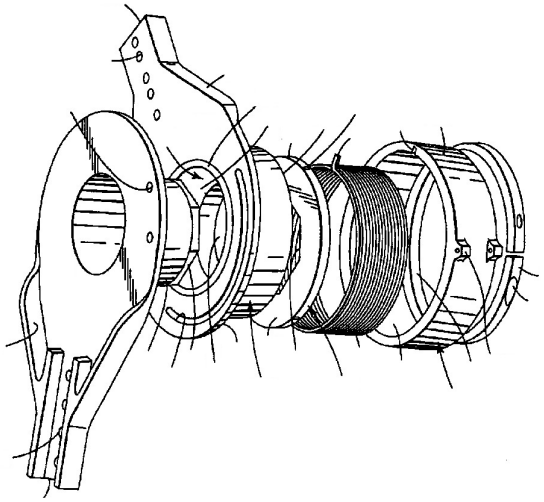

Figure 1.13: *Sensor Walk*'s mechanism (Irby et al., 2004)

Figure 1.14 presents the *Sensor Walk*. The highlight goes to element G in the Figure 1.14b namely, the *Sensor Selection Switch*. Sensor Walk allows to chose which foot sensor triggers the microcontroller to unlock the orthosis, as it is shown in Figure 1.15.

The *Sensor Walk* has some important additional characteristics (Healthcare, 2010b):

- The *Sensor Walk* maximum user bodyweight is 136kg;
- *Sensor Walk* users must have muscular force in the lower limbs equal or greater than Grade 3 and a step length over the opposite foot.

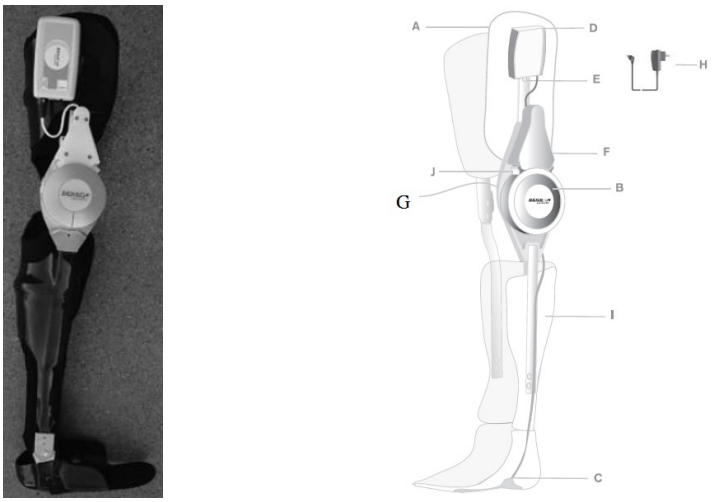

(a) *Ottobock Sensor Walk* (b) *Sensor Walk* diagram

Figure 1.14: *Ottobock - Sensor Walk* (Healthcare, 2010a)

The *Sensor Selection Switch* (see Figure 1.15) has advantages and disadvantages. The main advantage is that it allows to save energy because only one sensor is energised. The disadvantage is that the selected sensor has to be the right one that triggers the mechanism, if it is not the correct one, this situation will cause performance problems.

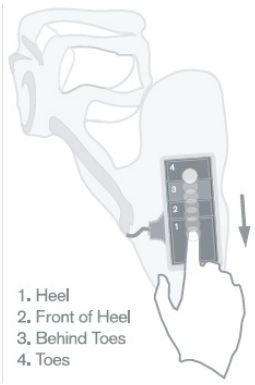

Figure 1.15: *Sensor Selection Switch* (Healthcare, 2010a)

The *Ottobock* created a device called *E-MAG Control* which is a locking mechanism that can be assembled with other orthosis from *Ottobock* company. *E-MAG* is an automatic locking mechanism without being controlled by the movement of the ankle or by sensors located on the foot. The gait cycle is detected by two gyroscopes, which read the angular accelerations from the lower limb and according to the values those accelerations the orthosis is locked or unlocked. In Figure 1.16a is shown the various parts that compose the *E-MAG* are listed below (OttoBock, 2008a):

1. Knee joint with bearings;
2. Electromagnetic joint;
3. End position sensor;
4. Electronic part (sensor, microncontroller, and others);
5. Buttons to manual operation;
6. Batteries (not shown);
7. Auto-calibration and test buttons.

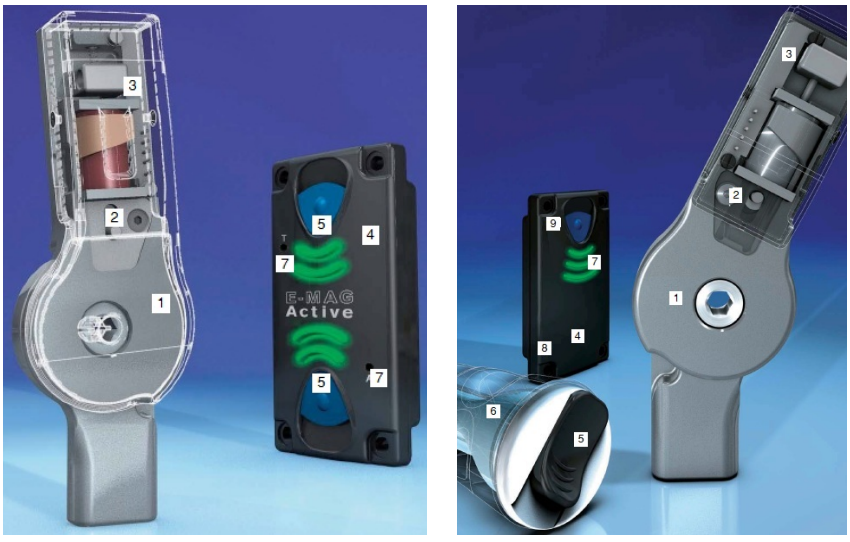

(a) *E-MAG* (b) *E-MAG* Control System

Figure 1.16: *Ottobock* - *E-MAG* (OttoBock, 2008a)

The *E-MAG* was a working principle similar to *E-Knee* or *Sensor Walk* is controlled by a microcontroller, which requires a battery to supply the locking mechanism because it is a mechatronic device instead of a purely mechanical device like *Free Walk* or *UTX*. According to Ottobock, the *E-MAG* has an autonomy of the battery is 10.000 steps.

The control system by *E-MAG* that is displayed in Figure 1.16b, has (OttoBock, 2008a):

1. Knee joint with bearings;
2. Electromagnetic joint;
3. End position sensor;
4. Electronic part (sensor, microncontroller, and others);
5. Remote control to manual locking and unlocking;
6. The remote control can be installed on the waist;
7. Feedback system is composed by LEDs to ensure that is locked;
8. 2.4Ghz microcontroller for wireless communications;
9. Manual operation

Becker also presented *E-MAG Active*, an orthosis that is equipped with *E-MAG Control* and the bodyweight of the user limit is 85kg. This orthosis is indicated for persons with poliomyelitis, post-polio syndrome, or partial paraplegia. It is also indicated for persons that need a higher mobility.

Chapter 2

Biomechanics of the Human Gait

2.1 Human Gait: Non pathological

In order to better understand the human gait, it is necessary to analyze the gait cycle and the corresponding phases and sub phases. The gait cycle can be divided in two parts: the swing phase and the stance phase. The swing phase can be described as the part of the gait cycle where there is no contact between the ground and the foot. The stance phase begins in the exact instant when the heel touches the ground and ends when the toe rises from the ground, interrupting the contact between the foot with the ground.

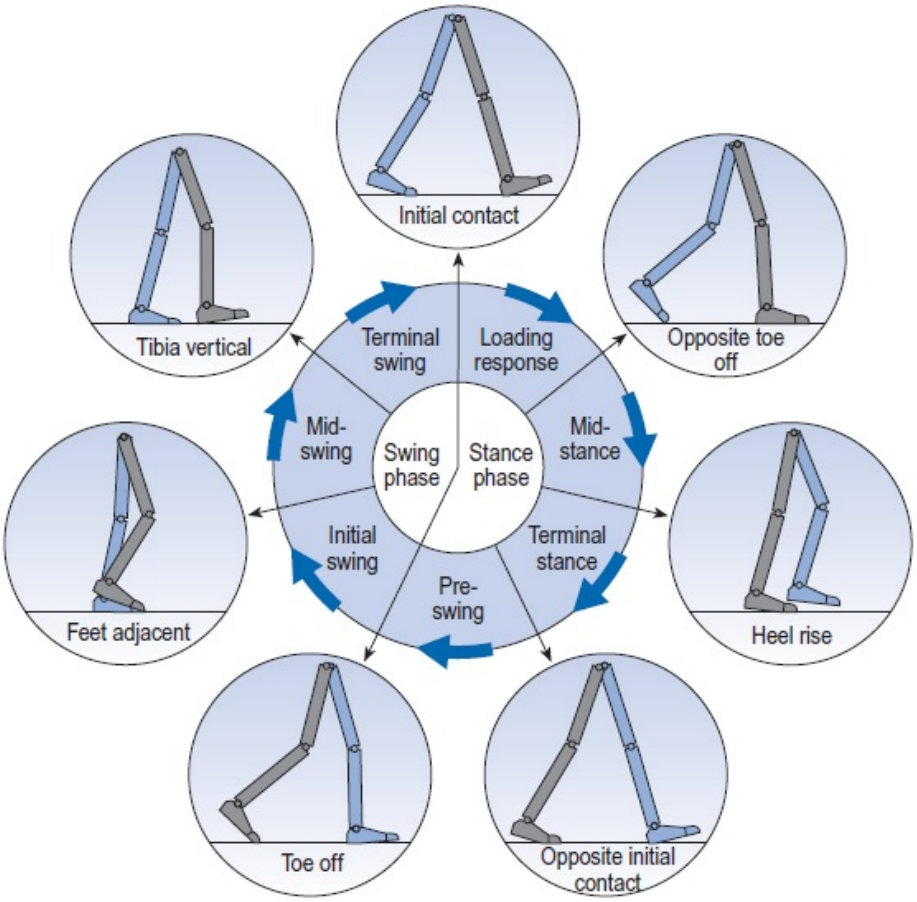

Figure 2.1: Gait cycle (Whittle, 2007)

In Figure 2.1, several parts of the human gait are illustrated. The swing phase can be divided in three sub-phases:

- Initial swing
- Mid-swing
- Terminal swing

The stance phase is divided in four sub-phases:

- Loading response
- Mid-stance
- Terminal stance
- Pre-swing

The sub-phases above described are separated by seven instants as it is shown in Figure 2.1:

- Initial contact (IC);
- Opposite toe off (OT);
- Heel rise (HR);
- Opposite initial contact (OI);
- Toe off (TO);
- Feet adjacent (FA);
- Tibial vertial (TV).

The transition between swing phase and stance phase happens in the instant named *initial contact*, in this situation the point of contact between the ground and the foot is trough the heel. The opposite transition occurs when the instant named *toe off* initializes the swing phase.

According to Whittle (2007), the range of the human gait cycle time is between 0,80 seconds and 1.48 seconds. The values depend on gender and age. In Table 2.1 it is presented the duration of the women gait cycle, in Table 2.2 it is presented the the men gait cycle duration. Thus, the women's gait are less susceptible to aging.

Table 2.1: Gait cycle timing: Female (Whittle, 2007)

Age (years)	Cycle time (s)
13 - 14	0.80 - 1.17
15 - 17	0.83 - 1.20
18 - 49	0.87 - 1.22
50 - 64	0.88 - 1.24
65 - 80	0.88 - 1.25

The women's minimum gait cycle duration varies from 0,8 seconds (from 13 to 14 years) to 0,88 seconds (from 65 to 80 years), 0,08 seconds of difference. The women's maximum gait cycle time is between 1,17 and 1,25 seconds, the same 0,08 seconds of difference. In men's gait cycle the differences are larger. The minimum gait cycle time is between 0,81 (from 13 to 14 years) seconds and 0,96 seconds (from 65 to 80 years), 0,15 seconds of difference. The men's maximum gait cycle time goes from 1,20 seconds to 1,48 seconds, 0,28 seconds of difference. This aspects shows that men gait are more influenced by aging.

Table 2.2: Gait cycle timing: Male (Whittle, 2007)

Age (years)	Cycle time (s)
13 - 14	0.81 - 1.20
15 - 17	0.85 - 1.25
18 - 49	0.89 - 1.32
50 - 64	0.95 - 1.46
65 - 80	0.96 - 1.48

There is another important issue that should be taken in account namely, the joint angles. The joint angles are very relevant to human gait analysis, by retrieving the angles of the various joints it is possible to know in which part of the human gait the person is situated. In Figure 2.2, is shown the evolution of the joints during a entire cycle is illustrated.

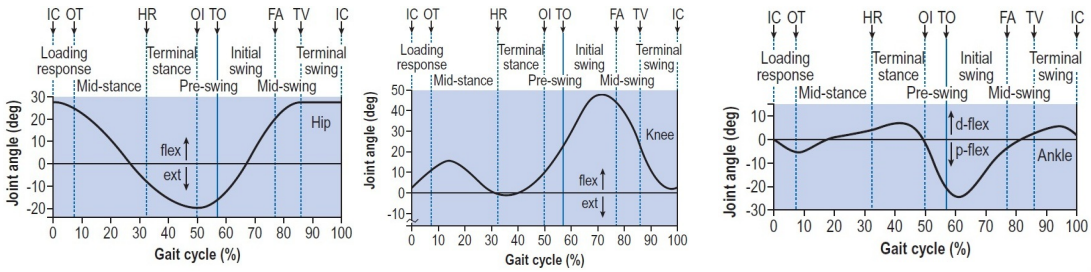

(a) Hip (b) Knee (c) Ankle

Figure 2.2: Joints angles (Whittle, 2007)

Figure 2.2a shows that in the *initial contact* the hip angle is close to 30°. From IC to OI the angle of the hip keeps lowering to values around -20°. In the transition from stance phase to swing phase (given by Toe Off) the angle is not in the lower value anymore. The angle rises until it reaches TV, then stays constant during the terminal swing.

Figure 2.2b shows that in the IC the knee is almost fully-extended. After the IC, the knee flexes slightly in the beginning of the stance phase. With lifting of heel the knee starts to flexing until the maximum value in the initial swing, nearly 50°, then the knee starts extending to repeat the gait cycle.

Finally, the ankle (see Figure 2.2c) stays almost in the same position, except the negative peak in the initial swing, this is moment when the person rises the foot from the ground.

2.2 Human Gait: Pathological

There are several diseases that can affect the normal gait of a human being, these diseases can be divided into three main groups: central neurological diseases; peripheral neurological diseases; and muscular diseases. The central neurological diseases can be subdivided into six (Moreira and Flores, 2011):

- Multiple sclerosis
- Cerebral palsy
- Parkinson disease
- Brain injury
- Stroke
- Spinal Cord Injury

In turn, the diseases that belong to the peripheral neurological diseases group are as follows (Moreira and Flores, 2011):

- Poliomyelitis
- Post-polio syndrome
- Spina bifida
- Poly neuropathy
- Stroke
- Spinal Cord Injury

Finally, the muscular diseases can be listed as (Moreira and Flores, 2011):

- Duchenne muscular dystrophy
- Becker's muscular dystrophy
- Myasthenia gravis

These diseases produce an abnormal gait, which may vary according to the type of disease. Lateral trunk bending is one of the abnormal gaits, in this situation it is normal for the patient to bend the torso sideways to reduce the pressure in the hip joint while supporting the weight only in one leg. When the person starts the swing phase with one leg, the torso leans towards the other leg, making easier the movement of swing of the first leg. Figure 2.3 shows a person using a prothesis, which causes a lateral trunk bending.

Figure 2.3: Laterial trunk bending (Craig, 2012)

The common reasons to this abnormal gait are: Painful hip, hip abductor weakness, abnormal hip joint, wide walking base and unequal leg length. There is also anterior and posterior trunk bending, in these cases the torso moves erratically in the sagittal plane. With anterior trunk bending the person flex the torso in the stance phase to compensate the muscular weakness of the muscles responsible for the movement of knee extension. The posterior trunk bending is the inverse movement of the anterior trunk bending where the person moves the torso backwards in order to compensate the muscular weakness of the muscles responsible for the movement of hip extension.

Some users of lower limbs orthosis have functional leg length discrepancy. In order to compensate this problem, it is frequently used one of these abnormal gaits: circumduction, hip hiking, steppage and vaulting. Circumduction is the circular movement that the person of the swing leg to compensate the leg discrepancy, as it is shown in Figure 2.6.

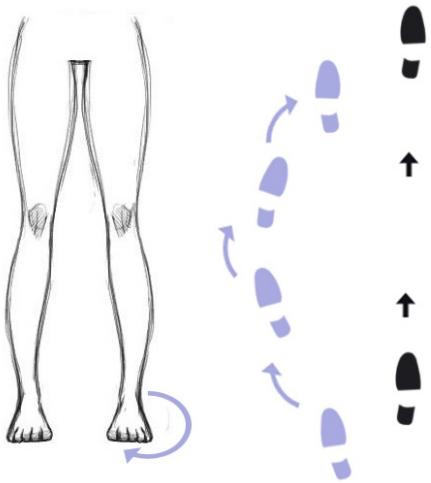

Figure 2.4: Circumduction

With the hip hiking gait (see Figure 2.5a) the person moves the swinging leg side of the hip upwards to compensate the leg discrepancy. The steppage (see Figure 2.5b), is the gait abnormality where the person flex the knee and the hip more than on a natural gait. In the gait with vaulting (see Figure 2.5c) the stance phase is made on the person's toes, with this the person gains height, and does not needing to over-flex the knee or the hip.

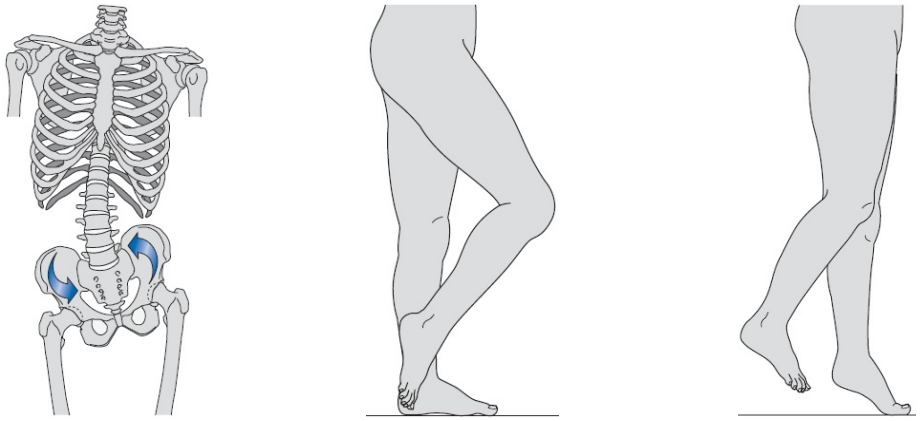

(a) Hip hiking (b) Steppage (c) Vaulting

Figure 2.5: Pathological gaits (Whittle, 2007)

The excessive knee extension/flexion is another pathological gait. If the person has excessive knee extension the stance phase is not normal, instead of a normal stance phase as shown in Figure 2.2, the person extend the knee to a negative angle. With excessive knee flexion, the person can not fully extend the knee in the stance phase, originating a abnormal gait.

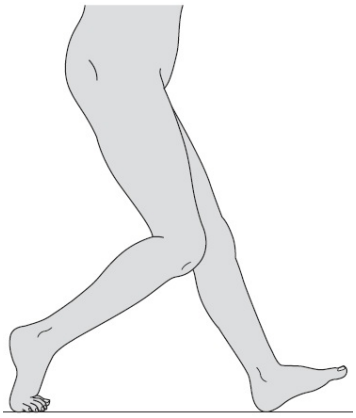

Figure 2.6: Excessive Knee Flexion (Whittle, 2007)

Abnormal foot contact is also a pathological gait very important to the development of an orthosis, because the orthosis performance depends on the movement of the dorsiflexion that is able to unlock the orthosis (e.g. *Becker UTX*). There exits three types of origins for abnormal foot contact: *talipes calcaneus*, *talipes equinus* and *talipes equinovarus*, as it is shown in Figures 2.7a, 2.7b, and 2.7c, respectively. The *talipes calcaneus* reduces the time of stance phase in that foot, therefore causes an asymmetrical gait. If a person has *talipes equinus*, the first contact between the foot and the ground is the entire foot or the metatarsal instead of the heel, this causes a problem to the orthosis that is activated by the foot sensors. With the *talipes equinovarus* the weight is supported by the outside of the foot.

(a) *Talipes calcaneus* (b) *Talipes equinus* (c) *Talipes equinovarus*

Figure 2.7: Abnormal foot contact (Dorland, 2007)

Abnormal foot rotation consists of the rotation of the foot during the swing phase, this pathology can cause a disturbance in the readings of the typical knee sensors, such as gyroscopes or accelerometers.

It must be noticed that there is also others diseases that affects children and causes a pathological gait, namely:

- *Metatarsus varus*: Adduction of the forefoot
- *Genu varum*: Leg bowing
- *Blount's disease*: Growth disorder of the shank or tibia
- *Developmental Dysplasia of the Hip* (DDH): The femur is not attached firmly to the hip

2.3 Experimental Studies of the Human Gait

In order to complement the information of the human gait given in the subchapters 2.1 and 2.2 it is necessary to add experimental studies of the human gait. A person with a non pathological gait, as the one shown in Figure 2.8, it is possible to see the different leg positions during the gait.

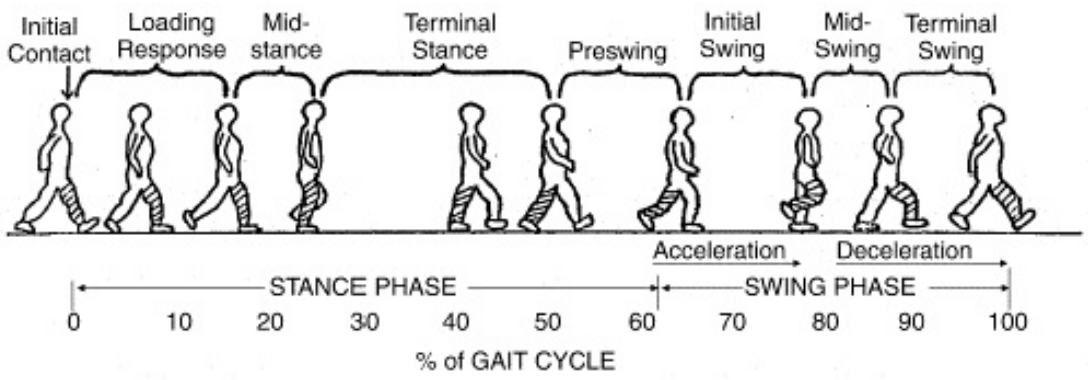

Figure 2.8: Non pathological gait (NCBI, 2012)

The evolution of the knee angle can be defined as it is illustrated in the Figure 2.9, the grey curve demonstrates the normal pattern while the green curve shows the experimental study made by Whittle (2007). In this case, both gates are very similar only with small differences, the experimental gait (green trace) is shorter than the normal pattern, the maximum flex angle in the stance phase is smaller than the normal pattern, and it has a hyperextension of the knee from the IC to the loading response.

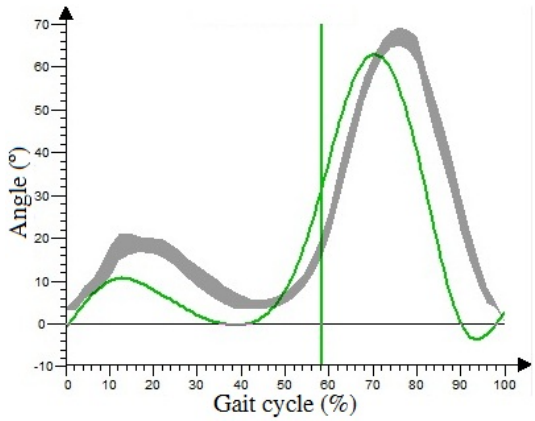

Figure 2.9: Knee angle on normal gait (Whittle, 2007)

In a normal gait, when the initial contact occurs the knee is fully-extended. During the loading response and mid-stance there is a small flexion of the knee. After the mid-stance (approximately at 40% of the gait cycle) the knee is extended once again until the heel rising. With the heel rising, the knee follows that movement and compensates by flexing the knee. During the swing phase (from 48% until 90% of the gait cycle) the knee stays flexed, extending only to repeat the initial contact once again.

The movement of the ankle, this experimental case is very similar to the normal pattern (see Figure 2.10a). The hip has the same behaviour comparing to the normal pattern but with a negative difference of 10° in the first 50% of the gait cycle (Figure 2.10b).

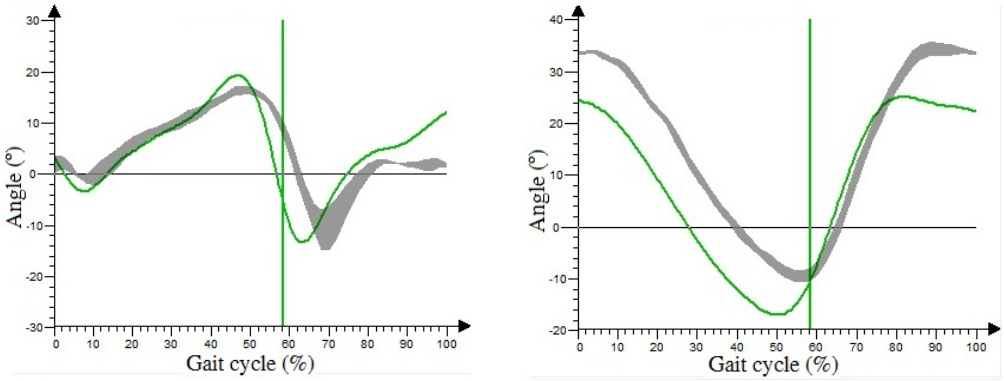

(a) Ankle (b) Hip

Figure 2.10: Ankle and hip angle on normal gait (Whittle, 2007)

Figure 2.11 shows a pathological gait called crouch gait. This particular gait is defined by an excessive knee and hip flexion in swing and stance phase. The crouch gait is one of the effects caused by cerebral palsy.

Figure 2.11: Crouch gait (Whittle, 2007)

The angle of the knee (see Figure 2.12) with crouch gait is almost constant comparing with the normal gait. The minimum value is approximately 62°, while the maximum value is nearly 80°, this clearly shows the over flexing of the knee. At the beginning of the stance phase or initial contact, the knee angle is 62°, rapidly rises to 70° during the loading response and keep rising (more slowly) up to 78° at the mid-swing when the feet are adjacent, then drops again to the initial value during the mid-swing and terminal swing.

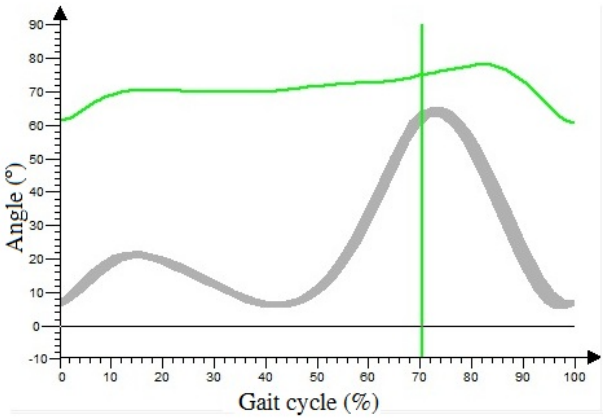

Figure 2.12: Knee angle with crouch gait (Whittle, 2007)

The ankle movement of the crouch gait (see Figure 2.13a) has the same behaviour of the ankle in the normal gait, but has a difference: the ankle is over flexed in the pathological gait. The hip (see Figure 2.13b) has also a similar behaviour to the normal gait, as result of increased stance phase, the pathological swing phase presents a lag in relation to the normal gait (Whittle, 2007).

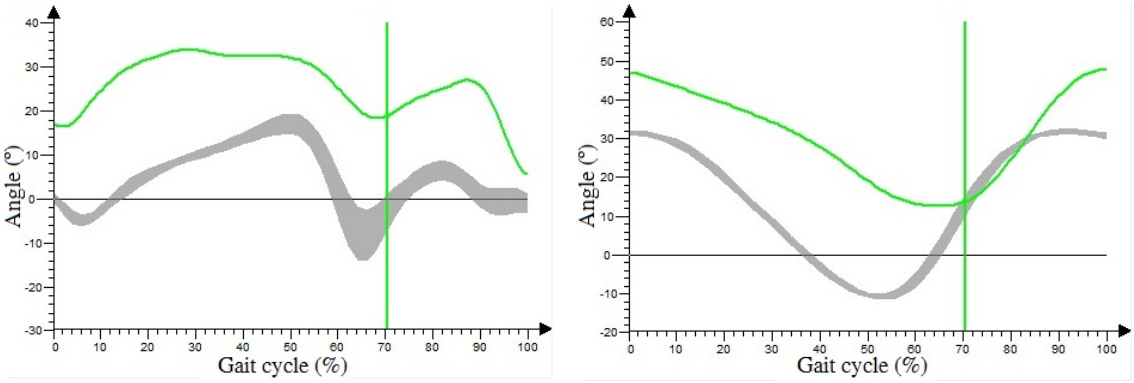

(a) Ankle (b) Hip

Figure 2.13: Ankle and hip angle with crouch gait (Whittle, 2007)

Equinus gait is another pathological gait caused by cerebral palsy. In this situation the person is unable to control the dorsiflexion of the foot, placing only the toes and the metatarsal heads on the ground. Figure 2.14 shows a child with equinus gait, specifically in two instants: Initial contact (see Figure 2.14a) and Opposite toe off (see Figure 2.14a). It is possible to observe that when the right foot (or pink leg) of the person touches the ground can not endure the weight of the body forcing a leg sliding to the outside.

(a) Initial contact (b) Opposite toe off

Figure 2.14: Equinus gait (Whittle, 2007)

The dynamics analysis (see Figures 2.15 and 2.16) shows that the ankle is always extended which will lead to a disturbance in the rest of the lower limb. In the knee the behaviour is almost the same with the exception of the terminal swing, the behaviour of the child's foot requires this movement of the knee to compensate the incapability of dorsiflexion, so the child overflex the knee (Whittle, 2007).

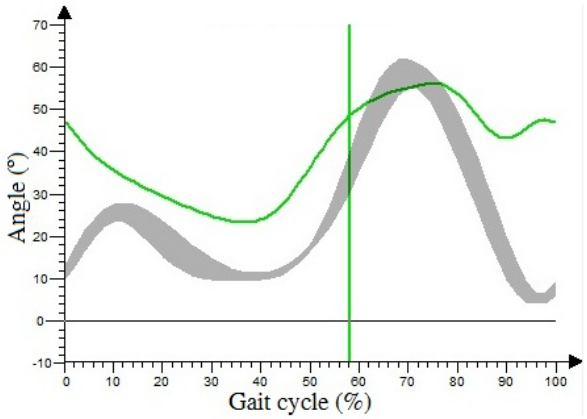

Figure 2.15: Knee angle with equinus gait (Whittle, 2007)

Figure 2.16a shows the child's inability of dorsiflexion in which, the angle is always bellow 0° in the entire gait cycle and the maximum value read was -23°, which is less than the minimum value in the natural gait (-14°). The hip (see Figure 2.16b), has exactly the same behaviour of a non pathological gait with a over flexion of approximately 25° during the entire gait.

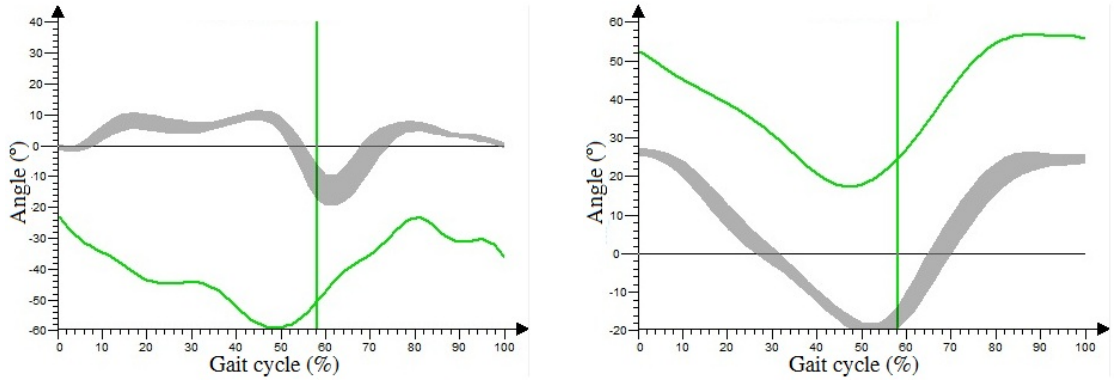

(a) Ankle (b) Hip

Figure 2.16: Ankle and hip angle with equinus gait (Whittle, 2007)

The stiff knee is another pathological gait caused by cerebral palsy. In this abnormal gait, the knee is the most affected articulation of the lower limbs. Comparing with the normal gait, the ankle and the hip stay the same. As visible in the Figure 2.17, the angle of the knee in the swing phase is much smaller than in the natural gait, the maximum angle is even smaller than the knee in the stance phase. This shows the incapability of controlling the knee flexors. The gait behaviour is the same of the Figure 2.6 (circumduction).

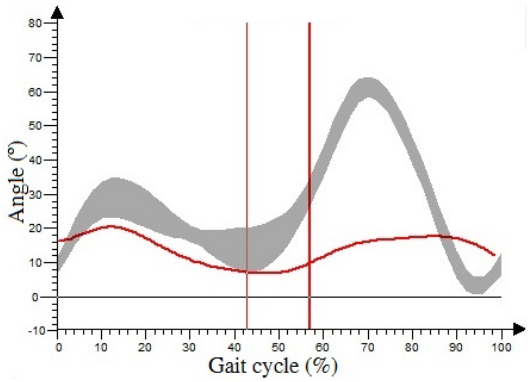

Figure 2.17: Knee angle with stiff knee gait (Whittle, 2007)

2.4 Chapter Summary

In this chapter a lower limb description was presented and the pathologies that affects them were also described. The human gait includes two main phases: stance phase and swing phase. In turn, these two phase can be subdivided into seven parts, these parts are devided by seven movements that defines the end of one part and sets the beginning of the next. The gait cycle times through the different ages and genders was also discussed.

The three main type of diseases were discussed. A list of the central neurological diseases, peripheral neurological diseases and muscular diseases were made, also can be found how these diseases affects the human gait.

Experimental studies performed by some authors were discussed in this chapter with a comparison to the normal pattern and to the theoretical data. These studies include the results of some diseases in the articulations and how it is possible to identify the diseases at naked eye according to the gait.

Chapter 3

Preliminary study of the locking mechanism

3.1 Problem description

The main goals when designing a functional SCKAFO are: allowing knee flexion during the swing phase and immobilizing it during the stance phase. According to Moreira et al. (2011) and Yakimovich et al. (2006b) a SCKAFO must accomplish several requirements in addition to the main goals:

- To switching between phases in less than 6ms;
- To switch from lock to unlock without requiring a fully-extended knee;
- To be silent or at least the most quiet possible;
- To allow knee extension at anytime and knee flexion movement up to 110° in order to allow the user to climb stairs and sit;
- To be as light as possible, preferably with a weight less than 2kg;
- In cosmetic terms, the orthosis should be discrete and should be appealing to the user, this reduces the chances of late rejection;
- The knee joint mechanism should not have more than 2cm of thickness;
- The orthosis should resist to a moment of 77Nm (90kg user);
- Resist to fatigue and have a mean-time of six months between the maintenance.

In resume the orthosis should be light, noiseless, durable and with a fast reaction time.

The knee joint mechanism should be produced from a material of high hardness that allows to withstand the forces to which the mechanism is subjected. This type of mechanism is made of metallic materials, such as steel. Usually these type of mechanisms are made from steel with treatment to increase the hardness and also the corrosion resistance. The steel increases the weight of the mechanism but has a better strenght/weight ratio compared to the aluminium or other common metal.

The thickness of the mechanism should as small as possible. The companies that produce electro-mechanical orthosis are leaving this part to second plan due to the emphasis given to the reliability of the locking system. The size is compromised, but by ignoring it the companies ensure that the orthosis has a strong locking mechanism capable of support the patients weight.

3.2 Material

The metal selected for the manufacturing and tests was the *Stainless Steel - Grade 304*, which is an inexpensive and widely used metal. According to AZoM (2012), eFunda (2012), and ASM (2012) the Stainless steel 304 is composed as described in Table 3.1.

Table 3.1: Stainless Steel 304 composition

Weight (%)	C	Mn	Si	P	S	Cr	Mo	Ni	N
min	-	-	-	-	-	18.0	-	8.0	-
max	0.08	2.0	0.75	0.045	0.030	20.0	-	10.5	0.1

In general, metals can also be defined according to others characteristics, such as mechanical, physical and thermal characteristics. Density and yield strength are two of those properties. The values of their properties are used, not only to better understand this metal, but also to perform computational simulations in *Autodesk Inventor*. According to AZoM (2012), eFunda (2012), and ASM (2012) the Stainless steel 304 characteristics are as listed in Table 3.2.

Table 3.2: Stainless Steel 304 characteristics

Property	Value
Ultimate Tensile Strength (MPa)	515 (minimum)
Yield Strength (MPa)	205 (minimum)
Poisson's Ratio	0.29
Density (kg/m^3)	8000
Elastic Modulus (GPa)	193
Thermal Expansion (mm/m/°C)	17.2
Thermal Conductivity (W/m.K)	16.2
Specific Heat (J/kg.K)	500

3.3 Mechanical Solutions

The mechanisms utilized in the orthosis considered in this work can have different configurations and geometries. The first objective of this work was to study different mechanisms to create a basis for comparison between them in order to be able to select the most adequate solution.

Figure 3.1: Ratchet/Pawl mechanism

Thus, the first presented mechanism consists of a two parts, namely a ratchet and a pawl as Figure 3.1 shows. This mechanism can lock the orthosis at any angle, eliminating the need to fully extend the knee. In the transition from stance phase to swing phase, a motor with small dimensions pulls the pawl away from the ratchet allowing to the user flex the knee (see Figure 3.2a). In the sub-phase initial swing the knee reaches the maximum flexion moment, and at this instant the motor releases the pawl back into the ratchet allowing the extension movement and blocking the flexion movement (see Figure 3.2b). The pawl should bs assisted by a spring that accelerates the locking movement and does not allow for the pawl move away from the ratchet while is in the locked position.

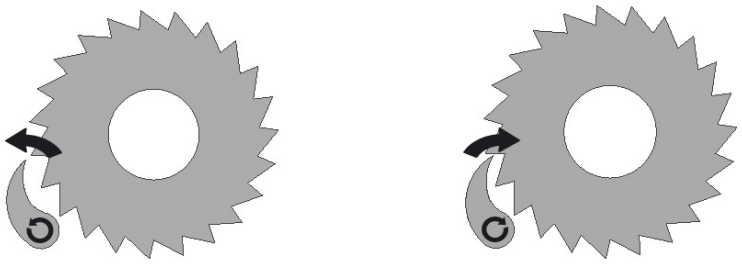

(a) Unlocked (b) Locked

Figure 3.2: Ratchet/Pawl mechanism positions

The main dimensions of this mechanism are presented in the Figure 3.3. The diameter of the ratchet is less than 30 mm, and has a hole of 10 mm for the main shaft, that connects the lower part of the orthosis to the upper part. The thickness of the ratchet is equal to 10 mm, which leaves 10 mm to the housing and other parts in order to follow the requirements advised by Moreira et al. (2011) and Yakimovich et al. (2006a). The outer diameter can be smaller, but a smaller mechanism will have less resistance to the applied moments to the mechanism during operation. A compromise between size and strength should be taken in account.

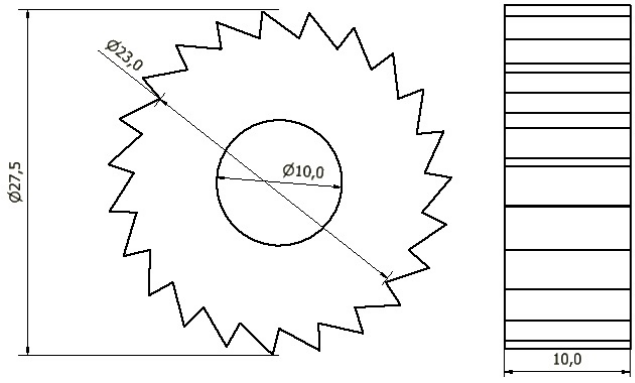

Figure 3.3: Ratchet dimensions

The pawl (see appendix A) has a height of 10 mm and a minimum thickness of 10 mm. At the center of rotation of the pawl a motor shaft is connect, in the drawing is defined with 10 mm in length and with a diameter of 2 mm. This values may vary according to the chosen motor, for instance, a Radio Control Servo (RC Servo) can not be connect directly to the pawl because is too long. In this case the motor is differently located and it is necessary a small mechanism to transmit the movement of the motor.

In order to perform the computational simulation, it is first necessary to know the value of the load to apply on the mechanism parts. For this purpose, the material properties of the stainless steel grade 304 presented in Table 3.2 were used. According to Yakimovich et al. (2006a), the mechanism has to support a moment of 77 Nm, which represents a 90 kg orthosis user climbing stairs. In order to know the pressure, it necessary to convert the moment created by the user to pressure (MPa), according to Hall et al. (1999), moment is given by equation 3.1:

$$M = F.d \tag{3.1}$$

F represents the applied force to the object and d is the distance to the center. In this case is the radius of the mechanism. The values of M (77 Nm) and d (or r) (13.75 mm) are known. Thus, the equation 3.1 yields:

$$\begin{aligned} F &= \frac{M}{d} \\ &= \frac{M}{r} \\ &= \frac{77}{0.01375} \\ &= 5600\ N \end{aligned} \tag{3.2}$$

Then, the pressure can be calculated as:

$$p = \frac{F}{A} \tag{3.3}$$

Where A represents the area where the force is applied. By checking the mechanism dimensions the pressure applied to the mechanism is given by:

$$\begin{aligned} p &= \frac{5600}{10x2.2} \\ &= 254.5\ MPa \end{aligned}$$

The obtained results of the stress simulation using the *Autodesk Inventor* software applying to the mechanism a moment of 77 Nm are illustrated in Figure 3.4.

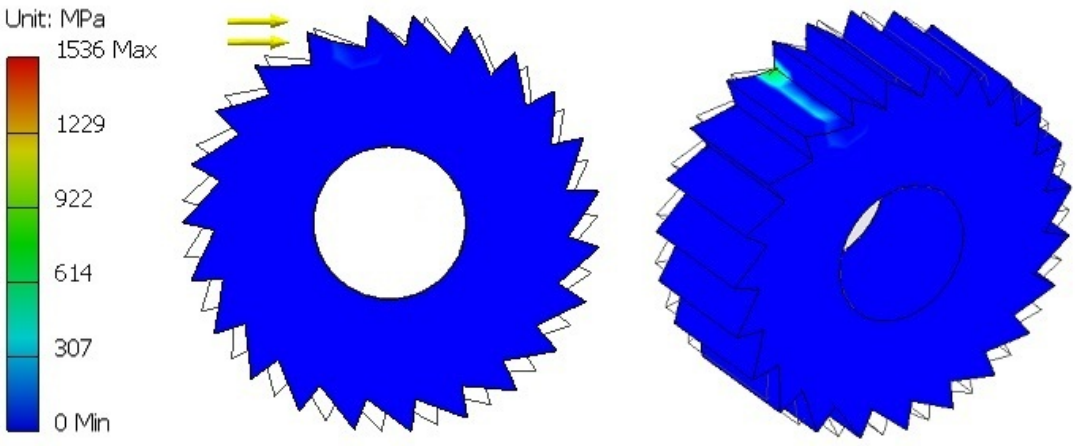

Figure 3.4: Ratchet - stress distribution

The results show that this mechanism is unsuitable for the present purpose. The maximum Von Mises Stress of 1536 MPa that occurs in this mechanism is greater than the yield strength of the stainless steel 304 (see Table 3.1). Thus, there are two possibilities to overcome this difficulty namely, changing the material to a metal with a higher yield strength or changing the geometry of the mechanism in order to endure the pressure applied. The first alternative will result in a increased costs due manufacturing and material costs. Therefore, the simplest way is to change the mechanism. The summary of the stress analysis can be found in appendix A.

Figure 3.5 shows the alternative mechanism. This mechanism is the first solution to the previous problem, with larger bumps this mechanism should endure the pressure that will be submitted. This mechanism works with the same principle and it has the disadvantage of not locking so fast as the previous mechanism because the distance between the bumps is bigger. For this mechanism the pawl is also different, two different versions of which were considered, a normal pawl and a double pawl as shown in Figure 3.6. The double pawl was created to distribute the pressure applied in the mechanism.

Figure 3.5: Ratchet 2 mechanism

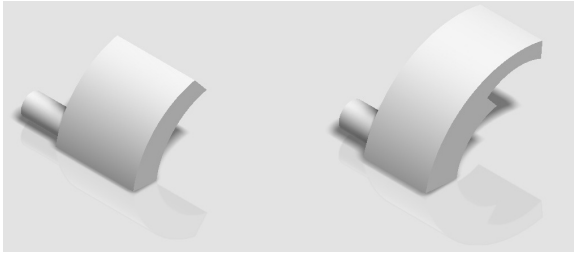

Figure 3.6: Pawl 2 and 3

As previously mentioned, the general dimensions of this mechanism is slightly higher comparing to the mechanism present in Figure 3.1, as shown in the Figure 3.7 and appendix B.

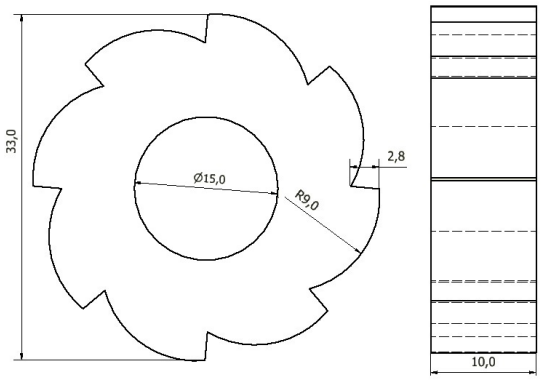

Figure 3.7: Ratchet 2 dimensions

Using now the dimensions of the Figure 3.7 and applying them to the equations (3.2) and (3.3), the results obtained are the follow:

$$F = 4667\,N$$
$$p = 166,7\,MPa$$

The computational results of the stress simulation, when a moment of 77 Nm is applied are shown in Figure 3.8. This simulation was made with the normal pawl, the force is applied only in one place (bump). The maximum Von Mises Stress is 281.7 MPa, a much smaller value than the one obtained in the previous mechanism (see Figure 3.4).

This mechanism made of stainless steel 304 should be strong enough because the value of 205 MPa is the minimum value for the yield strength and typically stainless steel 304 yield strength is 290 MPa or 300 MPa, also the value of 77 Nm is a peak value and not a continuous value.

Using the double pawl the stress values are lower. The pressure applied to the mechanism divides into to two pressures of 83.35 MPa each, as it is shown in Figure 3.9. With the double pawl the security of the mechanism is ensured, the maximum Von Mises Stress of 188.4 MPa applied to the mechanism is inferior to the minimum yield strength of the stainless steel. The result summary can be found in appendix B.

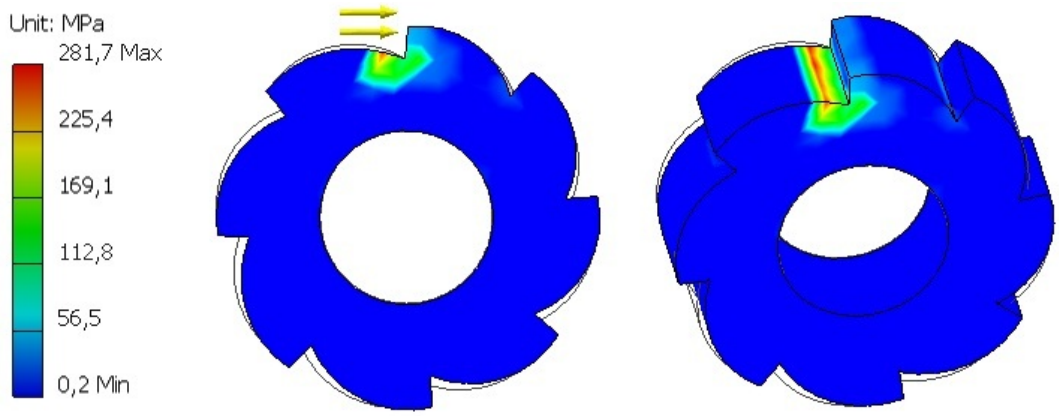

Figure 3.8: Ratchet 2 - stress distribution

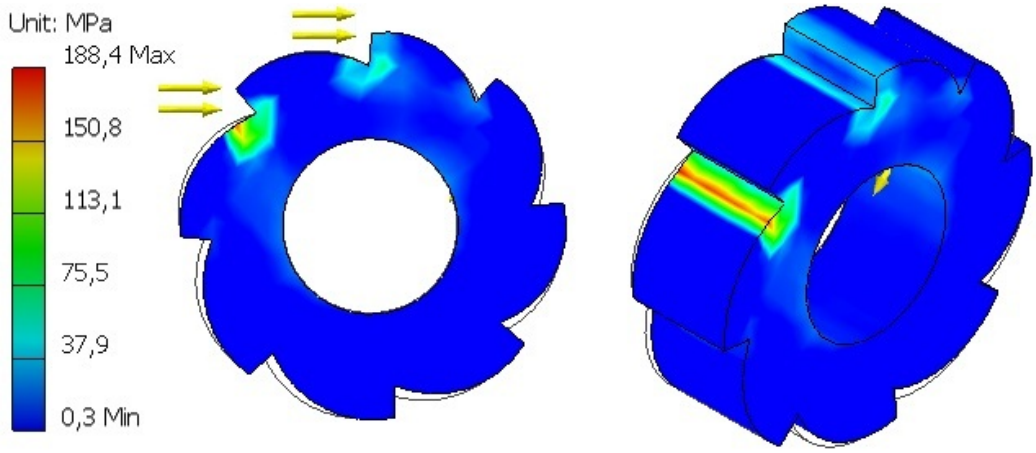

Figure 3.9: Ratchet 2 with double pawl - Stress distribution

It is necessary to know the shear stress of this mechanism to better design the desired solution. Thus, according to Hibbeler (2010) the average shear stress can be determined by:

$$\tau = \frac{V}{A} \tag{3.4}$$

When V represents the internal resultant shear force on the transverse section and A is the section. In this case V is equal to F because there is only one force perpendicular to the section.

Figure 3.10 shows the length of the section the width of the section is the same of the mechanism, 10 mm. The Force applied to this mechanism are: 4667 N with the normal pawl and 2333.5 N with the double pawl.

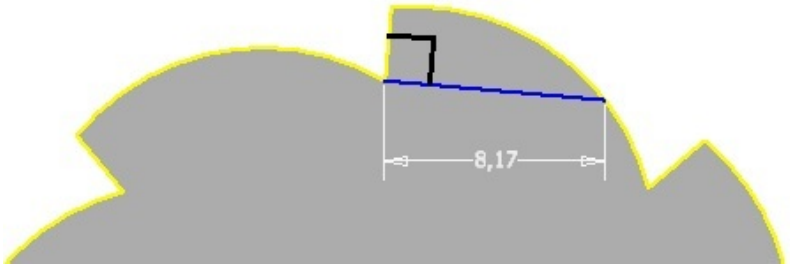

Figure 3.10: Ratchet 2 - Transverse section

Using the single pawl, the shear stress is given by:

$$\begin{aligned} \tau &= \frac{4667}{8.17x10} \\ &= 57.1\ Mpa \end{aligned}$$

Using the double pawl, the pressure is applied in two places, so the shear stress is calculated as:

$$\begin{aligned} \tau &= \frac{2333.5}{8.17 * 10} \\ &= 28.6\ Mpa \end{aligned}$$

It can be observed that for this case, the values are below the yield strength of the stainless steel 304, therefore ensures a good behaviour in terms of mechanical resistance.

It is also necessary to submit the pawls to the stress analysis in order to check if the they are suitable to the purpose. The normal pawl was subjected to a pressure of 166.7 MPa. The results are shown in the Figure 3.11 and appendix B.

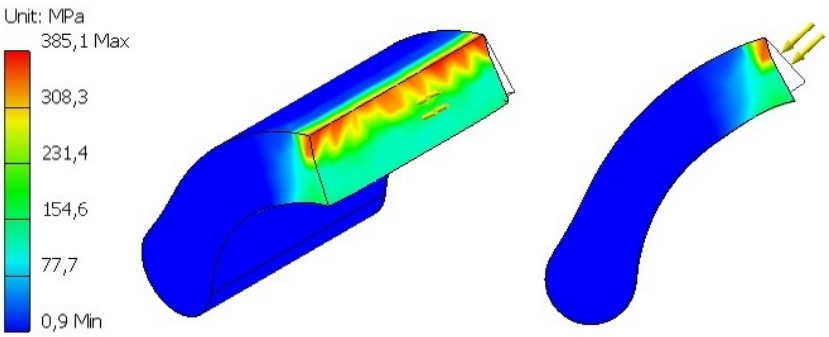

Figure 3.11: Pawl 2 - Stress distribution

As it is shown in Figure 3.11, this pawl it is not suitable when using the stainless steel 304. One alternative solution is change to the double pawl or use another material (e.g. Stainless Seel - Grade 440C). The adopted alternative for this case is to change to the double pawl, thereby the pressure is applied in two parts of the pawl. Figure 3.12 shows the results of applying two pressures of 83.35 MPa each, the maximum Von Mises Stress is 172.7 MPa, a value below from the yield strenght of stainless steel 304. This ensures that this pawl made of stainless steel 304 will work without yielding when a moment of 77 Nm was applied. The result summary can be found in appendix B.

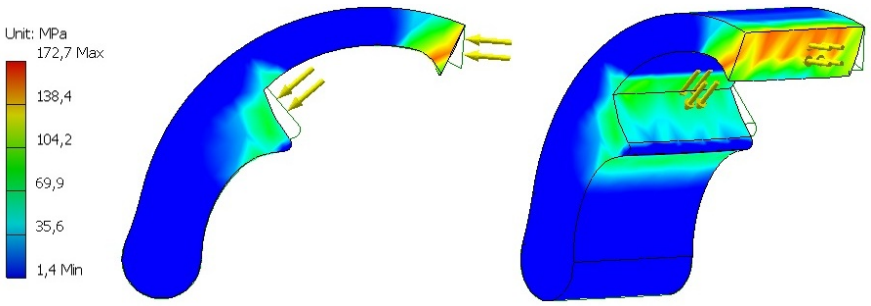

Figure 3.12: Pawl 3 - Stress distribution

The housing of these mechanisms (see Figures 3.1 and 3.5) is presented in the Figure 3.13. The lighter gray part is the ratchet, the green part is the pawl and the orange part is the part that pulls the pawl into the ratchet, can be a spring or a cam.

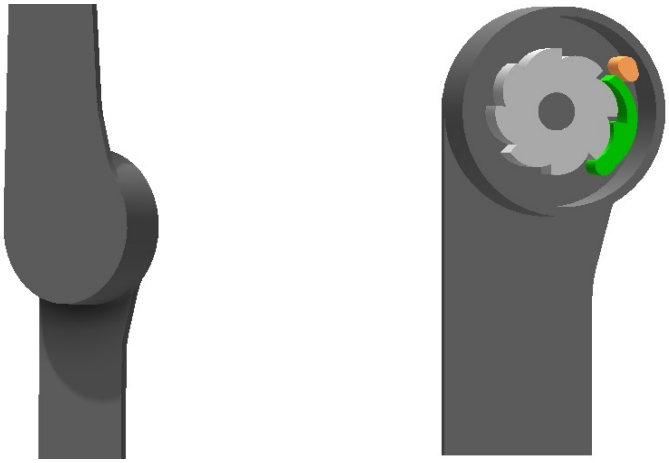

(a) Outside view (b) Inside view

Figure 3.13: Ratchet housing

Figure 3.14 shows another developed mechanism. Instead of a ratchet, this mechanism has eight slots with a circular shape.

The circular slots of the mechanism presented in Figure 3.14 allow an higher contact area between the parts of the mechanism, and as consequence supports higher pressures. The locking is made using only one slot, this reduces the weight of the pin.

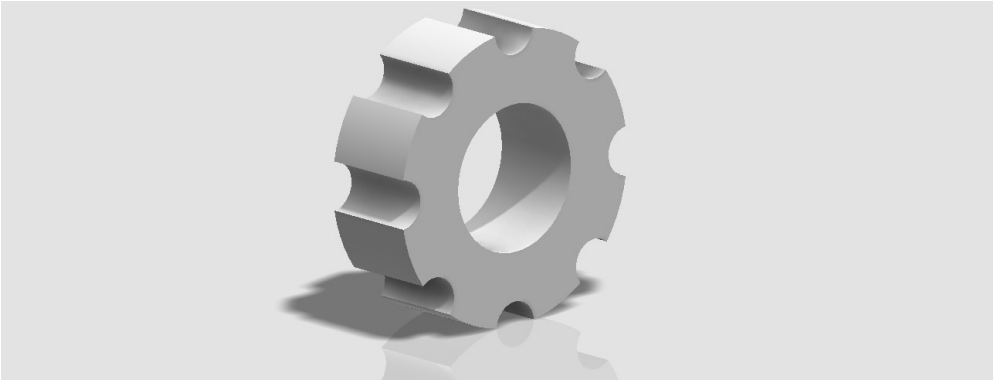

Figure 3.14: Slot mechanism

The general dimensions of this mechanism are shown in Figure 3.15 and in detail in appendix C. Using the dimensions of Figure 3.7 and applying them to equations (3.2) and (3.3), the contact force and the corresponding pressure are:

$$F = 5133.3\ N$$
$$p = 65.4\ MPa$$

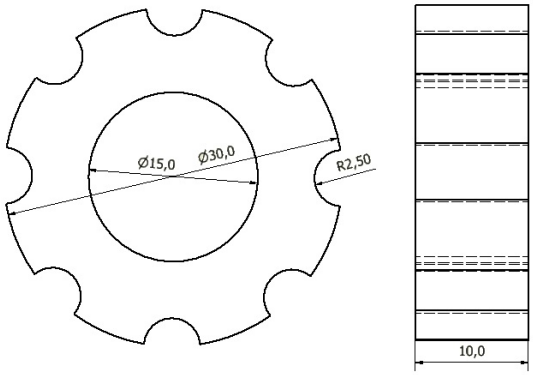

Figure 3.15: Slot mechanism dimensions

The results relative to the stress analysis are shown in Figure 3.16. The maximum Von Mises Stress is 129.6 MPa, a inferior value comparing to the yield strength of the saintless steel 304. The result summary can be found in appendix C.

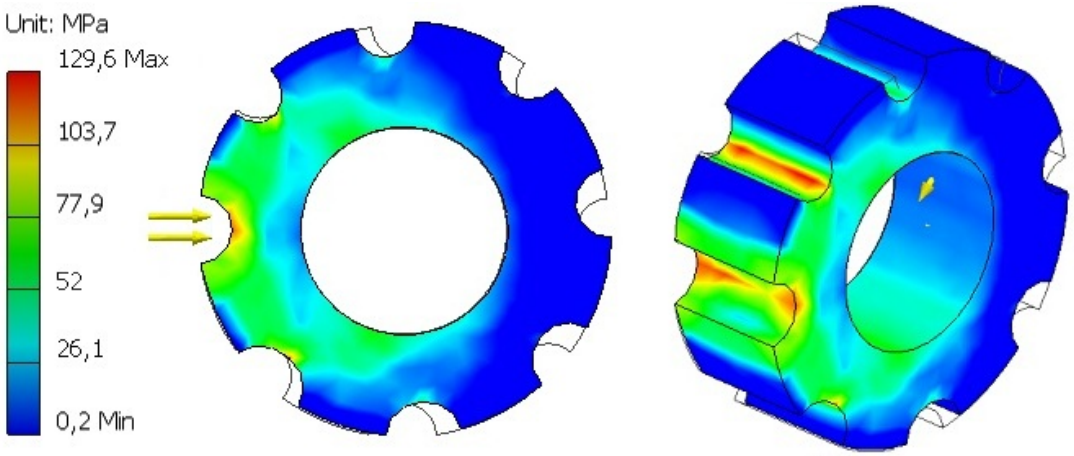

Figure 3.16: Slot mechanism - Stress distribution

Figure 3.16 shows that the critical spots of this mechanism are the innermost part of the slots. While the slot where the pawl is inserted (yellow arrows) tends to fracture, the upper slot is compressed due to the applied moment.

The shape of pawl allows for an easier locking and unlocking of the mechanism. Due to the shape of the mechanism, it has the disadvantage of not allowing auto-lock when the pawl is pushed away from the mechanism. When a slot is found, the stays locked to both ways (flexion and extention). In short, this solution is more stronger with an easier transition between phases but needs a faster actuator in order to quickly lock and unlock.

Applying 65.4 MPa to the pawl, the results (see Figure 3.17 and appendix C) show that this pawl is suitable to be part of the locking mechanism. The only critical spots (red color) are the lower corners of the mechanism, removing the corners using fillets will result in a higher Von Mises Stress.

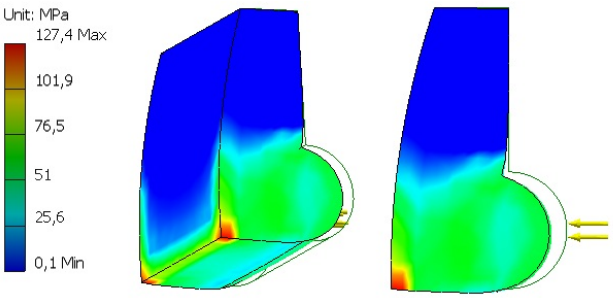

Figure 3.17: Pawl 3 - Stress distribution

The result of the assembling of the different parts (excluding the actuator) is illustrated in Figure 3.18.

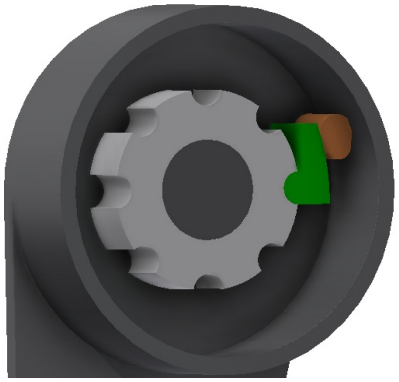

Figure 3.18: Assembly with slot mechanism

In order to reduce the manufacture costs, a generic mechanism that can be easily modified was considered. The parts of this mechanism were designed with a thickness of 2 mm. In the Figure 3.19 the mechanism is shown.

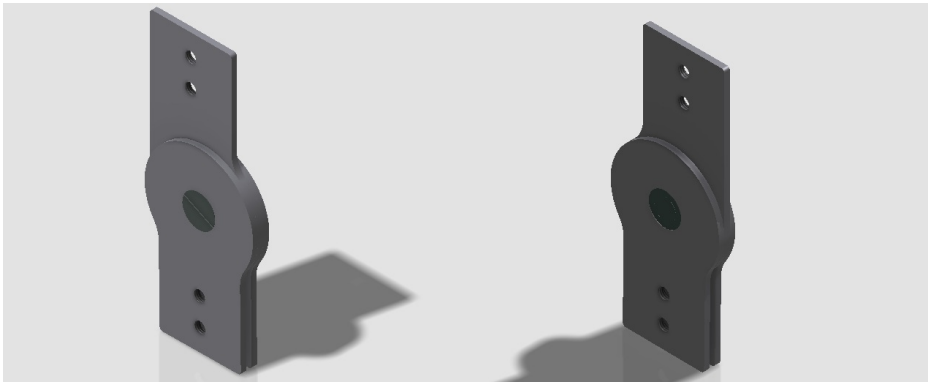

Figure 3.19: Generic mechanism

This mechanism was not created intending to endure real tests with patients. The purpose of this mechanism is to have a laboratorial prototype. Figure 3.20 shows the different models of this mechanism. The first mechanism (named v1) has a traditional locking system, it is necessary to have the knee fully extended in order to lock, only has one locking position. The second mechanism (named v2) is similar to the first but has two locking positions, which removes the need to be necessary to fully extend the knee and allows a small flexion when the foot touch the ground. The third mechanism (named v3) is similar to the mechanism presented in Figure 3.14, it has several locking positions, this mechanism allows to study the behaviour of a mechanism that has several locking positions. The last mechanism (named v4) allows the extending movement while blocking the flexion movement.

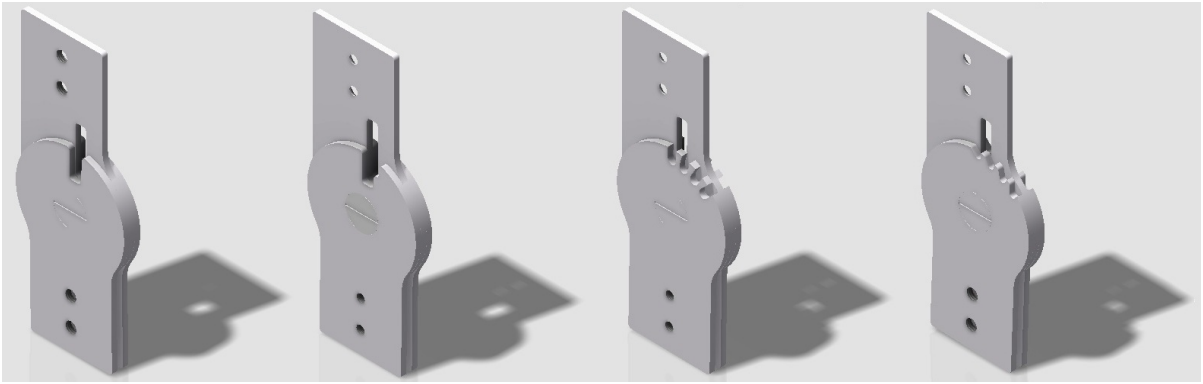

Figure 3.20: Generic mechanism - different models

The general dimensions of the mechanisms are shown in Figure 3.21. The dimensions of the different models can be found in the appendix D. Comparing with other mechanisms, this mechanism has a smaller thickness. The holes in the top and bottom are to attach the mechanism to the rest of the orthosis.

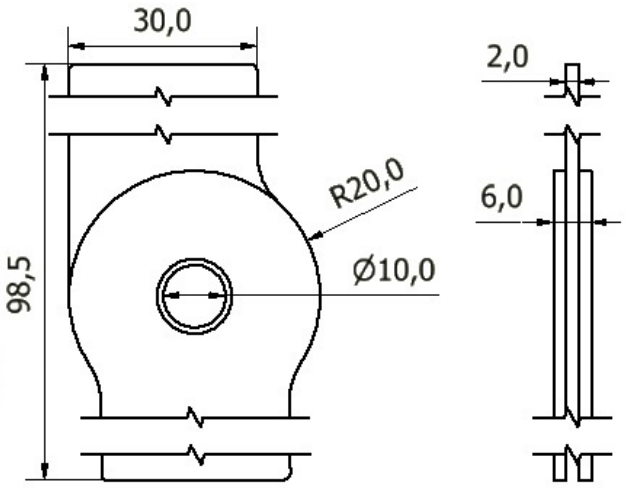

Figure 3.21: Generic mechanism dimensions

In order to simplify the tests, the mechanisms were divided in two parts, the upper part and the lower part. The upper part is common to all mechanisms, so only one test will be performed. The stress analysis of the upper part can not be known by applying a moment on the mechanism because it will subjected to a force on the pin slot and not to a moment produced by the user, in this case it is needed to calculate the pressure that will be applied to this part. The pin dimensions are: 3 mm Length (L) x 6 mm Width (W) x 5 mm Height (H). The area subjected to the force will be: 2 mm x 5 mm.

Using the dimensions of Figure 3.21 and applying them to equations (3.2) and (3.3), the values obtained are:

$$F = 6416.7\ N$$
$$p = 641.7\ MPa$$

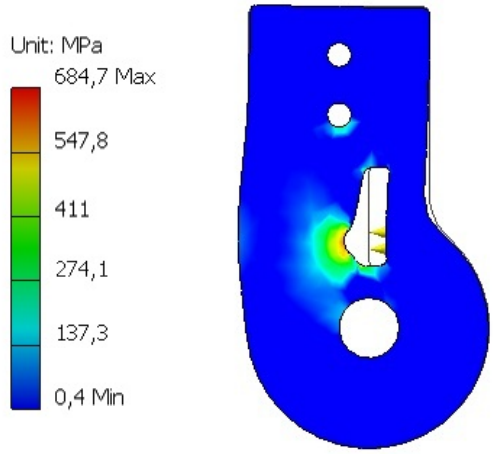

Figure 3.22: Generic upper part - Stress distribution

Figure 3.22 shows that this mechanism is not appropriate to actual use with patients, due to its small dimensions the mechanism it is subjected to very high pressures. The stress analysis of the lower part can be known by applying a moment of 77 Nm.

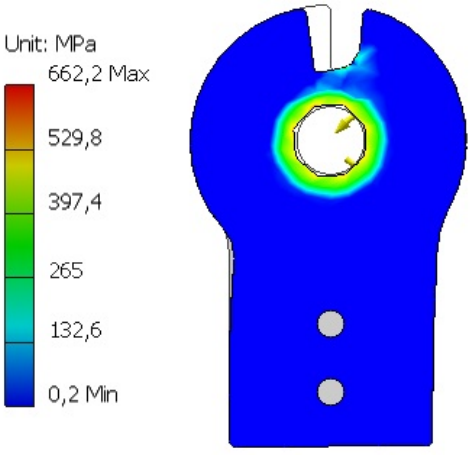

Figure 3.23: Generic lower part v1 - Stress distribution

Figure 3.23 shows a stress analysis result. This version is subjected to a maximum stress of 662.2 MPa, a value well above of the yield strength of the stainless steel 304. In this mechanism it is possible to observe that the slot widens due to the moment applied. If a moment of 77Nm is applied to the mechanism, it will rupture through the slot down to the shaft of the mechanism.

The second mechanism (see Figure 3.24) has two locking positions, position one and two. In position one the pin stays in the lower position. In position 2 the mechanism stays in the upper part, in this position the mechanism does not need the fully extension of the knee.

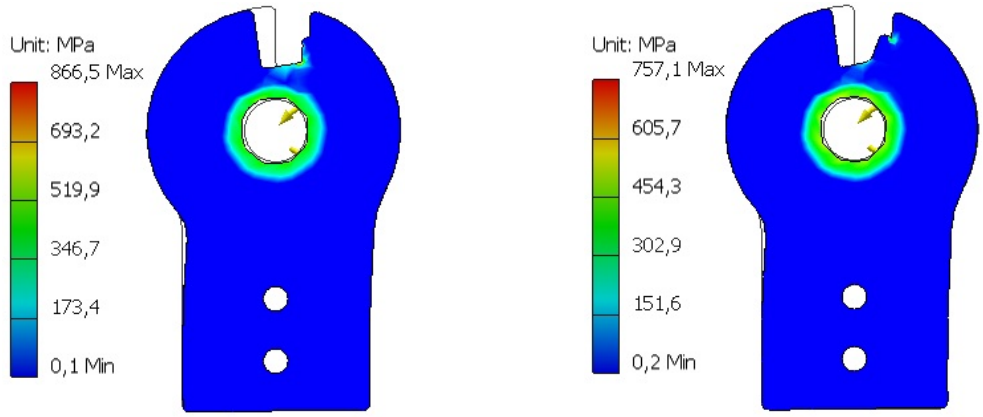

(a) Pin in position one

(b) Pin in position two

Figure 3.24: Generic lower part v2 - Stress distribution

In the position one (see Figure 3.24a) it can be observed that the maximum Von Mises Stress is 866.5 MPa while in position two (Figure 3.24b) is 757.1 MPa. From this test it is possible to know the most critical positions and it is also possible to compare the results with the mechanism with only one locking position. The v2 mechanism has a Von Mises Stress higher 31% to the most critical position and 14% to the less critical. It is a significative difference between the two versions.

The Figure 3.25 is composed by last two mechanisms, this mechanisms have several locking positions. The v3 mechanism (see Figure 3.25a) is composed by rounded slots while the v4 mechanism (see Figure 3.25b) has locking positions shaped as curved teeth.

These mechanisms have a much higher Von Mises Stress comparing to the v1. Instead of 662.2 MPa (v1) the values are 1461 MPa (v3) and 2847 MPa (v4), two and four times higher than the v1, respectively.

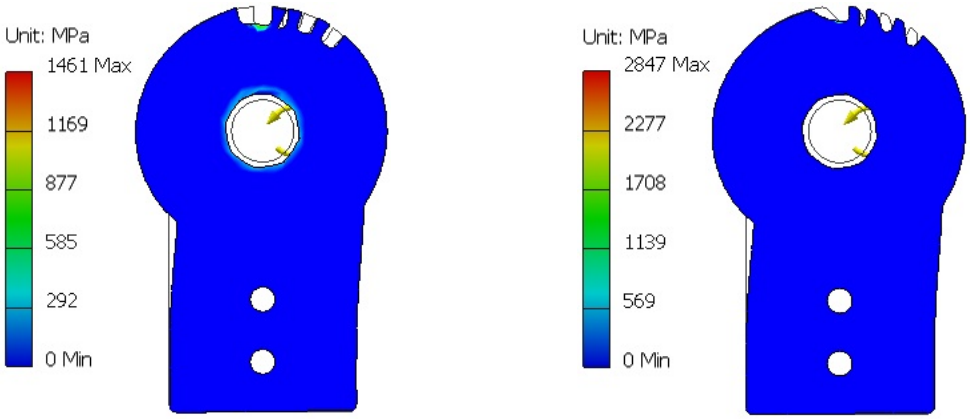

(a) Generic lower part v3 (b) Generic lower part v4

Figure 3.25: Stress distribution

Figure 3.25 shows that both mechanisms lose the shape when applied a moment of 77 Nm. Mechanisms with such shape may be easily damaged, showing that despite having several locking positions the mechanisms are more fragile.

The pin to these four mechanisms is the same, the dimensions of the pin are 3 mm (L) x 6 mm (W) x 5 mm (H). The stress simulation of the pin is presented in Figure 3.26. The simulation shows that this pin made of stainless steel 304 will not support the pressure applied to the mechanism. The area where the pressure is applied made by two parts, so the area has to be multiplied by two, the pressure applied to the mechanism is given by:

$$\begin{aligned} F &= 6416.7\ N \\ p &= \frac{6416.7}{2(2x5)} \\ &= 320.8\ MPa \end{aligned}$$

In the pin case the shear stress will be double shear stress because the pressure is applied by two elements and not only one. The double shear stress is given as:

$$\begin{aligned} \tau &= \frac{V}{2A} \\ &= \frac{6416.7}{2(3x5)} \\ &= 213.9\ MPa \end{aligned} \tag{3.5}$$

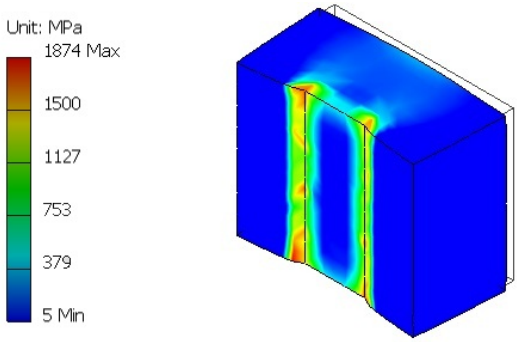

Figure 3.26: Locking pin

As shown previously the shear stress is inferior comparing to the maximum Von Mises Stress, the moment of 77 Nm is a very high value that forces the mechanisms to work above the calculated shear stress.

The traditional mechanisms presented in older orthosis (e.g. KAFOs) are similar to the mechanism presented in Figure 3.27. Composed by three parts, two for the main mechanism and the pin that locks the orthosis, these mechanisms were not made to lock and unlock during one gait cycle. They are made to stay locked during the entire gait. The locking is done manually by the user. This mechanism also has a bump which prevents the overextension of the knee.

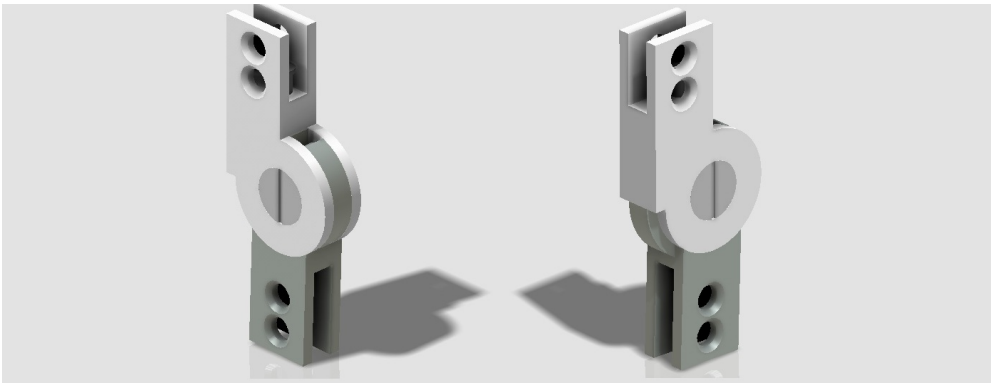

Figure 3.27: Tradicional mechanism

The computational stress simulation analysis is presented in Figure 3.28. The behaviour is similar to the other mechanisms, the critical spots are located on the same place. Usually the traditional mechanism is made of other metals, with higher yield strength. Normally the mechanisms are subjected to treatments in order to harden. The size of this mechanism is similar to que previous mechanism, has a height of 70 mm, shaft has 10 mm of diameter and the outer diameter has 25 mm.

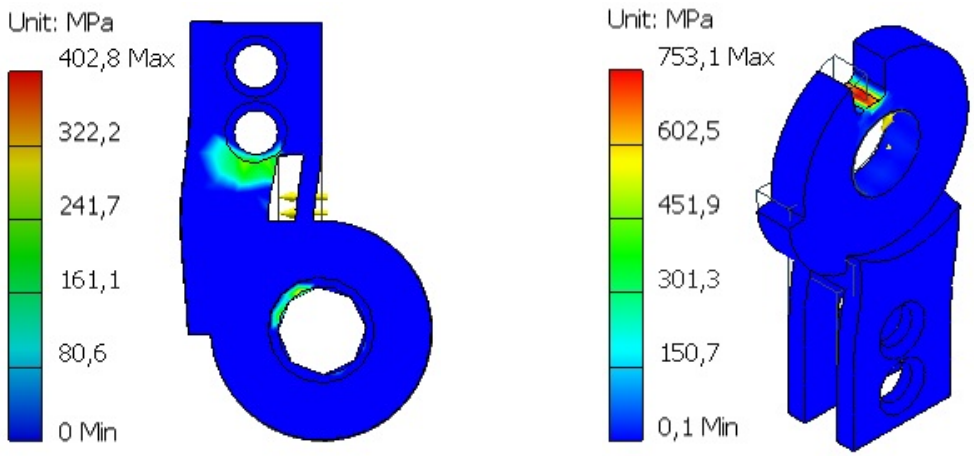

(a) Upper part (b) Lower part

Figure 3.28: Traditional mechanism - Stress distribution

3.4 Chapter Summary

In this chapter a problem description of the project was presented. All the goals and requirements that is needed to accomplish are also described in this chapter. The requirements can be aesthetically, can be associated with performance (velocity of locking and unlocking, knee extension requirement) dimensions, shape or strength.

The material of the mechanism was selected and characterized according to its composition and mechanical characteristics. The design of the mechanisms proved to be essential to the performance of the mechanism. A mechanism with more locking positions also has higher possibilities of failure. The stress simulations shown that because of the moment that acts on the mechanism (77 Nm), the pressures applied goes well beyond the theoretical shear stress. A mechanism with rounded slots can endure a higher moment but a mechanism with shaped-teeth slots allows the movement of extension while blocking the flexion movement. In this chapter a comparison between a mechanism with one locking position and two locking position was presented. A demonstration of a traditional mechanism performance is also shown.

Chapter 4

Preliminary study of the electronics

4.1 Sensors

The electronics is a very important and complex part of this project. The numerous existing sensors and actuators, each one with specific gamma and working principle require a weighted choice.

The models available in the market have limitations regarding their use. Each pathology create a very distinct gait pattern making it very difficult to create an orthosis capable to meet the different needs of each pathology. With electronics implementation in the system, it is expected to obtain a better monitoring of the gait cycle allowing to serve a wider range of pathologies with only one mechatronic system.

There are many types of measuring the human motion characteristics, to do so can be used devices such as accelerometers, gyroscopes, rotary encoders, among others. For this project it is necessary to choose sensors with low profile due to the dimensions limitations. Some devices combine several types of sensors in one Printed Circuit Board (PCB), being Inertial Measurement Unit (IMU) one of the devices. An IMU is a very good set of sensors to measure human motion, which is composed by an accelerometer and a gyroscope. The more expensive IMUs are also composed by magnometers and barometers. The less expensive IMUs are simply two sensors (sometimes of different companies) placed together, this will cause a problems when communicating with the sensors because each company defines communication for its sensors. The more expensive IMUs, usually made by companies that manufacture its own sensors, have an easier communication because they set a standard to all sensors and also the components are protected by a shell. IMUs have a couple of disadvantages namely, the range of used sensors are pre-defined, making it unsuitable for this project. For this project the dimensions are very important, so the dimensions of the PCB is essential.

Due to the good performance of IMU when measuring the human motion (Zhu and Zhou, 2004), it was decided to create a low-cost IMU with the required specifications. To be able to develop a good IMU it is necessary to make an exhaustive study of the currently available sensors about the range, output type, sensitivity, interface, mounting type, voltage supply and dimensions.

The sensors can be divided into two groups according to their output, (analog or digital). In analog accelerometers, the output is a variable voltage that depends on the measured value, while in digital sensors the output is made by digital communication, usually by Inter-Integrated Circuit (I^2C) or Serial Peripheral Interface (SPI).

Systems with analog sensors have an higher power consumption not only because of the sensors but using the analog channels of microcontrollers require more energy to work. Power consumption is a very important subject nowadays. For this project only was researched sensors with digital output due to low energy consumption.

There are many accelerometers manufacturers, for this project the first search was limited to the main stores that ship electronic material to Portugal, *Mouser Electronics* (www.mouser.com), *Digi-Key Corporation* (www.digikey.com), *RS* (www.pt.rs-online.com), and *Farnell* (www.farnell.com). The considered manufacturers are listed below:

- Analog Devices;
- Bosch Sensortec;
- Freescale;
- Kionix;
- STMicroelectronics;
- VTI Technologies.

In order to refine the search it was defined some pre-defined criteria namely, the acceleration range should be less than 2g, the output must be digital and the voltage supply must be between 3.3V and 5V because the microcontrollers operate within these values. Table 4.1 shows the sensors characteristics that meets these pre-defined criteria.

Table 4.1: Accelerometers - *Analog Devices*

Model		Axis	Accel. Range	Sensitivity	Voltage
ADIS16003	-	X,Y	1.7g	820 LSB/g	3V - 5.25V
ADIS16201	-	X,Y	1.7g	216.2 LSB/g	3V - 3.60V
ADXL312	-	X,Y,Z	1.5g - 12g	345LSB/g	2V - 3.60V

Table 4.2: Accelerometer - *Bosch Sensortec*

Model		Axis	Accel. Range	Sensitivity	Voltage
BMA180	-	X,Y,Z	1g - 16g	8192 LSB/g	1.62V - 3.6V

Table 4.2 shows that *Bosch Sensortec* only has one sensor that meets the requirements. In turn, the companies Freescale, Kionix and STMicroelectronics does not have sensors

that meet the specified requirements, these companies manufacture accelerometers with a range higher then 2g.

The company VTI Technologies such as Bosch only has one sensor that meets the pre-defined criteria, as it is shown in Table 4.3

Table 4.3: Accelerometers - *VTI Technologies*

Model		Axis	Accel. Range	Sensitivity	Voltage
SCA1000	-	X,Y	1.7g	1.2V/g	5V

Another similar sensor to the accelerometer is the inclinometer. Instead of linear accelerations an inclinometer measures the inclination of a object in relation to the earth gravity axis. The inclinometer has the advantage of having a higher immunity against other accelerations comparing to the accelerometer. In order to narrow the search were defined some requirements that an inclinometer for this project should have. The inclination range should be higher than 180° (negative and positive), which result in a total range of 360°, the output must be digital and the voltage supply must be between 3.3V and 5V. The considered manufacturers of inclinometers are:

- Analog Devices;
- VTI Technologies.

Selecting the sensors by the requirements, only two of them are suitable, which are presented in Table 4.4

Table 4.4: Inclinometers - *Analog Devices*

Model		Axis	Angle Range	Sensitivity	Voltage
ADIS16203	-	X or Y	360°	0.025°/LSB	3V - 3.6V
ADIS16209	-	X or Y	180°	0.025°/LSB	3V - 3.6V

The gyroscopes that read angular accelerations, are ideal to measure angular movements of the lower limbs. The main manufacturers of gyroscopes are:

- Analog Devices
- VTI Technologies

The major requirement is to have digital output, as previously stated. According to the requirements, there are few sensors that can be selected for this type of project.

The sensors from the company *Analog Devices* that can be selected are presented in Table 4.5, which the sensors from *VTI Technologies* are presented in the Table 4.6. VTI Technologies also has other sensors, but due to a high price were excluded.

Table 4.5: Gyroscopes - *Analog Devices*

Model	Axis	Angle Range	Sensitivity	Voltage
ADIS16060 -	Yaw	80°/s	0.0122°/sec/LSB	4.25V - 5.25V
ADIS16080 -	Yaw	180°	0.09766°/sec/LSB	4.75V - 5.25V

Table 4.6: Gyroscopes - *VTI Technologies*

Model	Axis	Angle Range	Sensitivity	Voltage
CMR3000 -	Yaw	2000°/s	1.33 count/°/s	2.5V - 3.6V

4.2 Actuators

The electronic part is not only composed by sensors, but also includes an actuator in order to lock and unlock the orthosis. The actuator can be an electric motor, a linear actuator or any similar device. The electric motor can be divided into two main parts, Alternating Current (AC) motors and Direct Current (DC) motors. Since the device must be portable, only DC motors will be be considered. According to Pansini (1996) the DC motors can be divided into three main parts:

- Shunt motor;
- Series motor;
- Compound motor.

In the Shunt motor the coils are connected in parallel with the rotor. In the Series motor the coils are connected in series with the rotor. The Compound motor has two types of coil, one is connected in parallel and another is in series Pansini (1996).

In the search of motors it was used the same methodology of search of the sensors, a search based in the largest stores with shipping to Portugal. For this purpose was defined some presuppositions, a motor should be small and light as possible, and voltage supply should be inferior to 12V. Another important characteristic to consider is that the motor will always be starting and stopping, therefore it is necessary a motor with fast acceleration and not made for continuous rotation. Taking this consideration into account, were found namely, two types of DC actuators:

- RC Servo;
- Stepper motor.

RC servo (see Figure 4.1) is a small DC motor which is often used in robotic applications. The most common are a brushed motor with three or five pole armature, but there is also with a version coreless motor. A five pole motor has a smoother operation, comparing with the three pole motor. The torque can be lower if the magnets stay between two poles, with the coreless version this situation does not exist because there is no core. A RC Servo usually have a maximum range of operation of 180°. (hooked-on-rc airplanes, 2012)

A RC Servo can also be defined according to its control, which can be an analog or a digital servo.

Figure 4.1: RC Servo (PyroElectro, 2012)

The RC Servo is controlled by Pulse Width Modulation (PWM) as it is illustrated in Figure 4.2. The time in high (5V) will define the position of the motor the pulse has a time of 20 ms. An analog servo is slower than a digital servo, but as a lower power consumption.

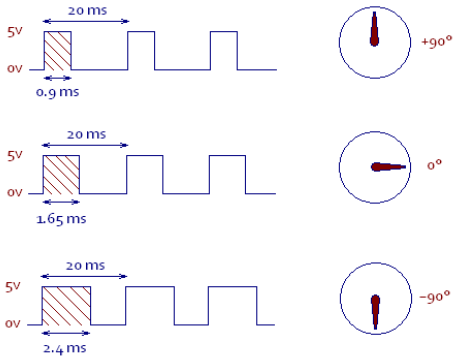

Figure 4.2: RC Servo control (Television, 2012)

The number of available servos is high, therefore three models were only chosen. One with a high torque (RC-1), one with high speed (RC-2), and the last taking into account dimensions and weight (RC-3). The information is presented in the Table 4.7. All the presented RC Servos work at 4.8V.

A stepper motor is a motor with several applications. With a working principle similar to the RC Servo, the Stepper motor has two main differences comparing to RC Servo. The first is that instead of being necessary a single pulse it is necessary a parallel pulses to activate the motor, another difference is that the poles are activated directly instead of having a circuit with an amplifier.

Table 4.7: RC Servos (Servodatabase, 2012)

Property	RC-1	RC-2	RC-3
Model	GWS S777CG 6BB	MKS DS 760	Protech B1021
Modulation	Analog	Digital	Analog
Weight	189.9 g	75.0 g	2.1 g
Dimensions	65.0 x 32.0 x 70.4 mm	40.0 x 20.0 x 40.0 mm	20.1 x 6.1 x 6.1 mm
Torque	35.1 kg-cm	3.90 kg-cm	0.30 kg-cm
Speed	0.15 sec/60°	0.03 sec/60°	0.20 sec/60°
Motor type	Coreless	Coreless	Coreless

In order to have have a better understanding of stepper motors, was chosen a stepper with a high torque (Stepper-1), and the other taking into account dimensions and weight (Stepper-2). The characteristics are presented in Table 4.8.

Table 4.8: Stepper Motors - Portescap (Digi-Key, 2012)

Property	Stepper-1	Stepper-2
Model	23HX18D	15M020D1B
Coil type	Bipolar	Bipolar
Voltage	6.84V	5V
Amps	1A	0.1A
Step angle	1.8°	18°
Torque	13 kg-cm	0.01 kg-cm
Diameter (body)	57.15 mm	15.50 mm

4.3 Data Acquisition

In order to process the information retrieved from the sensors and act according to that information. For this functionality was chosen a microcontroller with a incorporated transceiver for *ZigBee* and *IEEE 802.15.4*, known as *One chip solution*. The model is ATmega128RFA1 (Figure 4.3) from *Atmel*. Among all the features, the ones that stand out are (Atmel, 2011a):

- Up to 16 MIPS;
- 128K Bytes of In-System Self-Programmable Flash;
- 4K Bytes EEPROM;
- 16K Bytes Internal SRAM;
- JTAG Interface with On-chip Debug;
- Real Time Counter with Separate Oscillator;
- Master/Slave SPI Serial Interface;
- Fully integrated Low Power Transceiver for 2.4 GHz ISM Band;
- Hardware Security;
- Supply voltage range 1.8V to 3.6V;
- Ultra Low Power consumption less than 18.6 mA.

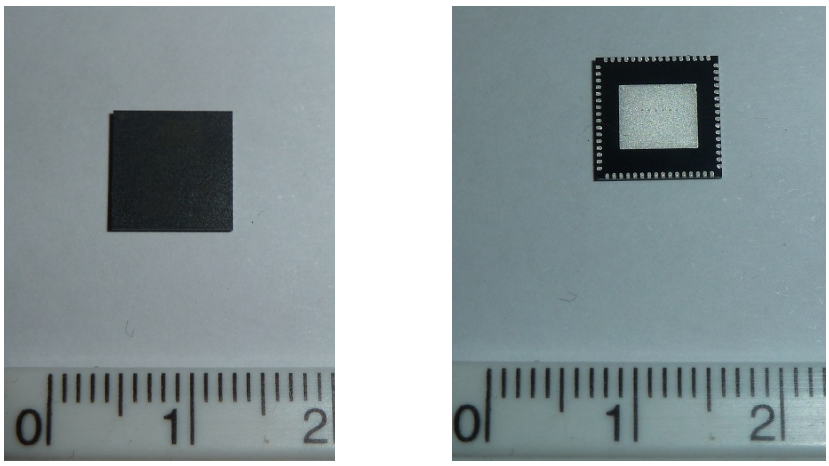

(a) Front view (b) Back view

Figure 4.3: ATmega128RFA1

To make the data acquisition the software *Labview* was chosen. The microcontroller will send the information of the four sensors and will calculate the knee angle as shown in the Figure 4.4.

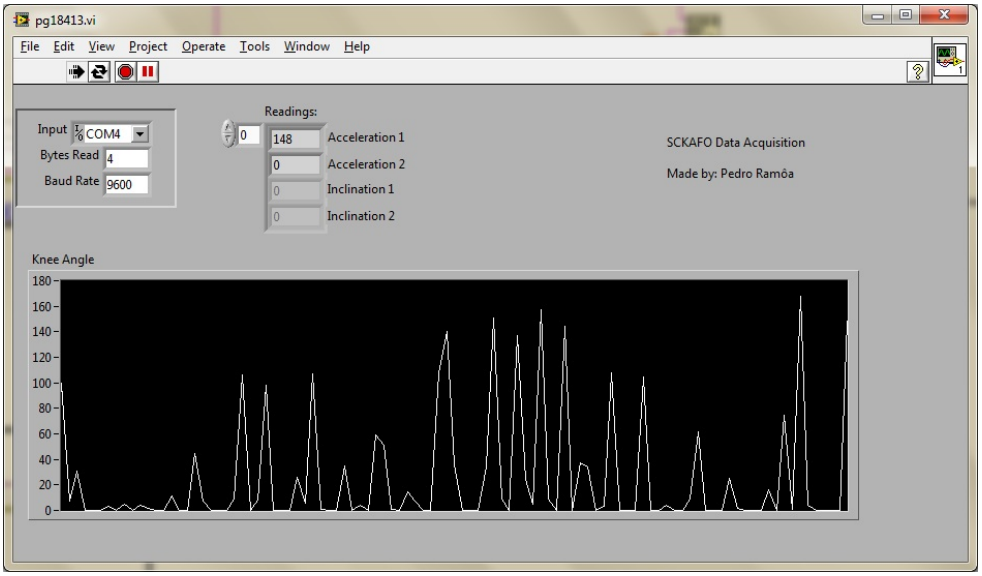

Figure 4.4: General view of the software

The main used functions were:

- Visa Serial;
- Visa Set I/O Buffer Size Function;
- Visa Read Function;
- Error Handling Function;
- String Reading Function.

4.4 Chapter Summary

A search of suitable sensors for this project was made. Despite the large number of existing sensors, this chapter presemted the number of sensors suitable for this kind of project is small. The best type of sensors for measuring the human motion are: accelerometers, gyroscopes and inclinometers. The main manufactures of this type of sensors were also indicated. A sample of suitable actuators were also shown in this chapter, due to a large offer of motors a comparison was made based on their characteristics and also their working principle.

The selected microcontroller was the ATmega128RFA1 from *ATmega* due to its characteristics, that is, it has a built-in transceiver which reduces the size of PCB and also reduces the price.

Finally, in this chapter a brief description of the functions used on the developed program is shown. The *Labview* was the chosen platform.

Chapter 5

Development of a New Concept of Locking System for an Orthosis SCKAFO

5.1 Operation and Performance of the Mechanical Device

Writen the context of this work, the mechanism selected for the orthosis is the one illustrated in Figure 5.1, which has one locking position, but can support higher loads. The mechanism dimensions are presented in the appendix D.

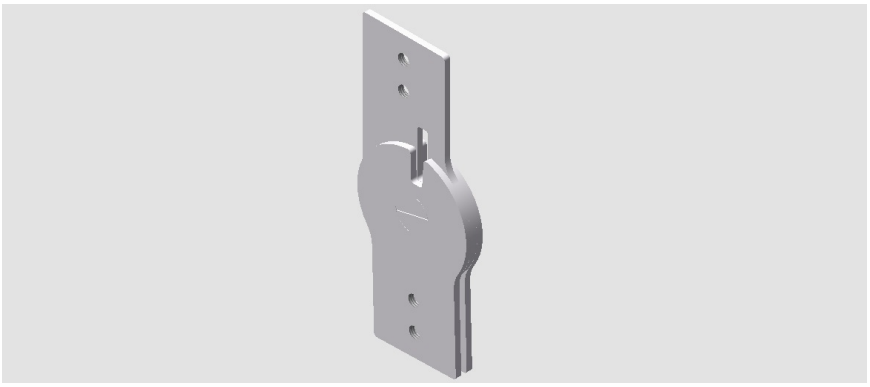

Figure 5.1: Generic mechanism - v1

In terms of performance the mechanism has to lock and unlock in a period less than 6 ms. In the locking process (see Figure 5.2a) the actuator pushes the pin downwards locking the orthosis. In turn, the unlocking process (Figure 5.2b), the actuator pulls upwards the pin unlocking the orthosis and allowing the knee flexion.

(a) Locked (b) Unlocked

Figure 5.2: Switching operation

This mechanism should allow knee flexion in the swing phase and stabilize the knee during the stance phase.

The sensors selected for this project were the gyroscopes and inclinometers/accelerometers. The gyroscopes will be used to measure the angular accelerations of the lower limb, as it is shown in the Figure 5.3a. The inclinometers/accelerometers will measure the angles of the lower limb, as illustrated in Figure 5.3b.

During the measuring process, a microcontroller will send the data retrieved from the sensors to a computer.

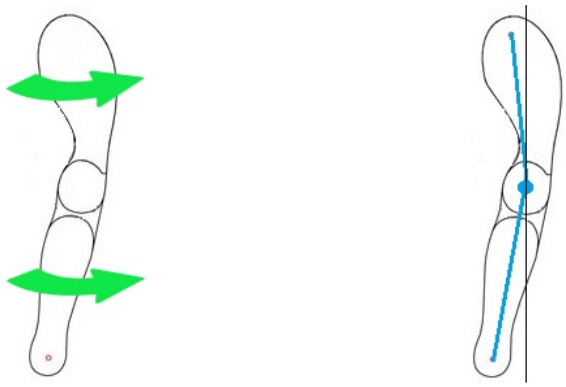

(a) Gyroscope (b) Inclinometer/Accelerometer

Figure 5.3: Sensor measurement

5.2 Construction of the Physical Prototype

The physical prototype constructed is made of a stainless steel plate with a thickness of 2 mm. The mechanism was manufactured by laser technique. Two different mechanisms were built, one with a slot as presented in the Figure 5.1, and another one without any slot. With this approach, a simplification is intended, it is needed only one actuator, and thus, a lower power consumption. The only disadvantage of this solution is that only one mechanism is subjected to the pressure. Figure 5.4 shows the mechanism built. The cost of this mechanism was 78,46 euros.

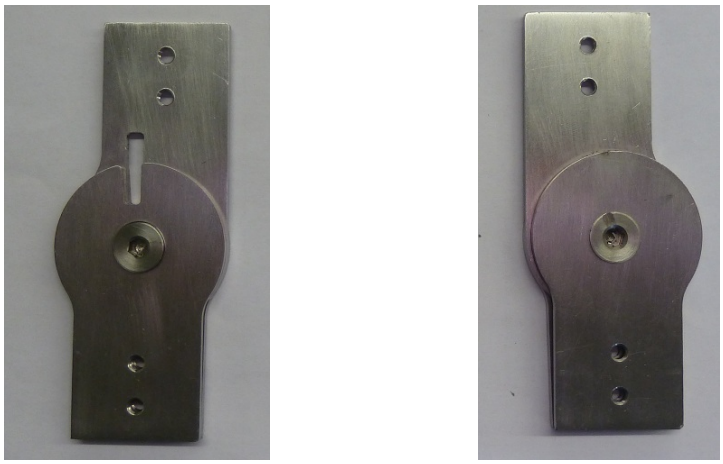

(a) With slot (b) Without slot

Figure 5.4: Built mechanism

Figures 5.5 and 5.6 show the five elements that constitute each mechanism. Three parts belong to the locking system and the remaining two parts belong to the shaft of the mechanism.

Figure 5.5: Elements of part one

Th following images include a scale in order to better understand the dimensions of the mechanism.

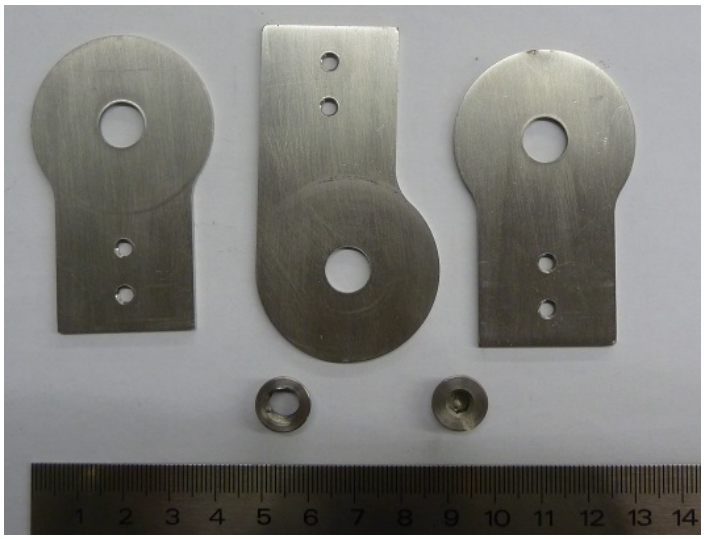

Figure 5.6: Elements of part two

Figure 5.7 shows the actual dimmensions of the locking system parts. The maximum deviation is 0,06 mm.

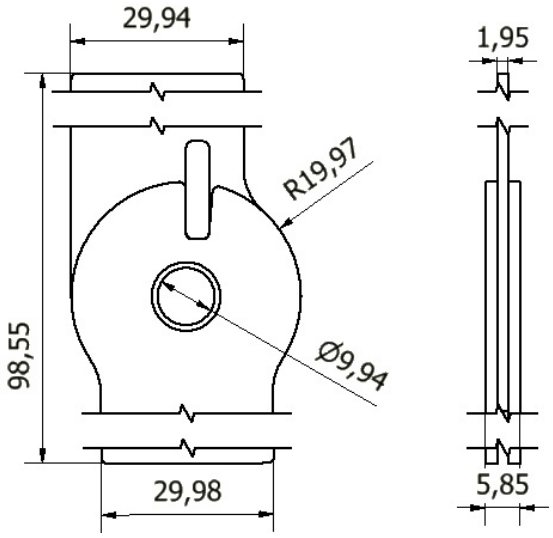

Figure 5.7: Measured values

The highlight in these figures go to the shaft, the shape of the shaft's head is different comparing to the original design. Figure 5.8 shows the details of the shaft. The dimensions of the shaft are: 9.90 mm of body diameter and 10.90 of head diameter.

(a) Interior (b) Exterior

Figure 5.8: Shaft

Figure 5.9 shows the locking mechanism assembled in a used orthosis, is is visible a small cable that will pull the cable upwards and downwards. The mechanism is fixed to the orthosis using only two screws due to the curvature of the aluminium bars.

Figure 5.9: KAFO with the built mechanism

5.3 Electronic System Implementation

With the purpose to develop a SCKAFO it is necessary to design a system that provides automatic actuation to the orthosis that is to lock and unlock without any human action. One possible way to provide this is to use electronics, by measuring the entire process and acting when it will be necessary according to the human gait progress. The measurement is made by using sensors, namely:

- Inclinometer: ADIS16203 from *Analog Devices*;
- Gyroscope: CMR3000 from *VTI Technologies*.

An inclinometer was selected instead of an accelerometer because it has greater immunity to noise from accelerations from other axis, for instance, when the foot makes the downward movement towards the floor the entire lower limb is subject to an acceleration that does not have interest in measuring and can interfere with the measurement of the angle of the lower limb. The choice of the sensors was limited due to the budget constrains and the available stock in stores.

Due to the low budget available for this project was not possible to work with development boards, so it was decided to make new development boards with the desired dimensions.

In order to make a successful development board it is necessary to study the datasheets of the sensors and corresponding development boards. The datasheet of the ADIS16203 sensor does not provide any kind of information about how a development board with this sensor should be, but searching the datasheet of the development board is retrieved the information presented in Figure 5.10.

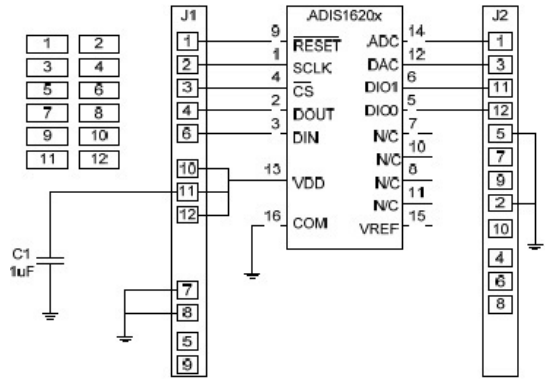

Figure 5.10: iSensor Inclinometer/Accelerometer Evaluation Board (Devices, 2007)

According to Devices (2007) an extra component is necessary to be added to this type of board, that is a capacitor of 1 uF. The datasheet from the sensor (Devices, 2010) shows that the sensor has 16 pins and the communication is made by SPI.

For this project the following pins are necessary:

- Pin 01 - SCLK: SPI Serial Clock;
- Pin 02 - DOUT: SPI Data Out;
- Pin 03 - DIN: SPI Data In;
- Pin 04 - CS: SPI Chip Select, Active Low;
- Pin 13 - VDD: Power Supply;
- Pin 16 - COM: Neutral.

According to the Technologies (revA.02) the communication can be done by SPI or I^2C. The selected protocol was the SPI because ADIS16203 can also communicates by SPI.

Figure 5.11 shows the necessary extra components to make a development board, namely three capacitors of 100 nF. All three capacitors are meant to provide additional power supply filtering.

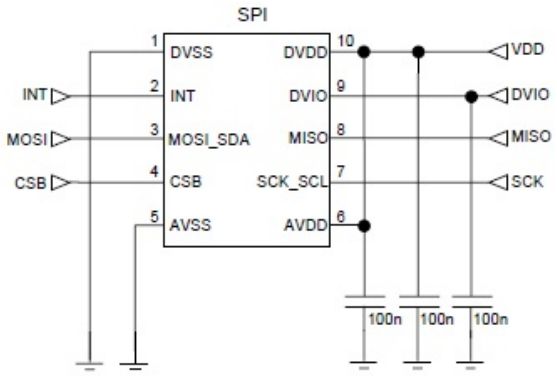

Figure 5.11: CMR3000 - Necessary components (Technologies, revA.02)

For this project it is necessary to use the following pins from CMR3000 sensor:

- Pin 01 - DVSS: Digital neutral;
- Pin 03 - MOSI: SPI Data In;
- Pin 04 - CSB: SPI Chip Select, Active Low;

- Pin 05 - AVSS: Analog neutral;
- Pin 06 - AVDD: Analog Power Supply;
- Pin 07 - SCK: SPI Serial Clock;
- Pin 08 - MISO: SPI Data Out;
- Pin 09 - DVIO: I/O Supply;
- Pin 10 - DVDD: Digital Power Supply;

The pins DVSS, AVSS will be connected to the same voltage (0V), while the pins AVDD, DVDD and DVIO will be connected to the same voltage (3.3V). This will make both sensors with the same connection type of six pins.

For the development of PCBs a freeware version of the software EAGLE 6.0 was utilized. For this project an entirely new library for the PCB design was created. Every component of the follow boards, has a personalized footprint in order to make the soldering easier by hand. A library with 44 devices was created. The objective of this subchapter is not to show how is created the PCBs, but to show the final result.

The board with the sensors should not be wider than the mechanism, so the first limitation is the width of the board, 30 mm. Following this requirement and the drawing of Figure 5.10 and 5.11 was obtained the PCB presented in Figure 5.12.

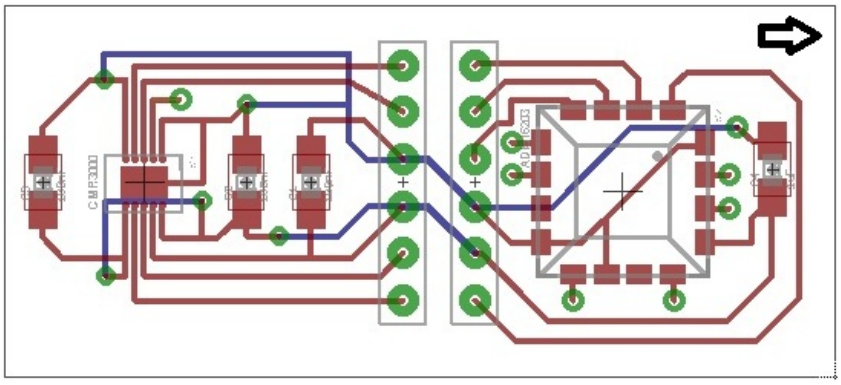

Figure 5.12: PCB with sensors

The black arrow shows side that should be facing up. The PCB presented in the Figure 5.12 follows the suggested designs recommended by *Analog Devices* and *VTI Technologies*. The non-used pins were connected to holes that in case of necessity can be soldered to connectors. The only exceptions is one pin of the sensor ADIS16203 that should not be connected to anything as explained in the respective datasheet.

In appendix E is shown the full schematic. The total price of the presented board are listed in Table 5.1.

Table 5.1: Sensor PCB cost

Element	Price (in Euros)
ADIS16203	49,91
CMR3000	22,48
Capacitor 1uF	0,06
3 capacitors 100nF	0,06
12 connectors	0,60
PCB	18.67
Total cost:	91,78

Table 5.1 shows that doing a personalized board is much cheaper than buying a made one. However, it has one big risk, that is a bad soldered or a bad designed board will not work.

According to Atmel (2011b), in order to design a PCB with ATmega128RFA1 microcontroller with wireless communication needs the configuration presented in the Figure 5.13. The full description can be found in the microcontroller datasheet.

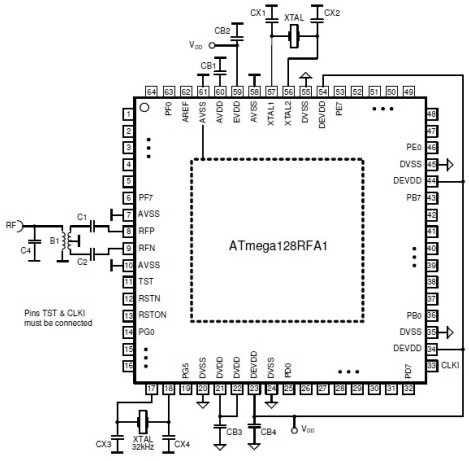

Figure 5.13: ATmega128RFA1 schematic

It should be mentioned that due to the delay in receiving some of the bought components, it was necessary to design two boards. One with communication by wire and another one with wireless communication, as Figures 5.14 and 5.15 depict, respectively.

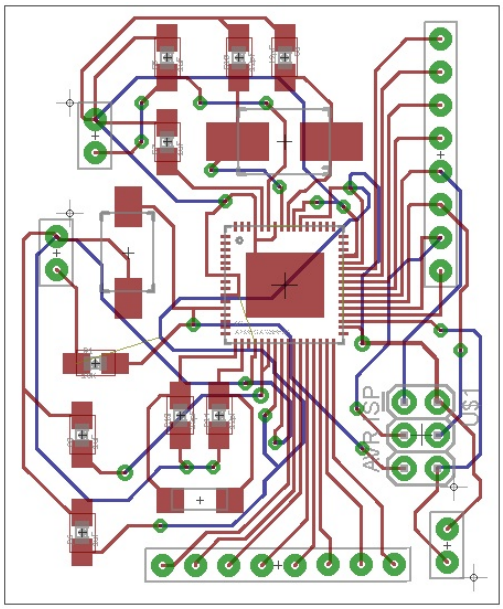

Figure 5.14: ATmega128RFA1 Board - communication by wire

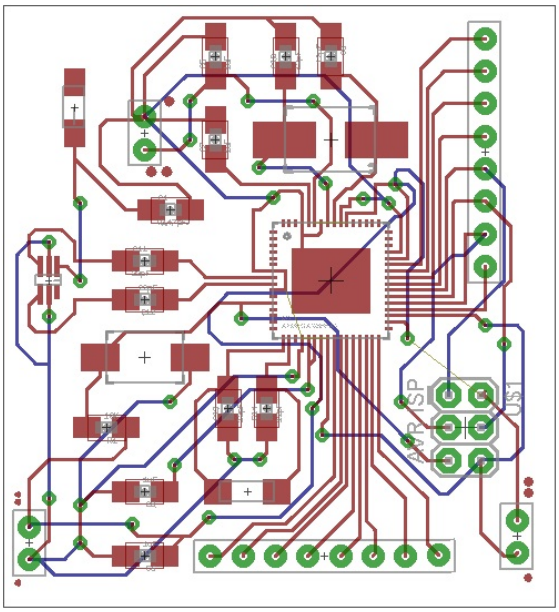

Figure 5.15: ATmega128RFA1 Board - wireless communication

The boards presented in Figures 5.14 and 5.15 (excluding the communication mode) have, programming circuit by ISP, capability to read sensors with the protocols SPI and I^2C, external interruptions. The analog inputs were not connected because they will not be used. The total costs of the presented board is listed in Table 5.2. The wireless board costs rise is 3,58 euros for the SMD Antenna, Balun and two capacitors of 22pF needed for wireless communication.

Table 5.2: ATmega128RFA1 PCB cost

Element	Price (in Euros)
ATmega128RFA1	8,03
Crystal 16MHz	1,00
Crystal 32kHz	1,11
4 capacitors 1uF	0,24
4 capacitors 12pF	0,24
Resistor 10k	0,02
Switch	0,35
20 connectors	1,00
6 headers	0,16
PCB	18.86
Total cost:	31,01

It was also necessary to design another board, a voltage regulator, made to regulate the power supply of the sensors and the microcontroller. For this purpose, it was used the LP2985 from *National Semiconductor* and the entire board had a cost of 3,95 Euros. The design was based on the LP2985 datasheet (Semiconductor, 2007)

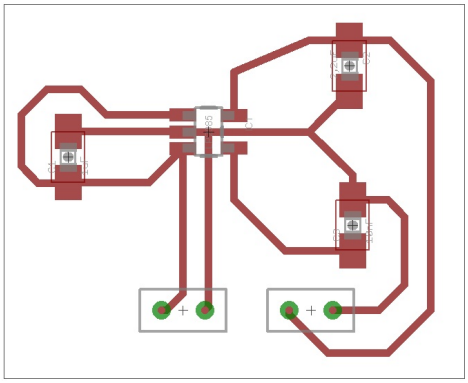

Figure 5.16: Voltage regulator

Finally, the result boards are shown in Figures 5.17 and 5.18.

The dimensions of the boards are respectively, 45 mm (H) x 20 mm (W) for the sensors board and 46 mm (H) x 38 mm (W) for the microcontroller board.

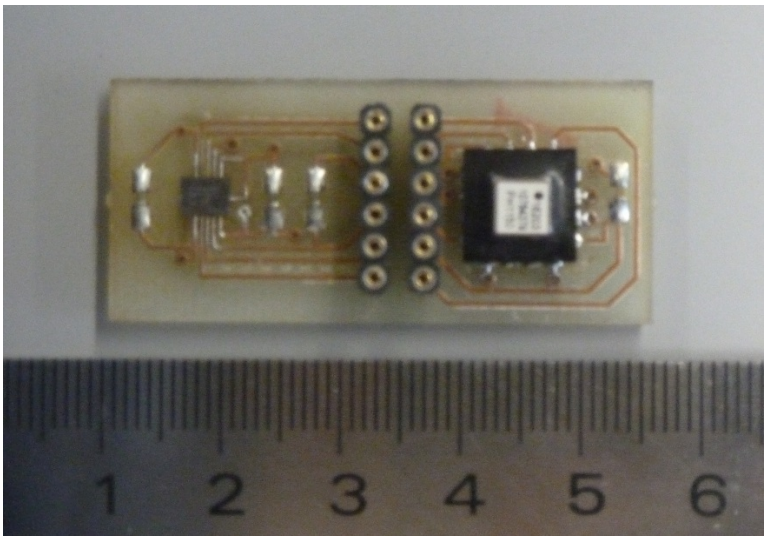

Figure 5.17: Built sensor board

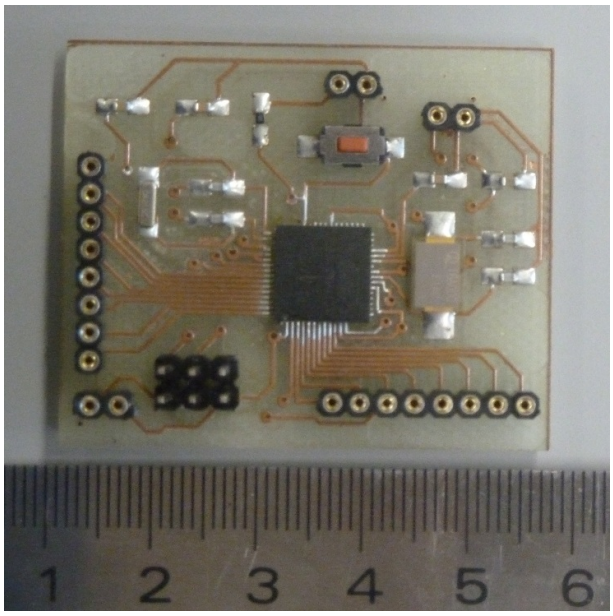

Figure 5.18: Built microcontroller board

Installing the sensor boards on the orthosis, the results are shown in the Figures 5.19a and 5.19b. The board with the microcontroller is shown in the Figure 5.20.

Unfortunately, due to budget limitations the actuators could not be bought. Thus it is expected that one the future tasks will be to buy motors and include them in the mechanisms.

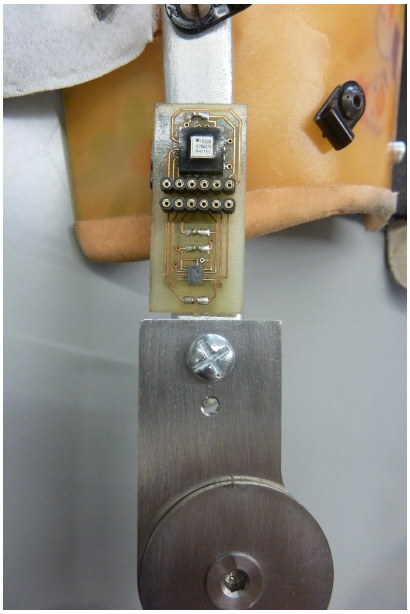

(a) Upper board

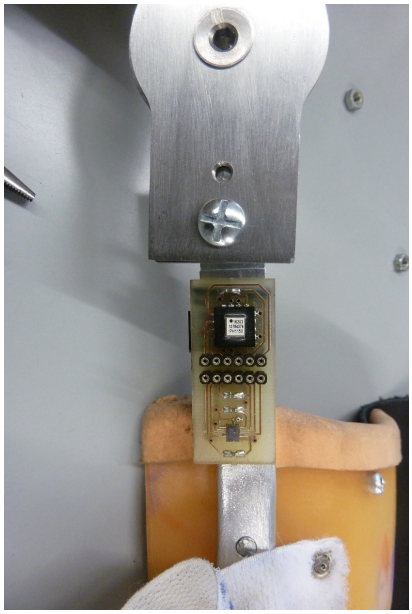

(b) Lower board

Figure 5.19: Installed boards

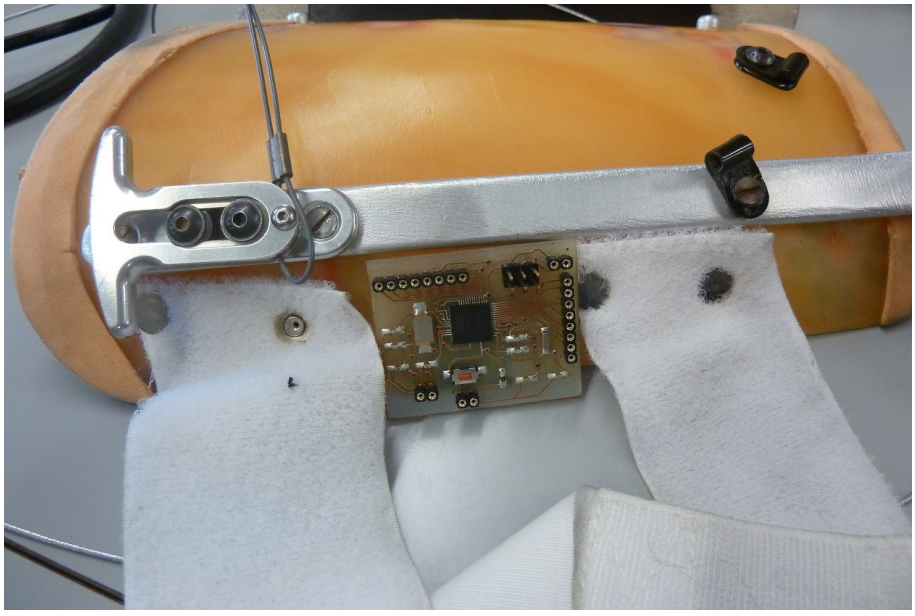

Figure 5.20: Installed microcontroller board

5.4 Concept Validation and Testing

The first test performed was on the efficiency of the mechanism. For this purpose a small motor was installed, but due to its low torque was not included in this work. Without any restrictions the motor raised pin, but when some pressure was applied to the pin holding it down, the motor was incapable of rising the pin. The alternative was locking and unlocking manually. With this method the mechanism performed well, but the fact of being used in an old orthosis, the mechanism does not connect well with the aluminum bars from the orthosis. This problem destabilizes the mechanism, making it unsecured as shown in Figure 5.21.

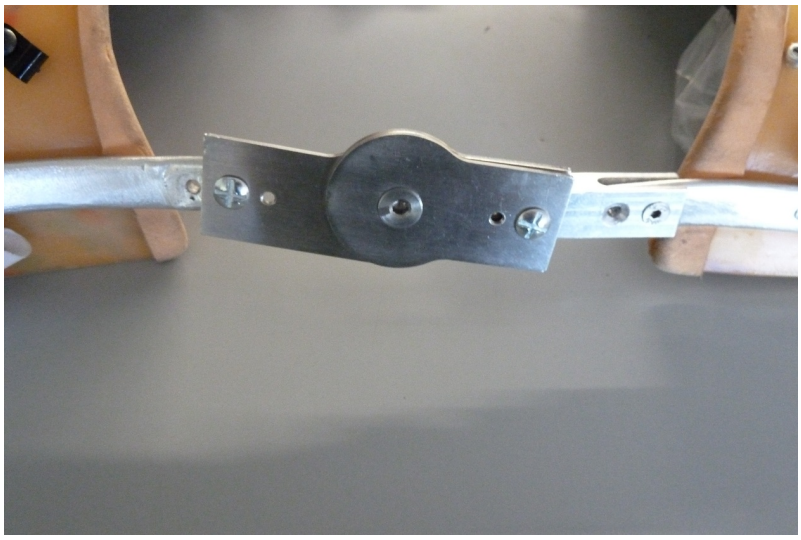

Figure 5.21: Unstable mechanism

There are two possible solutions to this problem:

- Cut the aluminum bars and assemble a new ones. This solution it is cheaper but does not solve the problem of discomfort when using this orthosis.
- Make a new orthosis will result in a more comfortable and better adjusted to this type of locking mechanism.

In order to perform tests with the sensors, they were installed in the upper part of the leg, but the continuous movement of the leg during the gait cycle constantly broke the wiring between the boards causing causing major delays in the testing process (see Figure 5.22). To solve this problem it is recommended to buy malleable wire in order allow real tests without constantly breaking the wires.

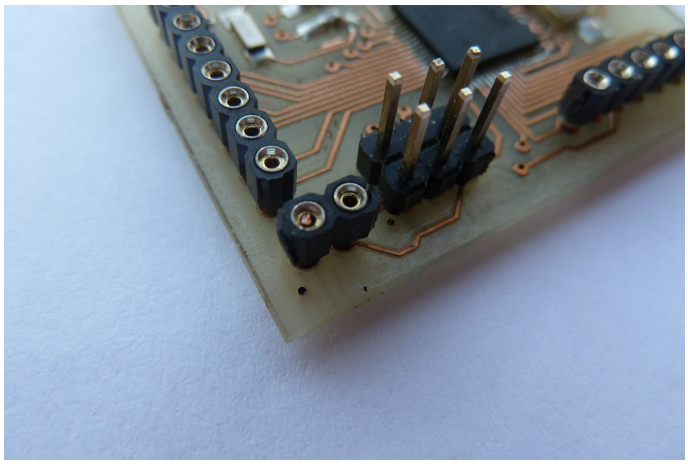

Figure 5.22: Broken wiring

In the Figure 5.23 it is shown the connection between the ATmega128RFA1 microcontroller and the sensors (ADIS16203 and CMR3000). The CMR3000 is connected to the microcontroller under the board, reducing the wiring from twelve wires to seven wires.

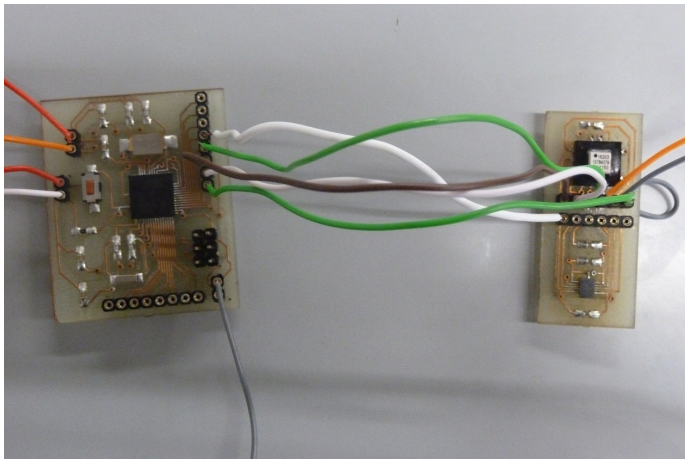

Figure 5.23: Connecting between the microcontroller and the sensors

The sensors stop working during the tests, probably because of a short-circuit or a bad connection between the pins and the board. Due to exposed paths on the PCB adding the small footprint of the sensors the board stayed to exposed and without proper protection the board failed. Next steps to solve this problem:

- Analyse with a magnifying glass if the components are well soldered.
- Analyse with a oscilloscope if the the communication is well done.

The voltage regulator was also tested. The test was done with four rechargeable batteries of 1.2V, as it is shown in Figure 5.24 the output is 3.78V when should be 4.8V, but this type of batteries lose voltage as they lose charge.

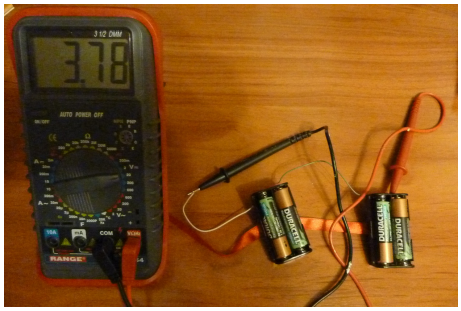

Figure 5.24: Batteries voltage

The LP2985 proves to be a efficient voltage regulator, in Figure 5.25 it is shown that the output voltage is 3.36V less than the maximum supported by the ATmega128RFA1 (3.6V).

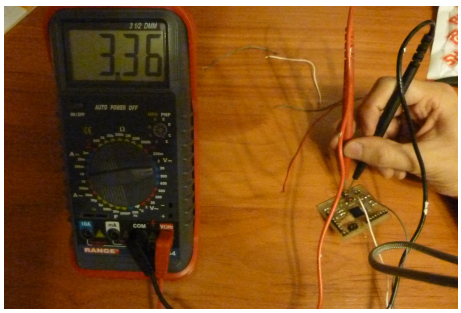

Figure 5.25: Voltage in the microcontroller

5.5 Chapter Summary

In this chapter a demonstration how the mechanism should work is presented, is also shown how many positions the mechanism have and how fast should actuate. In this chapter was shown how the measurement of the human gait is performed, the chosen sensors and those sensors work.

The built mechanism was also shown in this chapter. A set of two mechanisms constitutes the locking system, one has the locking system and the other is made to support the first one in order to help the operation of the orthosis. Meanwhile each mechanism is composed by five parts, three main parts and two are the shaft and hold all the parts together. In this chapter was demonstrated the differences between the mechanism made in the software *Autodesk Inventor* and the dimensions of the built mechanism. The adaptation of the mechanism to an old KAFO and the problems during the process of adaptation was explained.

The selected sensors for this project were an inclinometer and a gyroscope with the intention to buy two of each sensor in order to measure both parts of the leg. In this chapter can be found the drawings of the boards, the built boards and also the costs of each board. The process of adapting the PCBs to the orthosis is demonstrated and the difficulties of that process. The dimensions of the PCBs was also shown.

All the parts of this project were submitted to tests, some parts passed the tests like the mechanical part that was able to endure the pressures applied, other parts did not endure the entire tests (e.g. Sensors board). In this chapter can also be found the possible solutions to the presented problems.

Chapter 6

Conclusions and Future Work

6.1 Conclusions

In first place it must be said that this kind of project is a quite motivating and a very complex challenge. The opportunity to help person with the pathologies described in this project is something that motivates everyone involved in this project. The number of different solutions to compensate the muscular weakness of the lower limbs is not enough, specially in Portugal where almost orthosis utilized are KAFO and most of population does not have a financial capacity, so the idea of creating a low cost SCKAFO was a positive aspect of this project.

Since the development of the first mechanical SCKAFO in 1986, the orthosis did not suffer a significant evolution. The quality of the materials used improved in quality therefore, improving the quality and comfort of the SCKAFOs. Some SCKAFOs are still purely mechanics, such as, *Becker UTX*, *Ottobock Freewalk*, or *Becker SafetyStride* are some examples of mechanical SCKAFOs. Only in 2003 the companies start to present electromechanical SCKAFOs, such as, *Becker E-Knee* or *Ottobock Sensor Walk*. All the SCKAFOs presented until now show limitations in terms for which pathologies they can compensate.

The human gait is composed by two phases, stance phase and swing phase, and each one can be divided in several sub-phases. A behaviour of a non-pathological gait is similar between different people. The number of pathologies that affects the lower limbs is very high, which can be divided in three groups, central neurological diseases, peripheral neurological diseases and muscular diseases. Each disease causes a different pathological gait. Each disease produces in the joints of the lower limbs an effect that is very significant as the experimental data proves.

The mechanism for an orthosis SCKAFO must support pressures of very high values. A mechanism designed for this type of project must follow several requirements, such as: fast switching between phases, should be as quiet as possible, should be light, among others. Due to its price and abundance, the metal *stainless steel - grade 304* is a good material for this type of mechanism, is not the ideal for a long term use, but is very good for testing in order to reduce the costs of prototyping. To develop a good mechanism for an orthosis it is necessary to draw different models, in order to have a better understanding the behaviour of each mechanism. Several mechanisms were developed, these mechanism allowed to compare each mechanism to retrieve information in order to create the most suitable one.

Each mechanism developed in this project has its own advantages and disadvantages, but comparing each one the more promising ones are the *Ratchet 2* (see Figure 3.5) and the *Slot Mechanism* (see Figure 3.14). These two mechanisms have the capability of endure high pressures and also they also have several locking positions.

A IMU is a very good device to measure the human motion, usually composed by accelerometers/inclinometers and gyroscopes, these sensors are a good choice for this type of project due to their price and performance. An IMU should be adjusted to each project, the best way to adjust it is to make a market research about the available sensors and choose the sensors that are more suitable for the project and developing a customized IMU.

There are thousands of actuators in the market, to this project the more suitable are RC Servos and Stepper Motors due to their fast reaction. The choice of the actuators should be made taking in account mainly the torque, power consumption, and dimensions.

This project needs a higher budget, unfortunately for this project that budget was not available which limited the evolution of the project. These limitations were obvious in the development of the physical prototype. The results given the limitations were very positive and the results also show that this project is on the correct path.

6.2 Future Work

For future developments of this work, the main tasks are identified as follows:

- To develop other mechanisms in order to have a comparison basis
- To buy actuators to test with mechanisms
- To design a new orthosis to fit easily the developed mechanisms
- To perform tests with all the parts connected.

Bibliography

ASM. Aisi type 304 stainless steel, 2012. http://asm.matweb.com [Visited on: 15 August 2012].

Atmel. *ATmega128RFA1 Preliminary Summary*, 2011a.

Atmel. *ATmega128RFA1 Datasheet*, 2011b.

AZoM. Stainless steel - grade 304, 2012. http://www.azom.com [Visited on: 15 August 2012].

Gary G. Bedard. *Stance Control Overview Guide II*, nov. 2010.

Kathie A. Bernhardt, Steven E. Irby, and Kenton R. Kaufman. Prosthetics and orthotics international. *Consumer opinions of a stance control knee orthosis*, 30(3):246 – 256, 2006.

Cascade. Fillauer swing phase lock, 2012a. http://www.cascade-usa.com/ [Visited on: 29 May 2012].

Cascade. Fillauer swing phase lock 2, 2012b. http://www.cascade-usa.com/ [Visited on: 29 May 2012].

Dana Craig. Lateral trunk bending, 2012. http://www.freewebs.com/dcraig3 [Visited on: 02 June 2012].

Analog Devices. *iSensor Inclinometer/Accelerometer Evaluation Board - ADIS1620x/PCB*, 2007.

Analog Devices. *Programmable 360° Inclinometer - ADIS16203*, 2010.

Digi-Key. Stepper motors, 2012. http://www.digikey.com [Visited on: 25 August 2012].

Newman Dorland. *Dorland's Illustrated Medical Dictionary*. Saunders, 31 edition, 2007.

BIBLIOGRAPHY

Demet Edeer and Craig D. Martin. E-mag active, a newer stance control knee ankle foot orthosis (sckafo) in the context of workers' compensation. Technical report, WorkSafeBC Evidence-Based Practice Group, dec. 2010.

eFunda. Aisi type 304, 2012. http://www.efunda.com [Visited on: 15 August 2012].

Fillauer. Spl2 from fillauer llc, 2012. http://www.fillauer.com/pdf/AD278-SPL2.pdf [Visited on: 29 May 2012].

A.S. Hall, F.E. Archer, and R.I. Gilbert. *Engineering Statics*. University of New South Wales Press Ltd, 2 edition, 1999.

Otto Bock Healthcare. *Sensor Walk 17B500 Orthosis - Instructions for Use*, 2010a.

Otto Bock Healthcare. *Sensor Walk White Paper*, 2010b.

R.C Hibbeler. *Mechanics of Materials*. Prentice Hall, 8 edition, 2010.

hooked-on-rc airplanes. Choosing rc servos!, 2012. http://www.hooked-on-rc-airplanes.com [Visited on: 25 August 2012].

INE. Censos 2001. Technical report, Instituto Nacional de Estatística, 2002.

Steven E. Irby, Rochester MN, Kenton R. Kaufman, and Rochester MN. Electromechanical joint control device with wrap spring clutch, 12 2004. URL `http://www.patentlens.net/patentlens/patent/US_6834752/en/`.

Pedro Moreira and Paulo Flores. Biomechanical design of a new sckafo (stance-control-kneeankle-foot-orthosis). In *4º CONGRESSO NACIONAL DE BIOMECÂNICA*, 2011.

Pedro Moreira, Pedro Ramôa, Luís Silva, and Paulo Flores. On the biomechanical design of stance control knee ankle foot orthosis (sckafo). In *International Symposium on Multibody Systems and Mechatronics*, oct. 2011.

Jonathan M. Naft, Chagrin Falls OH, and Cleveland Heights OH Wyatt S. Newman. Orthosis knee joint, 02 2003. URL `http://www.patentlens.net/patentlens/patent/US_6517503/en/`.

NCBI. National center for biotechnology information - gait analysis, 2012. http://www.ncbi.nlm.nih.gov/books/NBK27235/ [Visited on: 31 July 2012].

European Assistive Technology Information Network. Kafo-system free walk, 2012. http://www.eastin.eu/ [Visited on: 29 May 2012].

BIBLIOGRAPHY

Geelong Orthotics. Geelong orthotics aftercare and resources, 2012a. http://aftercare-and-resources.geelongorthotics.com.au/ [Visited on: 29 May 2012].

T&S Orthotics. Safety stride information, 2012b. http://www.tandsorthotics.co.uk/ [Visited on: 29 May 2012].

OttoBock. *E-MAG Active - E-MAG Control*, 2008a.

OttoBock. *Free Walk Orthosis: Movement with Swing*, 2008b.

OttoBock. *Free Walk - Taking Measurements for Otto Bock Free Walk Orthosis*, 2008c.

Anthony J. Pansini. *Basics of Electric Motors*. PennWell Books, 2 edition, 1996.

PyroElectro. Servo motor control: The servo motor, 2012. http://www.pyroelectro.com/tutorials/servomotor/servomotor.html [Visited on: 25 August 2012].

J. Neil Russell, Gerry E. Hendershot, Felicia LeClere, L. Jean Howie, and Michele Adler. Trends and differential use of assistive technology devices: United states, 1994. Technical Report 292, Vital and Health Statistics of the CENTERS FOR DISEASE CONTROLAND PREVENTION/National Center for Health Statistics, nov. 1997.

National Semiconductor. *LP2985 Micropower 150 mA Low-Noise Ultra Low-Dropout Regulator*, 2007.

Servodatabase. Rc servo specifications and reviews, 2012. http://www.servodatabase.com [Visited on: 25 August 2012].

VTI Technologies. *Data Sheet - CMR3000-D01*, revA.02.

Toymaker Television. Rc servo basics, 2012. http://tymkrs.tumblr.com/post/16765013540/rc-servo-basics [Visited on: 25 August 2012].

Michael W. Whittle. *Gait Analysis - An Introduction*. Butterworth-Heinemann, 4 edition, 2007.

Terris Yakimovich, Edward Lemaire, and Jonathan Kofman. Design and evaluation of a stance-control knee-ankle-foot orthosis knee joint. *IEEE Transactions on Neural Systems and Rehabilitation Engineering*, 14(3):361 – 369, 2006a.

BIBLIOGRAPHY

Terris Yakimovich, Edward Lemaire, and Jonathan Kofman. Design, construction and evaluation of an electromechanical stance-control knee-ankle-foot orthosis. In *Engineering in Medicine and Biology 27th Annual Conference*, sept. 2006b.

Terris Yakimovich, Edward Lemaire, and Jonathan Kofman. Engineering design review of stance-control knee-ankle-foot orthoses. *Journal of Rehabilitation Research and Development*, 46(2):257 – 268, 2009.

Rong Zhu and Zhaoying Zhou. A real-time articulated human motion tracking using tri-axis inertial/magnetic sensors package. *Neural Systems and Rehabilitation Engineering, IEEE Transactions on*, 12(2):295 –302, june 2004. ISSN 1534-4320. doi: 10.1109/TNSRE.2004.827825.

Appendix A

Ratchet 1

A.1 Dimensions

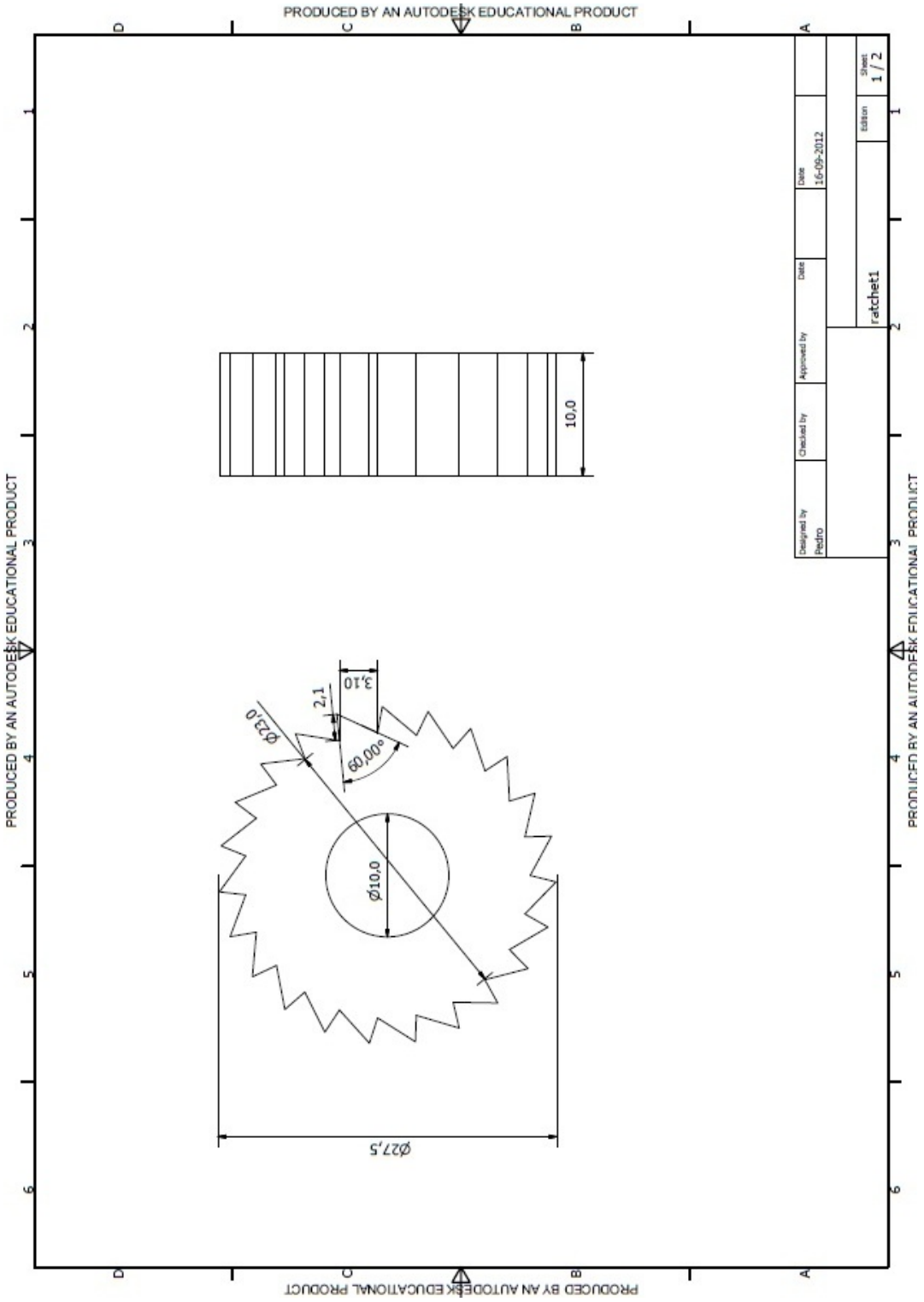

Figure A.1: Ratchet 1

Ratchet 1

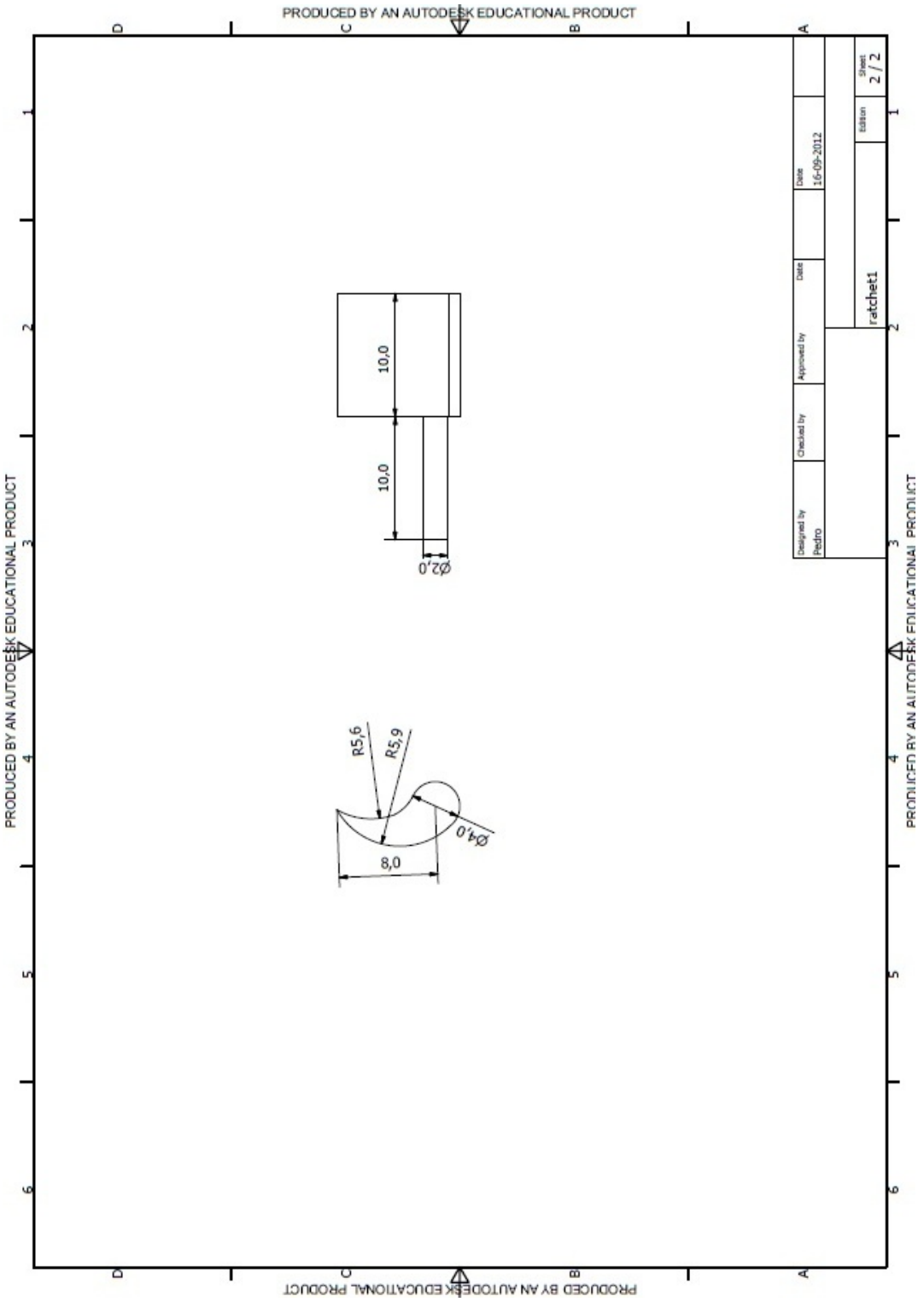

Figure A.2: Pawl 1

A.2 Stress Analysis

Reaction Force and Moment on Constraints

Constraint Name	Reaction Force		Reaction Moment	
	Magnitude	Component (X,Y,Z)	Magnitude	Component (X,Y,Z)
Fixed Constraint:1	6536,11 N	6534,35 N	5,33263 N m	-0,0293495 N m
		151,168 N		0,486966 N m
		10,5452 N		5,31027 N m
Pin Constraint:1	6537,35 N	-6535,59 N	0,510573 N m	-0,104826 N m
		-151,481 N		-0,499696 N m
		0 N		0 N m

Figure A.3: Reaction Force and Moment on Constraints

Name	Minimum	Maximum
Volume	4164,55 mm^3	
Mass	0,0333164 kg	
Von Mises Stress	0,175857 MPa	1535,82 MPa
1st Principal Stress	-136,946 MPa	1462,76 MPa
3rd Principal Stress	-1026,43 MPa	114,545 MPa
Displacement	0 mm	0,0134034 mm
Safety Factor	0,13348 ul	15 ul
Stress XX	-893,002 MPa	1074,89 MPa
Stress XY	-56,7271 MPa	804,551 MPa
Stress XZ	-454,472 MPa	295,133 MPa
Stress YY	-296,87 MPa	429,651 MPa
Stress YZ	-242,011 MPa	262,384 MPa
Stress ZZ	-348,259 MPa	603,237 MPa
X Displacement	-0,00604822 mm	0,0133751 mm
Y Displacement	-0,0105885 mm	0,0113358 mm
Z Displacement	-0,000927488 mm	0,000753864 mm
Equivalent Strain	0,000000835947 ul	0,00699498 ul
1st Principal Strain	0,000000831594 ul	0,00765648 ul
3rd Principal Strain	-0,00600453 ul	-0,000000403033 ul
Strain XX	-0,00498633 ul	0,00528357 ul
Strain XY	-0,000379161 ul	0,00537757 ul
Strain XZ	-0,00303766 ul	0,00197265 ul
Strain YY	-0,00148731 ul	0,002137 ul
Strain YZ	-0,00161759 ul	0,00175376 ul
Strain ZZ	-0,00189805 ul	0,00189714 ul

Figure A.4: Result Summary

Appendix B

Ratchet 2

B.1 Dimensions

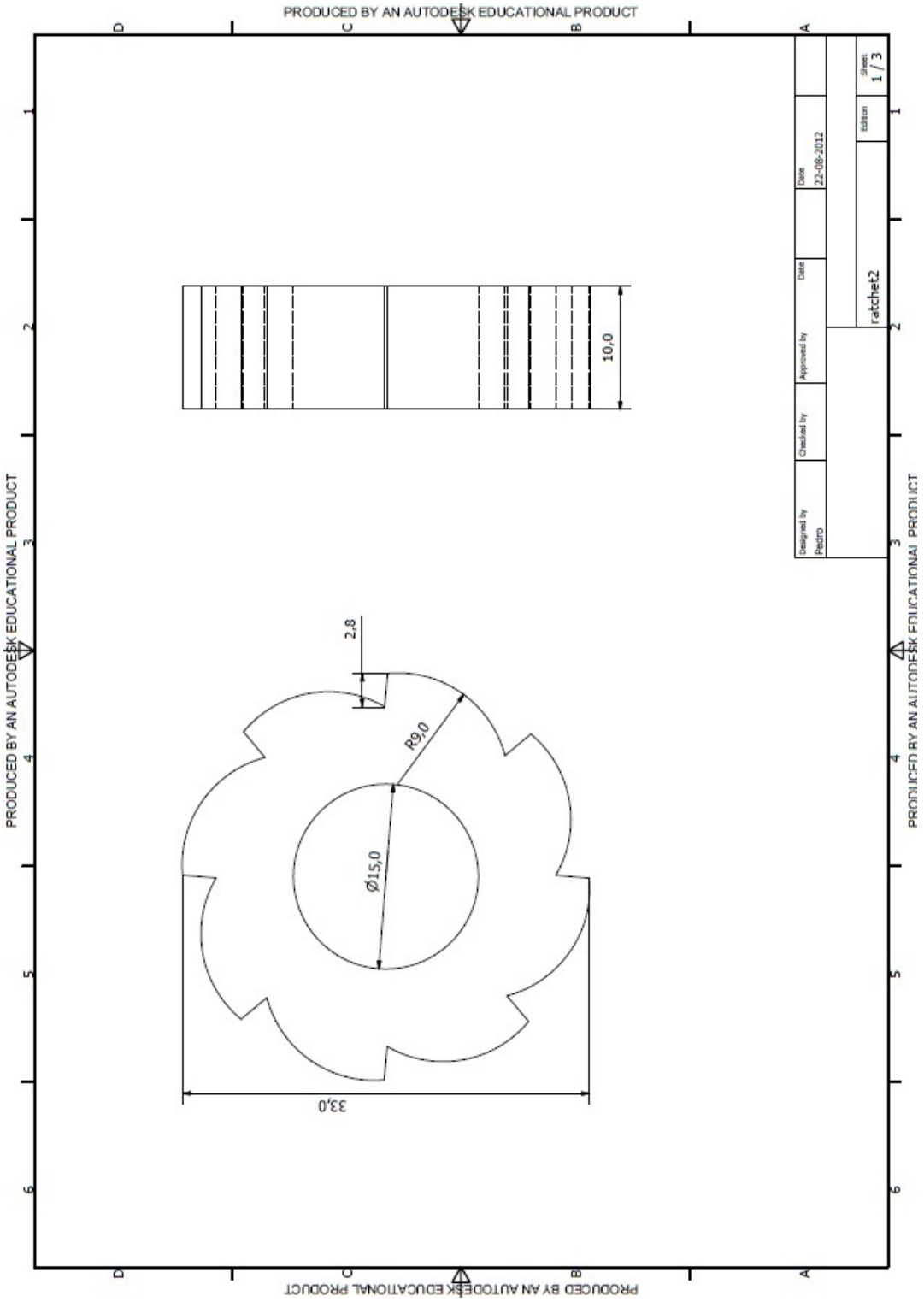

Figure B.1: Ratchet 2

Ratchet 2

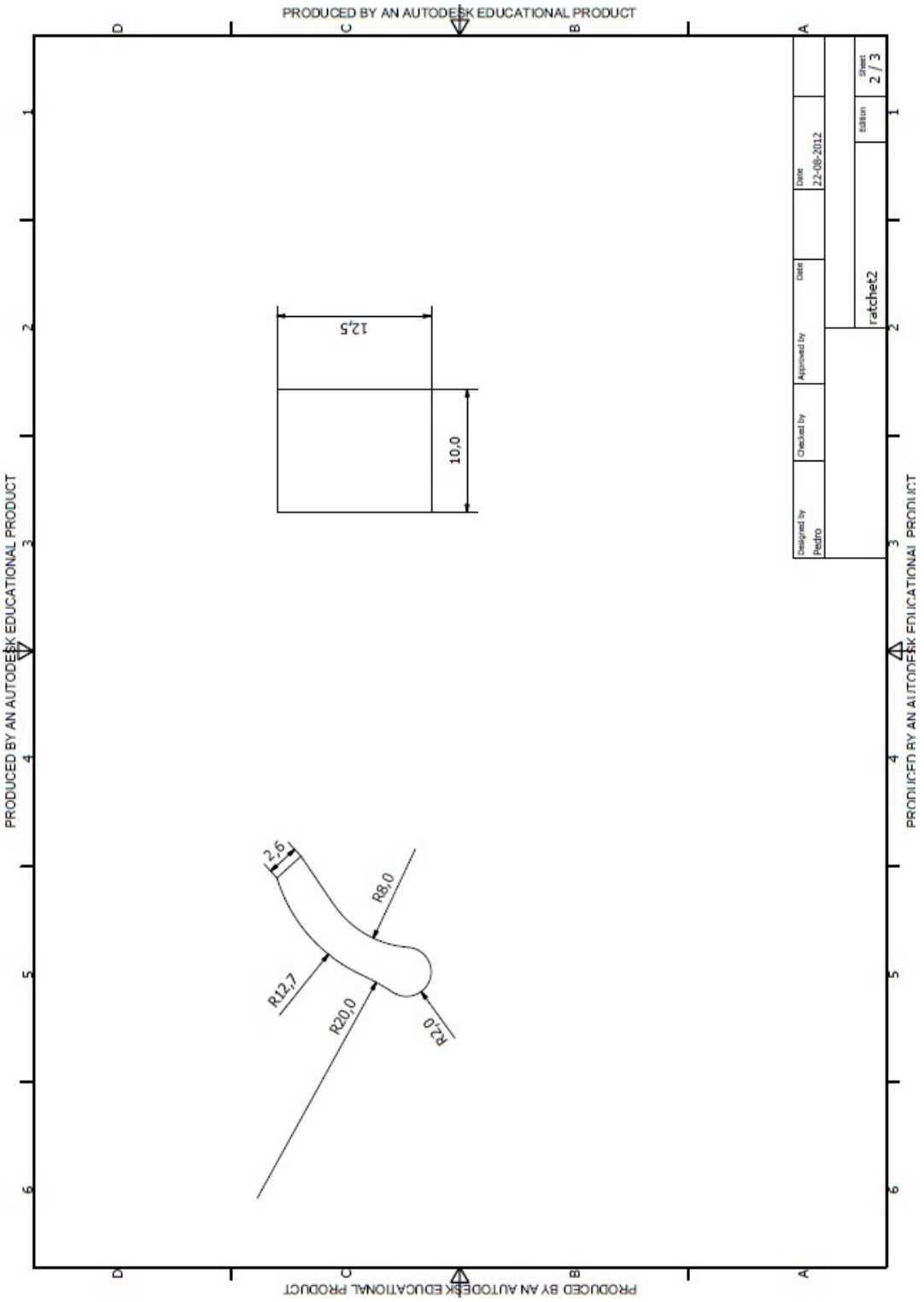

Figure B.2: Pawl 2

Ratchet 2

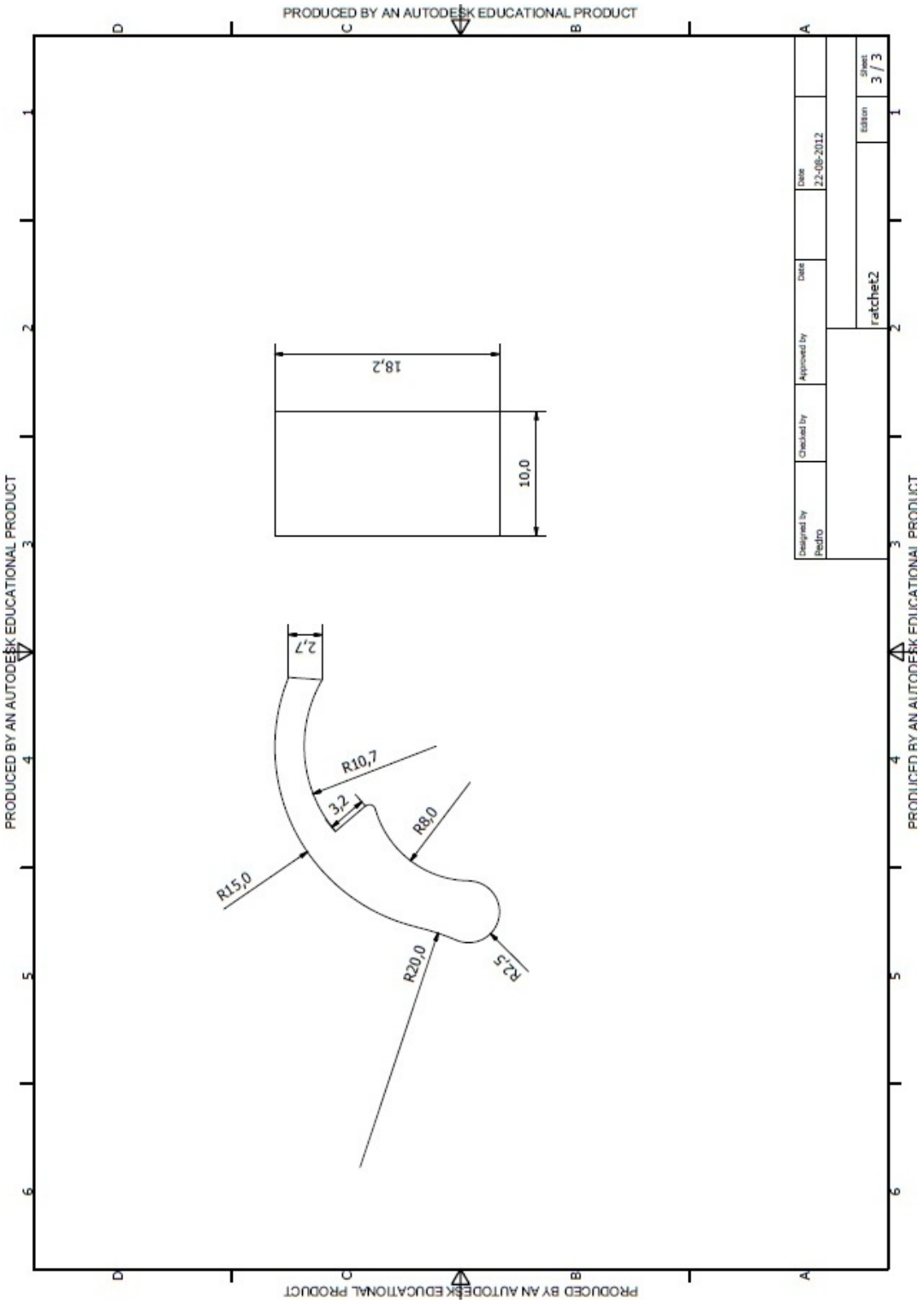

Figure B.3: Pawl 3

B.2 Stress Analysis

Constraint Name	Reaction Force		Reaction Moment	
	Magnitude	Component (X,Y,Z)	Magnitude	Component (X,Y,Z)
Pin Constraint:1	4663,98 N	-4484,25 N	0 N m	0 N m
		-1282,27 N		0 N m
		0 N		0 N m
Fixed Constraint:1	2732,2 N	2636,97 N	1,31704 N m	0,0290853 N m
		-715,048 N		-0,0100807 N m
		-1,81711 N		1,31668 N m
Fixed Constraint:2	2721,17 N	1847,97 N	2,79863 N m	0,0368097 N m
		1997,44 N		0,0209632 N m
		-2,96697 N		2,79831 N m

Figure B.4: Reaction Force and Moment on Constraints

Name	Minimum	Maximum
Volume	6070,15 mm^3	
Mass	0,0485612 kg	
Von Mises Stress	0,282656 MPa	188,387 MPa
1st Principal Stress	-26,6498 MPa	215,34 MPa
3rd Principal Stress	-97,1236 MPa	24,5611 MPa
Displacement	0 mm	0,00694357 mm
Safety Factor	1,08818 ul	15 ul

Figure B.5: Result Summary

Appendix C

Slot Mechanism

C.1 Dimensions

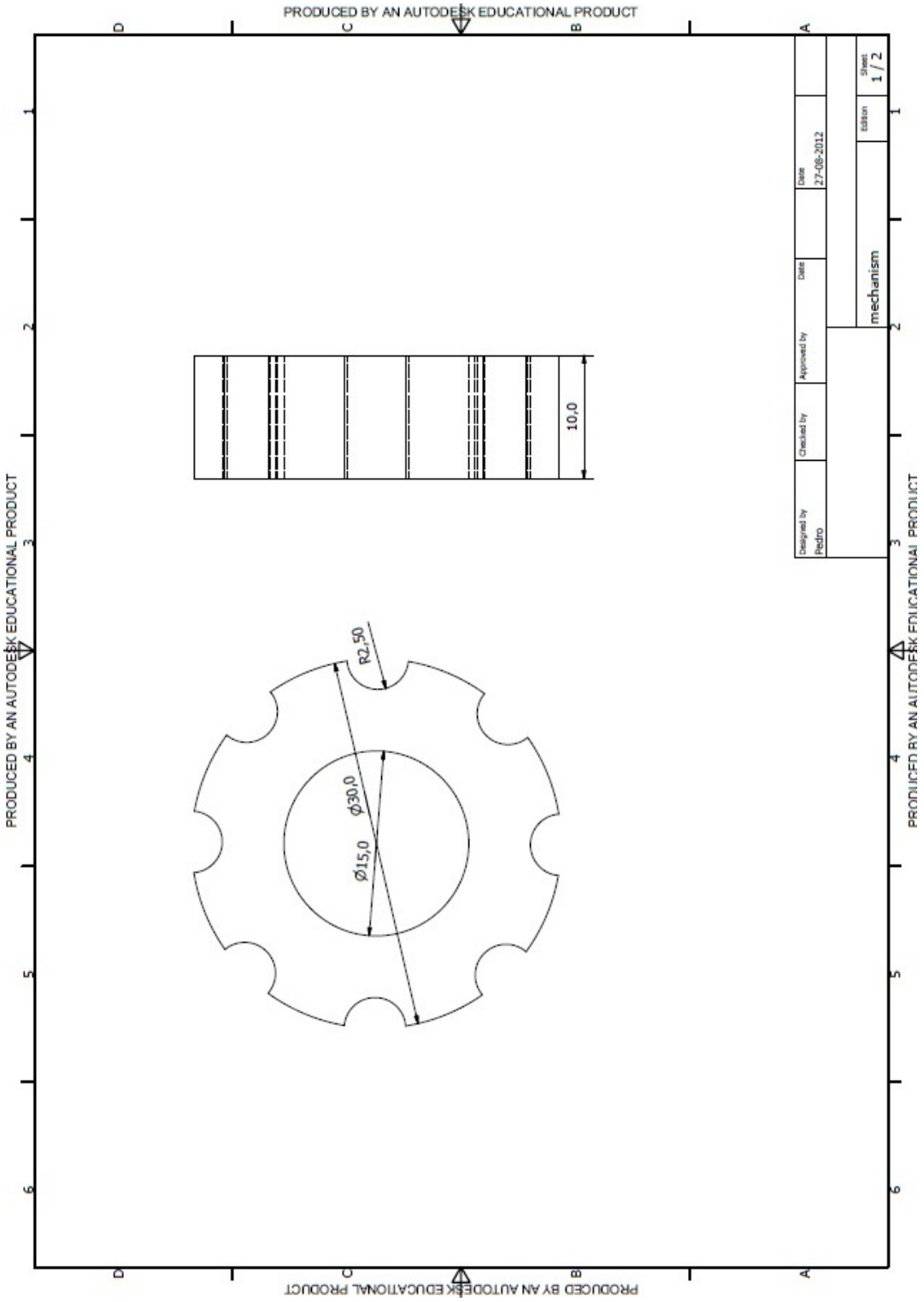

Figure C.1: Slot mechanism

Slot Mechanism

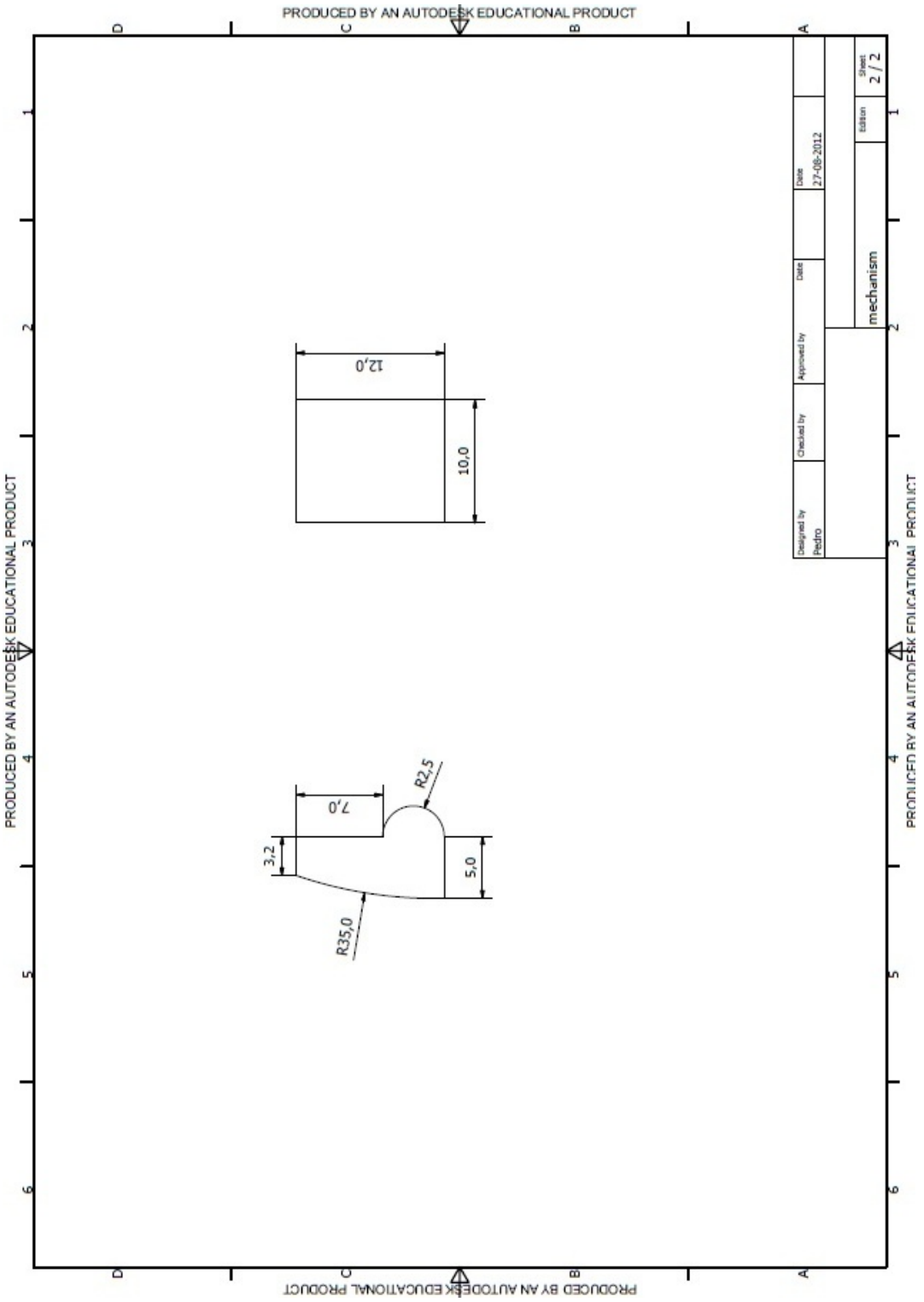

Figure C.2: Pawl 3

C.2 Stress Analysis

Constraint Name	Reaction Force		Reaction Moment	
	Magnitude	Component (X,Y,Z)	Magnitude	Component (X,Y,Z)
Fixed Constraint:1	5399,61 N	32,7027 N	5,03469 N m	0 N m
		5399,51 N		0,0342184 N m
		0 N		-5,03458 N m
Pin Constraint:1	5400,02 N	-32,4454 N	0 N m	0 N m
		-5399,93 N		0 N m
		0 N		0 N m

Figure C.3: Reaction Force and Moment on Constraints

Name	Minimum	Maximum
Volume	4543,9 mm^3	
Mass	0,0363512 kg	
Von Mises Stress	0,23999 MPa	129,617 MPa
1st Principal Stress	-33,5469 MPa	140,781 MPa
3rd Principal Stress	-140,977 MPa	33,1861 MPa
Displacement	0 mm	0,00906818 mm
Safety Factor	1,58159 ul	15 ul

Figure C.4: Result Summary

Appendix D

Generic Mechanism

D.1 Dimensions

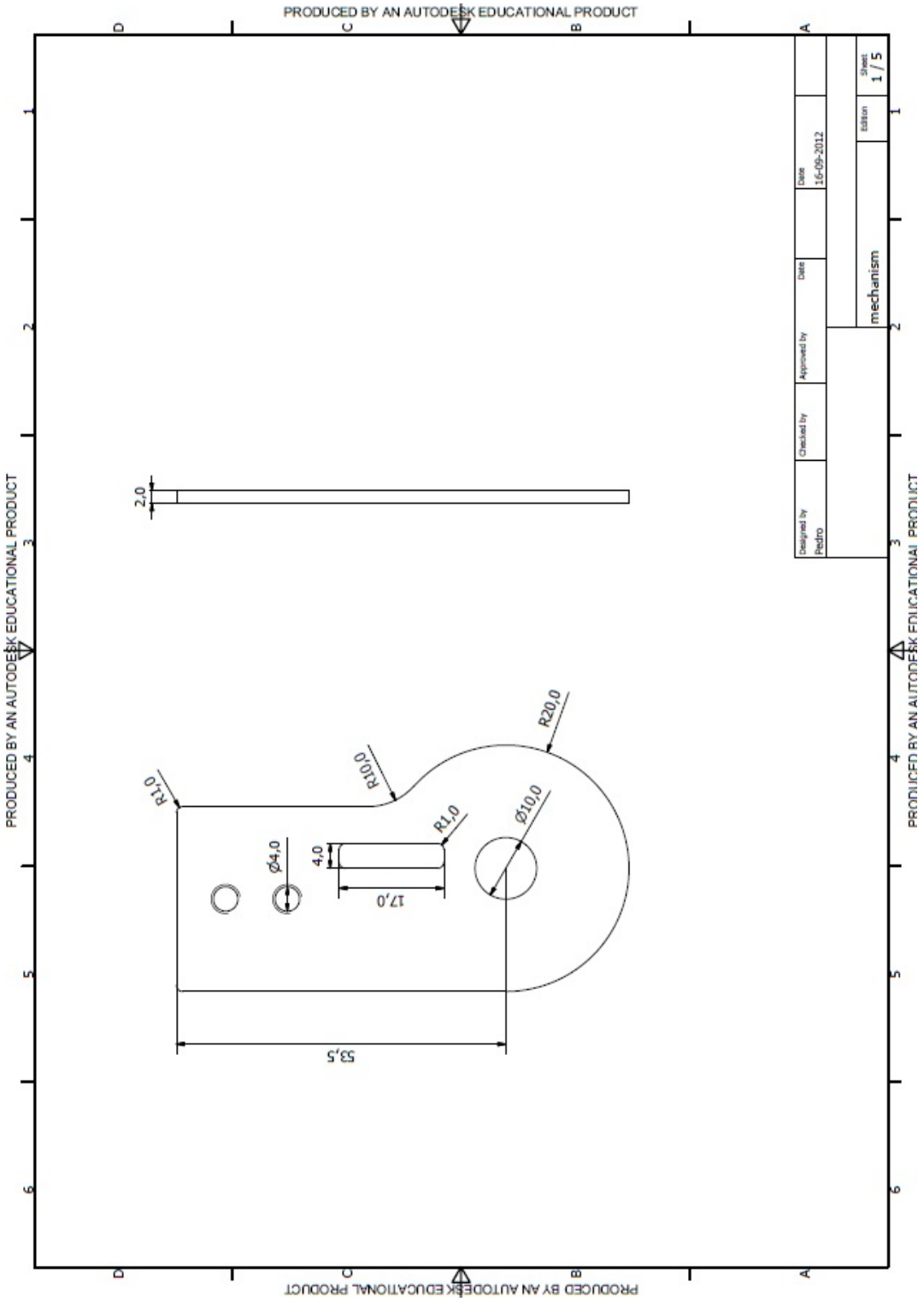

Figure D.1: Upper mechanism

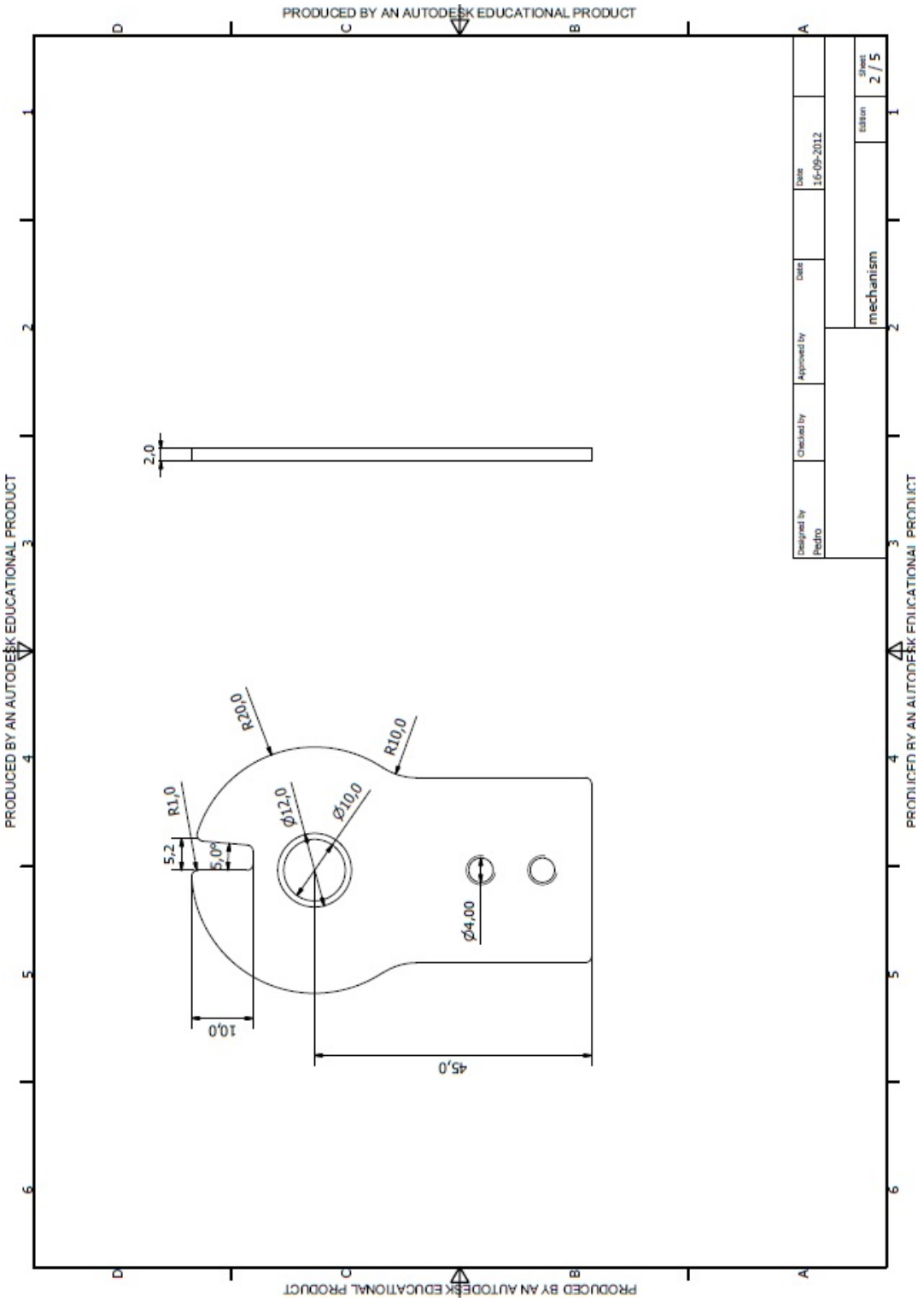

Figure D.2: Lower mechanism - v1

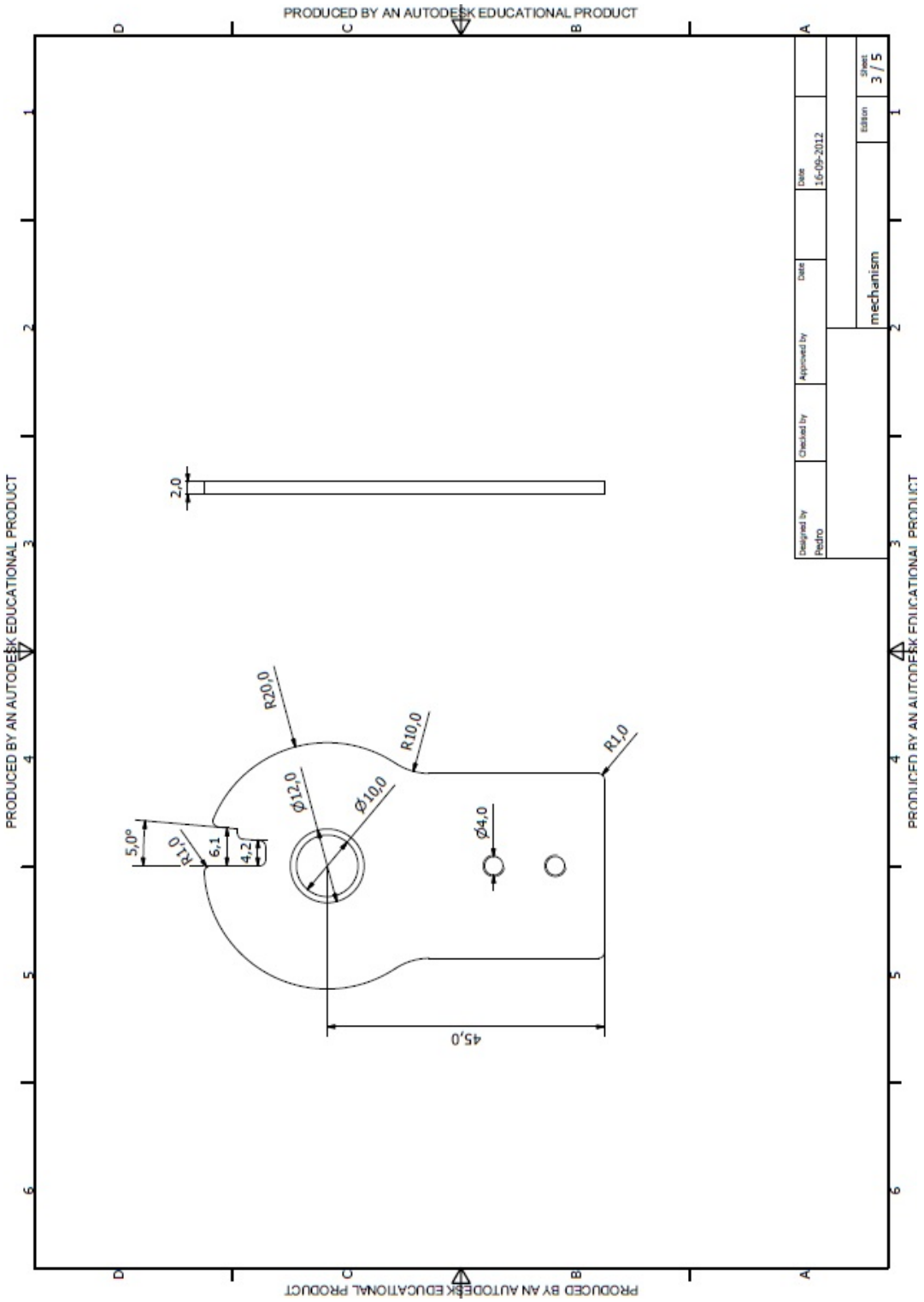

Figure D.3: Lower mechanism - v2

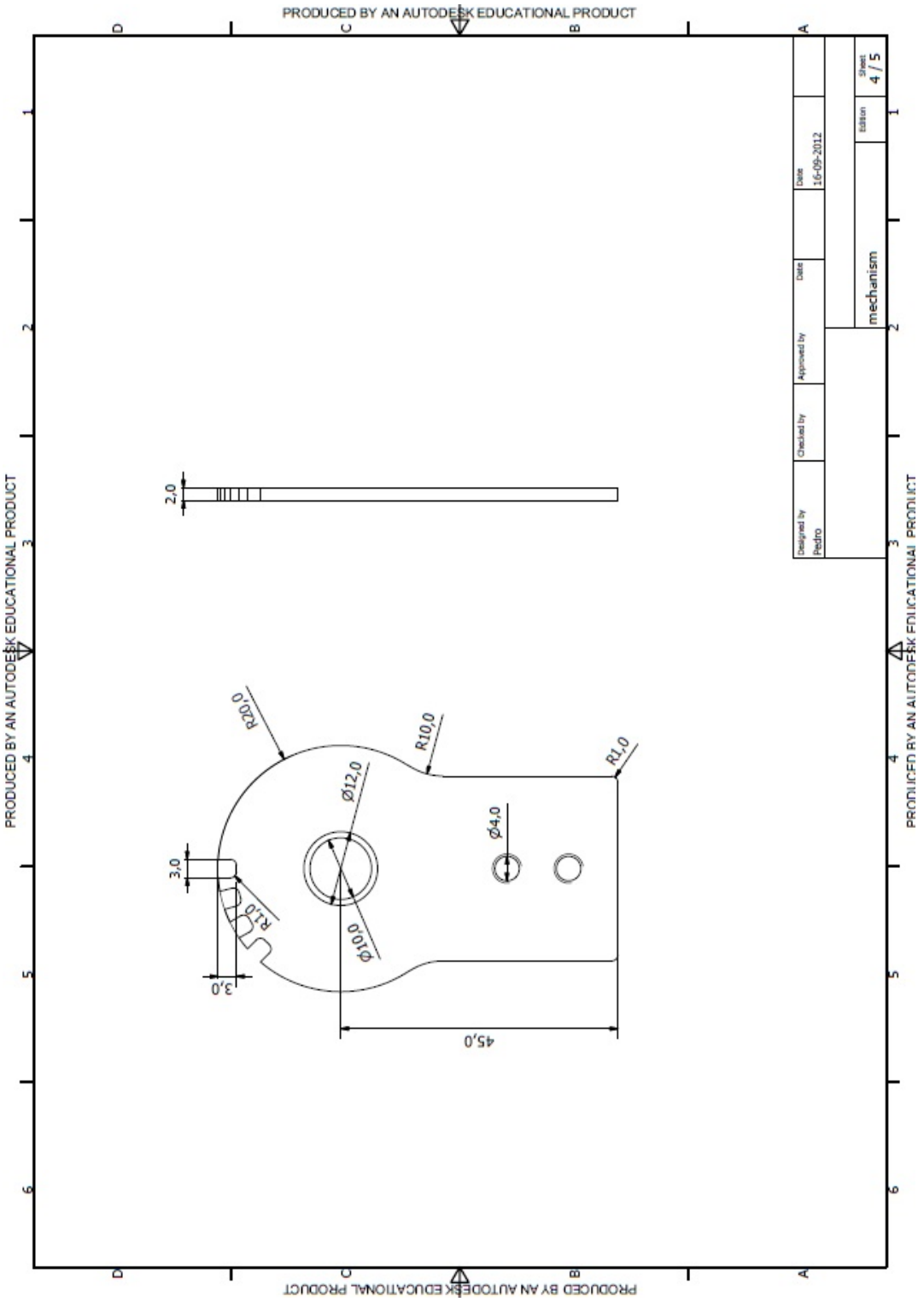

Figure D.4: Lower mechanism - v3

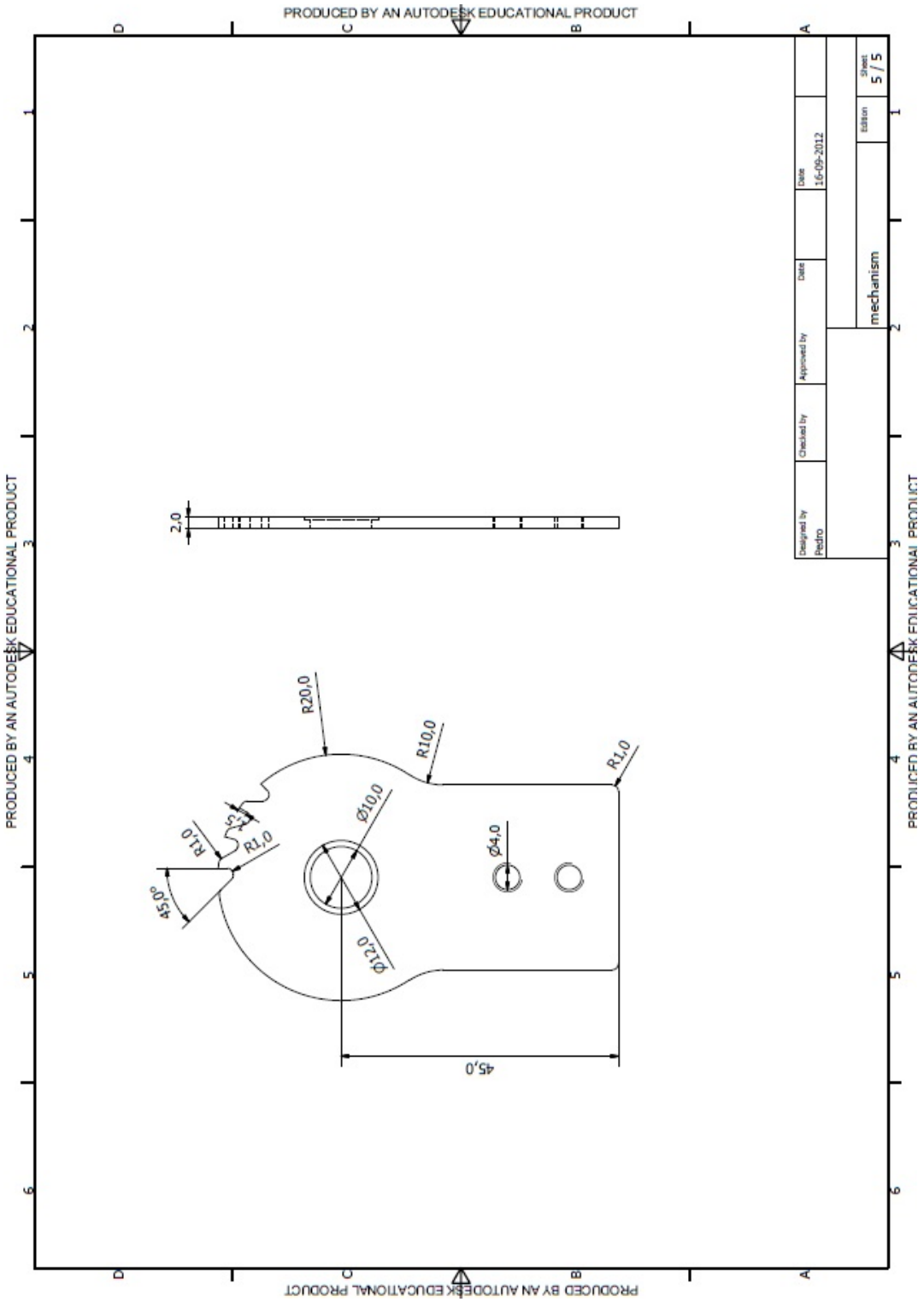

Figure D.5: Lower mechanism - v4

Appendix E

Schematics

Schematics

E.1 Microcontroller

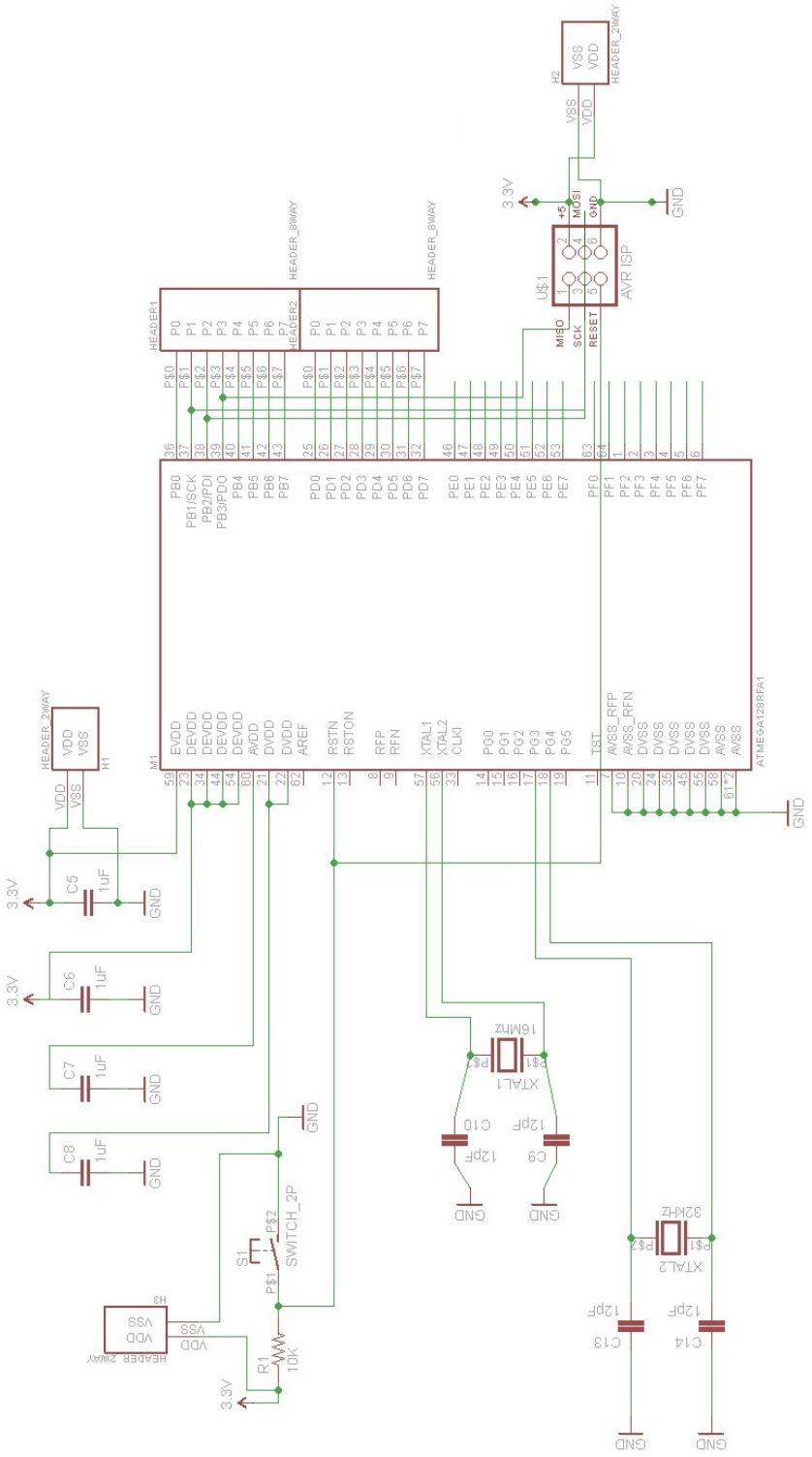

Figure E.1: ATmega128RFA1 Board - communication by wire

E.2 Sensors

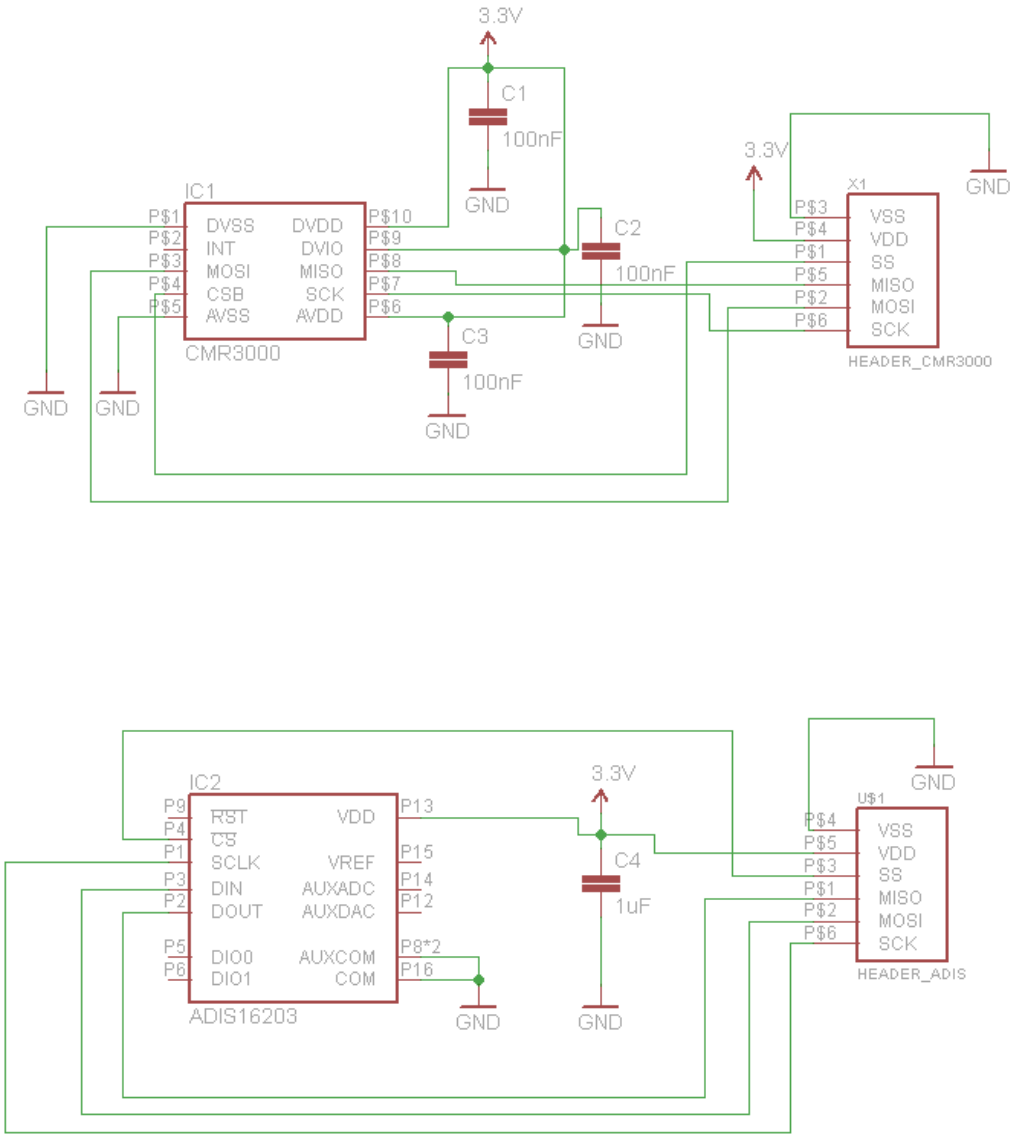

Figure E.2: PCB with sensors

E.3 Voltage Regulator

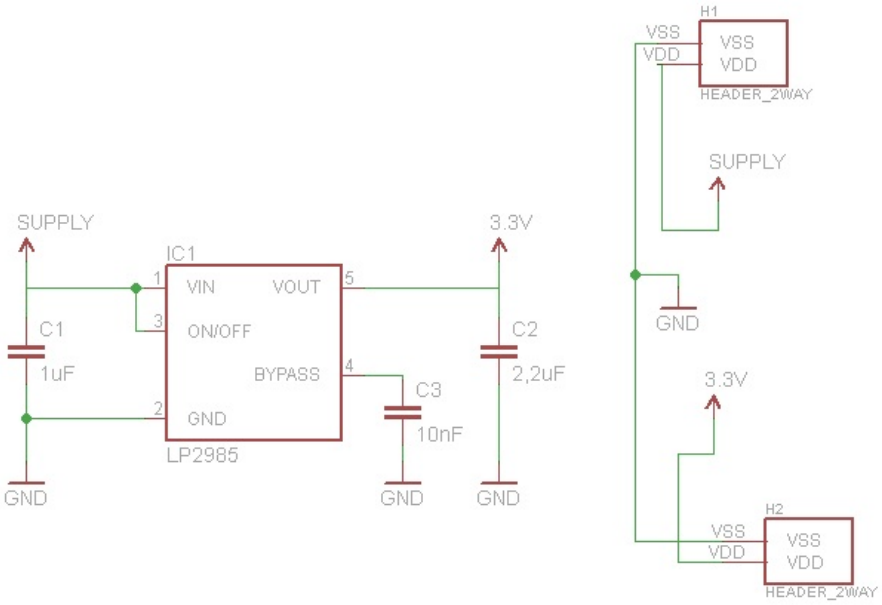

Figure E.3: Voltage regulator LP2985